uOttawa

L'Université canadienne
Canada's university

FACULTÉ DES ÉTUDES SUPÉRIEURES ET POSTOCTORALES

uOttawa

L'Université canadienne
Canada's university

FACULTY OF GRADUATE AND POSDOCTORAL STUDIES

Tyson Graber

AUTEUR DE LA THÈSE / AUTHOR OF THESIS

Ph.D. (Biochemistry)

GRADE / DEGREE

Department of Biochemistry, Microbiology and Immunology

FACULTÉ, ÉCOLE, DÉPARTEMENT / FACULTY, SCHOOL, DEPARTMENT

Post-Transcriptional Control of cIAP1

TITRE DE LA THÈSE / TITLE OF THESIS

Martin Holcik

DIRECTEUR (DIRECTRICE) DE LA THÈSE / THESIS SUPERVISOR

CO-DIRECTEUR (CO-DIRECTRICE) DE LA THÈSE / THESIS CO-SUPERVISOR

Jim Dimitroulakos

Bruce McKay

Martin Pelchat

Vincent Mauro
The Scripps Research Institute

Gary W. Slater

Le Doyen de la Faculté des études supérieures et postdoctorales / Dean of the Faculty of Graduate and Postdoctoral Studies

Post-Transcriptional Control of cIAP1

A Thesis

by Tyson E. GRABER, B.Sc. (Hons), Biochemistry

Presented to the Faculty of Graduate and Postdoctoral Studies in partial fulfillment of the requirements for the degree of **Doctor of Philosophy in Biochemistry.**

University of Ottawa, Ottawa, Ontario, Canada

Copyright © 2010 by Tyson E. Graber

Library and Archives Canada

Published Heritage Branch

395 Wellington Street
Ottawa ON K1A 0N4
Canada

Bibliothèque et Archives Canada

Direction du Patrimoine de l'édition

395, rue Wellington
Ottawa ON K1A 0N4
Canada

Your file Votre référence
ISBN: 978-0-494-73933-4
Our file Notre référence
ISBN: 978-0-494-73933-4

NOTICE:

The author has granted a non-exclusive license allowing Library and Archives Canada to reproduce, publish, archive, preserve, conserve, communicate to the public by telecommunication or on the Internet, loan, distribute and sell theses worldwide, for commercial or non-commercial purposes, in microform, paper, electronic and/or any other formats.

The author retains copyright ownership and moral rights in this thesis. Neither the thesis nor substantial extracts from it may be printed or otherwise reproduced without the author's permission.

AVIS:

L'auteur a accordé une licence non exclusive permettant à la Bibliothèque et Archives Canada de reproduire, publier, archiver, sauvegarder, conserver, transmettre au public par télécommunication ou par l'Internet, prêter, distribuer et vendre des thèses partout dans le monde, à des fins commerciales ou autres, sur support microforme, papier, électronique et/ou autres formats.

L'auteur conserve la propriété du droit d'auteur et des droits moraux qui protège cette thèse. Ni la thèse ni des extraits substantiels de celle-ci ne doivent être imprimés ou autrement reproduits sans son autorisation.

In compliance with the Canadian Privacy Act some supporting forms may have been removed from this thesis.

While these forms may be included in the document page count, their removal does not represent any loss of content from the thesis.

Conformément à la loi canadienne sur la protection de la vie privée, quelques formulaires secondaires ont été enlevés de cette thèse.

Bien que ces formulaires aient inclus dans la pagination, il n'y aura aucun contenu manquant.

Canada

Abstract

This dissertation examines post-transcriptional mechanisms controlling the expression of the cellular inhibitor of apoptosis protein 1 (cIAP1) - a key negative regulator of programmed cell death. Activation of post-transcriptional control mechanisms is especially evident in the cellular response to stress and thus represent potential targets for therapeutic intervention. Post-transcriptional control is mediated by trans-acting proteins and/or non-coding RNAs that interact with a mRNA to form a messenger ribonucleoprotein particle (mRNP). Identifying components of mRNPs is therefore an important first step towards understanding how they regulate the fate of mRNAs during the response to cell stress. The cIAP1 mRNA represents an ideal model of post-transcriptional control given its regulation at the level of stability and translation following various stress stimuli. Work presented herein identifies AU-rich elements within the 3' untranslated region (UTR) that negatively affect cIAP1 mRNA stability following ultraviolet radiation (UVR) stress. Additionally, our laboratory has previously shown that the cIAP1 5'UTR contains an Internal Ribosome Entry Site (IRES) that governs translation of cIAP1 mRNA in response to endoplasmic reticulum (ER) stress. These initial observations led to the hypothesis that trans-acting protein factors associated with cIAP1 mRNA play an essential role in modulating its stability and translational efficiency. Chapters 2 and 3 address this hypothesis by identifying p86 and NF45 as cIAP1 IRES trans-acting factors (ITAFs) required for IRES-mediated translation of cIAP1 following ER stress. Work presented in chapter 4 indicates that 5'UTR AU content can be reliably used to predict other NF45-dependent IRES; IRES that may function in a post-transcriptional RNA operon that maintains genomic stability, apoptotic threshold, and

appropriate NF-κB signalling. Finally, peer-reviewed work in chapter 5 identifies hnRNP A1 as an AU-rich element binding protein that destabilizes cIAP1 mRNA following exposure of the cell to ultraviolet radiation. The work embodied in this thesis contributes significantly to our understanding of how RNA binding proteins affect changes in RNA stability and translation and identifies novel targets for therapeutic strategies that modulate cIAP1 expression and its associated cytoprotective effects.

Acknowledgements

Many people have made it possible for me to complete this chapter of my professional life. They include friends, family, and colleagues; but also those anonymous members of various committees who decided to let me into graduate school, furnished me with a decent salary so that I could live like I wasn't in graduate school, and allowed me to keep a decent publication record. Of course, all of this would not have been possible without the absolute support and never waning optimism of my supervisor, Dr. Martin Holcik. I've learned much during my residency at the Apoptosis Research Centre, however two bits of wisdom stand out:

1) Contemporary science is driven by the networking meme.

2) A good experiment answers a question; a better experiment answers one question and begs the next.

Keep this in mind as you plough through this monolithic dissertation...

To the code-breakers.

Table of Contents

List of Abbreviations

ARE	AU-rich element
BclxL	B-cell CLL/lymphoma 2-like xenopus laevis
β-GAL	β-Galactosidase
BiP	Binding immunoglobulin protein
BVDV	Bovine viral diarrhea virus
c-myc	Cellular-myelocytomatosis onocogene
CAT	Chloramphenicol acetyl transferase
cIAP1	Cellular inhibitor of apoptosis protein 1
cIAP2	Cellular inhibitor of apoptosis protein 2
CrPV	Cricket paralysis virus
DAP5/p97	Death-associated protein 5/protein 97
DMSO	Dimethyl sulfoxide
eIF	Eukaryotic initiation factor
ELG1	Enhanced level of genome instability 1
ELISA	Enzyme-linked immunosorbent assay
EMCV	Encephelomyocarditis virus
ER	Endoplasmic reticulum
ES	Embryonic stem
GM-CSF	Granulocyte macrophage colony stimulating factor
HCV	Hepatitis C virus
HIAP2	Human inhibitor of apoptosis protein 2
HIV-2	Human immunodeficiency virus type 2
hnRNP A1	Heterogeneous ribonucleoprotein A1
hnRNP C1/C2	Heterogeneous ribonucleoprotein C1/C2
HRV2	Human rhinovirus type 2
HuR	Human antigen R
IGF2BP1	Insulin-like growth factor 2 mRNA-binding protein
IL-2	Interleukin-2
IRES	Internal ribosome entry site
ITAF	IRES trans-acting factor
La	La autoantigen
m7G	7-methylguanosine
MALDI-TOF	Matrix-assisted laser desorption/ionization-time of flight
miRNA	Micro RNA
mRNA	Messenger RNA
mRNP	Messenger ribonucleoprotein
MyoD	Myoblast determination protein 1
MYT2	Myelin transcription factor 2

NF-κB	Nuclear factor-kappa B
NF45	Nuclear factor 45
NF90	Nuclear factor 90
NIK	NF-kB inactivating kinase
NRF	NF-kB repressing factor
NTR	Non-translated region
ONPG	Ortho-nitrophenyl-β-galactoside
ORF	Open reading frame
PABP	PolyA-binding protein
PTB	Polypyrimidine tract binding protein
RHA	RNA helicase A
RIP	Receptor interacting protein
rpl26	Ribosomal protein large subunit 26
RRM	RNA recognition motif
rRNA	Ribosomal RNA
SDM	Site-directed mutagenesis
SNM1	Sensitivity to nitrogen mustard 1
TEK	Tyrosine endothelial kinase
TIA1	T-cell-restricted intracellular antigen-1
TNF-α	Tumour necrosis factor-α
TNFR1	Tumour necrosis factor receptor complex I
TRAF	Tumour necrosis factor receptor associated factor
TRAIL	TNF-related apoptosis-inducing ligand
Trn1	Transportin-1
UNR	Upstream of N-Ras
uORF	Upstream open reading frame
UPR	Unfolded protein response
UTR	Untranslated region
UVR	Ultraviolet radiation
VCIP	Vascular endothelial growth factor and type I collagen inducible protein
X-DC	X-linked dyskeratosis congenita
XIAP	X-linked inhibitor of apoptosis protein

List of Figures and Tables

Chapter 1

Chapter 2

Chapter 3

Chapter 4

Chapter 5

Chapter 6

CHAPTER 1

General introduction

1.1
Preamble

This introductory chapter consists of both unpublished (sections 1.2-3) and published (section 1.4) material. Section 1.2 introduces the reader to the various levels of post-transcriptional regulation and touches on its emerging importance in the post-genomic era. Section 1.3 provides the rationale, objectives and hypothesis for the research that was conducted. This section also gives the reader a brief introduction to the role of AU-rich elements in regulating RNA stability - a theme that is visited in chapter 5. Section 1.4 is a manuscript entitled "Cap-independent regulation of gene expression in apoptosis" and was first published as a review article in the periodical Molecular Biosystems (volume 3, December 2007). The article gives a detailed introduction to the control of mRNA translation and highlights the importance of these mechanisms during times of cell stress (in particular the response to endoplasmic reticulum stress) and in selected human pathologies. This theme will be visited in chapters 2-4.

Author list for section 1.4: Tyson E. Graber and Martin Holcik.

Author contributions for section 1.4: T.E.G. wrote the article. M.H. contributed ideas and editorial support.

1.2
The era of ribonomics

By the end of the twentieth century, fifty years of earnest work in the field of molecular biology had given the biologist a comprehensive doctrine that put control of proteome expression squarely in the hands of our genome; if the gene is transcribed, it must be translated. Work by Jacob and Monod in the late 1950s encapsulated this idea in their DNA operon model that explains how a prokaryotic cell can rapidly respond to changes in its environment by evolving groups of functionally similar genes that are coordinately expressed by a single protein regulator.[1] Little attention was paid at the time to the newly described "RNA messenger" whose appearance in the cytoplasm correlated perfectly with that of enzyme activity and thus was unlikely to be a point of control of gene expression. This viewpoint was espoused in the 1961 Cold Spring Harbor Symposium on Cellular Regulatory Mechanisms meeting report whose attendees included Jacques Monod, François Jacob as well as other notables such as Sydney Brenner and James Watson who were trying to understand what role RNA plays in peptide synthesis:

> "...regulation of protein synthesis appears to operate directly at the level of the genetic material. Since both the initiation and cessation of synthesis of an...enzyme follows almost immediately upon addition or removal of the specific effector, it appears that the information-carrying intermediate of protein synthesis must be both rapidly formed and rapidly destroyed." - Jacob and Monod [2]

Soon after however, eukaryotic cells (specifically invertebrate sea urchin eggs) were found to incorporate amino acids without de novo transcription immediately following fertilization.[3] Clearly, nuclear-enveloped eukaryotes had evolved mechanisms distinct from their prokaryotic cousins to regulate their proteome. Other examples of eukaryotic translational control would follow and the field of post-transcriptional regulation was born. Indeed, by the

time the human genome was deciphered at the start of this century it was realized that our genetic complexity arises, not from the number of genes in the nucleus, but from alternative splicing of gene transcripts. Thus, understanding the multiple levels of post-transcriptional regulation that includes splicing, export, stability, editing, localization and translation of cellular messenger RNA (mRNA) quickly became the next frontier in cell biology.

A common element to the life cycle of any mRNA molecule is its association with trans-acting proteins and/or non-coding RNAs. Together, these messenger ribonucleoproteins (mRNP) constitute the cellular ribonome. An mRNP particle is highly dynamic and is thought to be defined by RNA binding proteins interacting with sequence and structural elements within the untranslated regions (UTRs) of the mRNA.[4] Upstream signalling pathways that target the mRNP can alter the complement of trans-acting factors and therefore the overall fate of its mRNA cargo. As a modular unit of genetic information, mRNPs can act in a combinatorial fashion to regulate specific populations of transcripts in a manner analogous to the prokaryotic DNA operon (where gene expression is controlled in a time-dependent manner). Unlike their prokaryotic ancestors, eukaryotes* have evolved these RNA operons as an efficient method to control gene expression in a time- *and* space-dependent manner. Modelling individual mRNP units and defining RNA operons are therefore important first steps in determining how genetic information is organized in eukaryota and ultimately how perturbations in cellular homeostasis can lead to changes in phenotype.

* notable exceptions include nematodes; these organisms retain DNA operons as a method of gene regulation.

1.3
cIAP1: A model of post-transcriptional control

This dissertation focuses on identifying protein components that regulate stability and translational efficiency of the cellular inhibitor of apoptosis protein 1 (cIAP1[†]) mRNP. cIAP1 is a member of the highly conserved and critically important family of IAP proteins. Other members of this protein family include XIAP and cIAP2, that together with cIAP1, were initially reported to function as competitive inhibitors of caspases. While XIAP is indeed a potent competitive inhibitor of caspases, cIAP1 and cIAP2 have most recently been found to only weakly inhibit caspase activity in vivo.[5] Along with caspase binding activity, all three proteins possess E3 ubiquitin ligase activities that target proteins for proteasomal degradation (mediated by K48 poly-ubiquitin linkages) or for participation in specific signalling pathways (mediated by K63 poly-ubiquitin linkages). Intense research by several laboratories over the past three years has uncovered a critical role for IAP ubiquitin ligase activities in modulating inflammatory signalosomes that serve to regulate the pro-survival NF-κB transcriptional programme. More specifically, cIAP1/2-mediated K63-ubiquitylation of receptor interacting protein (RIP) kinase at the Tumour Necrosis Factor Receptor complex I (TNFRI) signalosome is necessary for TNF-α-mediated NF-κB pro-survival signalling.[6] Paradoxically, removal of either cIAP1 or cIAP2 in unstimulated cells enhances constitutive NF-κB signalling, possibly as the result of NF-κB-inducing kinase (NIK) stabilization that results in the induction of both the classical and alternative arms of the NF-κB response.[7] The broad range of NF-κB target genes that are involved in tumourogenesis and cancer

[†]cIAP1 is also known as "HIAP2". Note that published manuscripts presented in chapters 1 and 2 use the protein name "HIAP2", reflecting the accepted nomenclature at the time of publication.

progression coupled with frequent cancer-associated mutations in IAP alleles gives a strong rationale for studying the regulation of cIAP1 and cIAP2 expression.

Notwithstanding the apparent functional redundancy of cIAP1 and cIAP2 in the context of NF-κB signalling, expression of each protein is distinctly regulated and suggests specialized roles depending on the cellular context. For example, cIAP2 expression is primarily controlled at the level of transcription in an NF-κB-dependent manner and is held in check by cIAP1 which targets cIAP2 for proteasomal degradation. Previous work from our laboratory and others established that cIAP1 protein synthesis is significantly repressed in several cell lines. This repression of expression is the result of both a long (1.2 kilobases) 5'UTR that is postulated to hinder ribosomal scanning, and a small upstream open reading frame (uORF) that prevents initiation of translation at the authentic downstream AUG start codon (Figure 1.1 and Warnakulasuriyarachchi et al[8]). Our laboratory also previously identified a cis-regulatory element proximal to the authentic AUG that allows direct recruitment of the ribosome and initiation of protein synthesis.[9] This Internal Ribosome Entry Site (IRES) is only active following induction of the endoplasmic reticulum (ER) stress response and results in increased expression of cIAP1 protein. As discussed in section 1.2, such post-transcriptional regulation is generally mediated by RNA binding proteins. **Ergo, the explicit hypothesis stemming from these observations is that trans-acting protein factors associated with the cIAP1 mRNA play an essential role in modulating its translational efficiency.** Data presented in chapters 2 and 3 address this hypothesis by identifying components that modulate the activity of the cIAP1 IRES and thus translational efficiency of

Figure 1.1

Known cIAP1 mRNA sequence features and post-transcriptional regulatory nodes circa 2004. A diagram of the capped (m7G) and polyadenylated cIAP1 mRNA illustrating the size (in kilobases, Kb) and location of the 5' and 3' untranslated regions (UTR). Note that the drawing is not to scale. The IRES that enhances translation of this mRNA following ER stress is approximately 150 nucleotides long and is located proximal to the initiation codon (AUG) of the main open reading frame (ORF). An upstream ORF (uORF) whose CUG initiation codon bisects the IRES codes for a peptide of 21 amino acids. In addition, cIAP1 mRNA stability is reduced following exposure to ultraviolet C radiation. These preliminary observations were the basis of the hypothesis that RNA binding proteins mediate these phenomena.

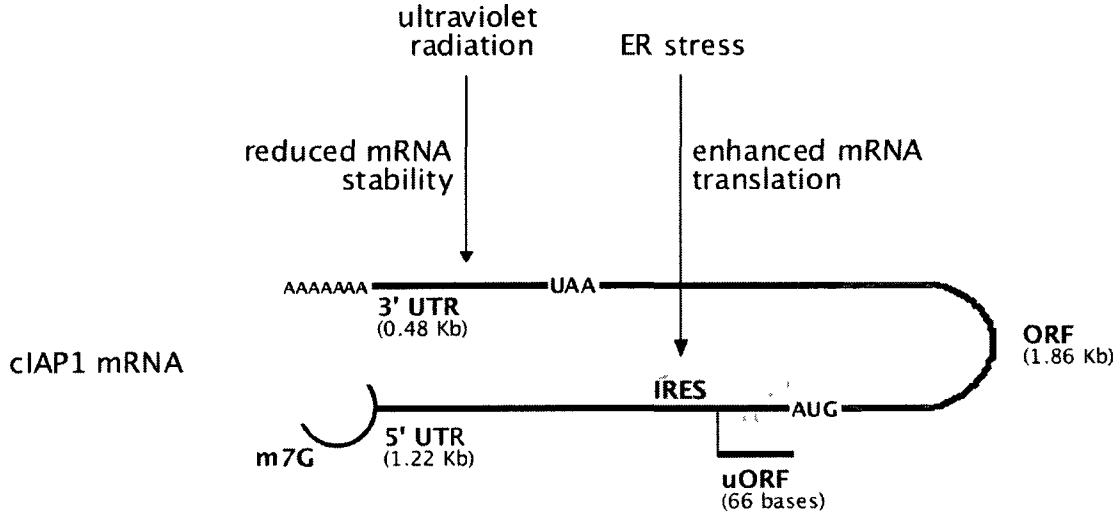
ultraviolet radiation
ER stress
reduced mRNA stability
enhanced mRNA translation
AAAAAAA
UAA
3' UTR
(0.48 Kb)
ORF
(1.86 Kb)
cIAP1 mRNA
IRES
AUG
m7G
5' UTR
(1.22 Kb)
uORF
(66 bases)

its mRNA. The data suggest the existence of an auxilliary translation initiation complex that is active during ER stress allowing for continued translation of this important regulator of apoptosis and NF-κB signalling during times when the cell has reduced general protein synthesis and proliferative potential in an effort to reduce the protein load in the ER and subvert apoptosis. Moreover, evidence is presented in chapter 4 that implicates a key component of this complex in the regulation of several other IRES. The data suggest that this component is not unique to the cIAP1 mRNP and may participate in a post-transcriptional RNA operon targeting IRES-mediated translation of critical mRNAs that function to maintain genomic stability and appropriate NF-κB signalling.

Besides regulation through its IRES, evidence is presented in chapter 5 that cIAP1 is additionally regulated at the level of RNA stability. Specifically, cIAP1 mRNA half-life is significantly reduced following exposure to ultraviolet radiation (UVR). The reduced stability of cIAP1 mRNA is mediated by AU-rich elements (ARE) in its 3'UTR. The classical ARE is defined by an AUUUA pentamer that generally targets the mRNA for degradation through the exosome.[10] Although the exact mechanism is unknown, it is clear that trans-acting protein factors are responsible for modulating ARE-dependent RNA stability. **Thus, the hypothesis addressing translational efficiency of cIAP1 mRNA in chapters 2-4 was extended in chapter 5 to propose that trans-acting protein factors play an essential role in modulating cIAP1 mRNA stability.** To this end, chapter 5 identifies a cIAP1 ARE trans-acting factor that undergoes nucleo-cytoplasmic transport after UVR stress allowing increased association with, and targeted degradation of cIAP1 mRNA. The work embodied in this thesis contributes significantly to our understanding of how RNA binding

proteins affect changes in RNA stability and translation and identifies novel targets for therapeutic strategies that modulate cIAP1 expression and its associated cytoprotective effects.

1.4
Cap-independent regulation of gene expression in apoptosis

Abstract

Expression of the proteome is tightly regulated at the level of protein synthesis. Translational control is a critical homeostatic mechanism that allows the cell to rapidly change its phenotype in the face of an intra- and extra-cellular environment in constant flux. It is becoming increasingly clear that when it comes to protein translation during cell stress, all mRNAs are not treated equally. The translation of the majority of mRNAs is compromised during cell stresses that induce programmed cell death such as hypoxia, or DNA damage. However, cellular messages harbouring Internal Ribosome Entry Site elements (IRES) within their 5' untranslated regions are insensitive to stress-induced repression of global translation. Instead, these IRES-containing mRNAs use a poorly understood alternative mechanism of translation that allows continued expression of proteins that are required for the cell to recover from a transient stress or to proceed down the path toward apoptotic death. This review will highlight recent literature that suggests why global translation rates are impaired during stress and apoptosis and how these conditions mediate a switch in the mechanism by which pertinent proteins are synthesized. In addition, recent advances towards our understanding of the physiological role and mechanism of IRES-mediated translation in the context of cell stress-induced apoptosis and human disease will be examined.

Apoptosis 101

Apoptosis, a form of programmed cell death, is constantly threatening the very existence of the cell. The specter of death arises at various checkpoints throughout the life of a cell.

Differentiation, development and growth are all subject to apoptotic signalling that will lead to the organized demolition of the cell should any of these processes go awry.

Many cellular stresses such as hypoxia, DNA damage, osmotic shock, or viral infection can initiate the apoptotic programme. More subtle growth-related stressors such as amino acid availability and cell cycle arrest can also trigger apoptosis if not readily corrected.

Apoptosis can begin from without via paracrine and/or autocrine death signals, or from within via perturbations in mitochondrial membrane integrity (Figure 1.2). Extrinsic signals can activate caspase-8 directly, which can in turn activate the effector caspases-3 and -7. Convergence of intrinsic pro-apoptotic signals at the mitochondria promotes release of cytochrome C into the cytosol resulting in the recruitment of the cysteine protease zymogen pro-caspase 9 and protease-activating factor 1 (APAF-1), that together form the apoptosome. The activation of caspase-9 within this protein complex results in the cleavage and activation of effector caspases-3 and -7. Alternatively, activation of caspases-2,4 (or caspase-12 in mouse) within the endoplasmic reticulum (ER) can directly activate pro-caspase-9.[1] These three distinct but inter-connected apoptotic cascades effectively amplify levels of active caspase-3 and -7 in the cell and, if not properly controlled, will lead to cell death.

Paradoxically, while global rates of protein translation are reduced during this process, several proteins that are required to mount an appropriate response to apoptosis (i.e. increase survival signals or increase death signals) are able to be synthesized via an alternative mechanism of protein translation. This review will highlight the progress of the

Figure 1.2

IRES-Mediated translation initiation regulates the expression of key players in apoptosis. Distinct stressors can trigger a cellular response that attenuates global translation within the cytoplasm. Downstream signalling events can induce an endoplasmic reticulum-mediated and/or mitochondria-mediated caspase activation cascade that leads to amplification of the effector caspases-3 and -7 and cell death. Despite a reduction in global translation, IRES-mediated translation of many anti- and pro-apoptotic proteins persists during apoptosis and serves to increase or decrease the apoptotic threshold in response to changes in the cellular environment.

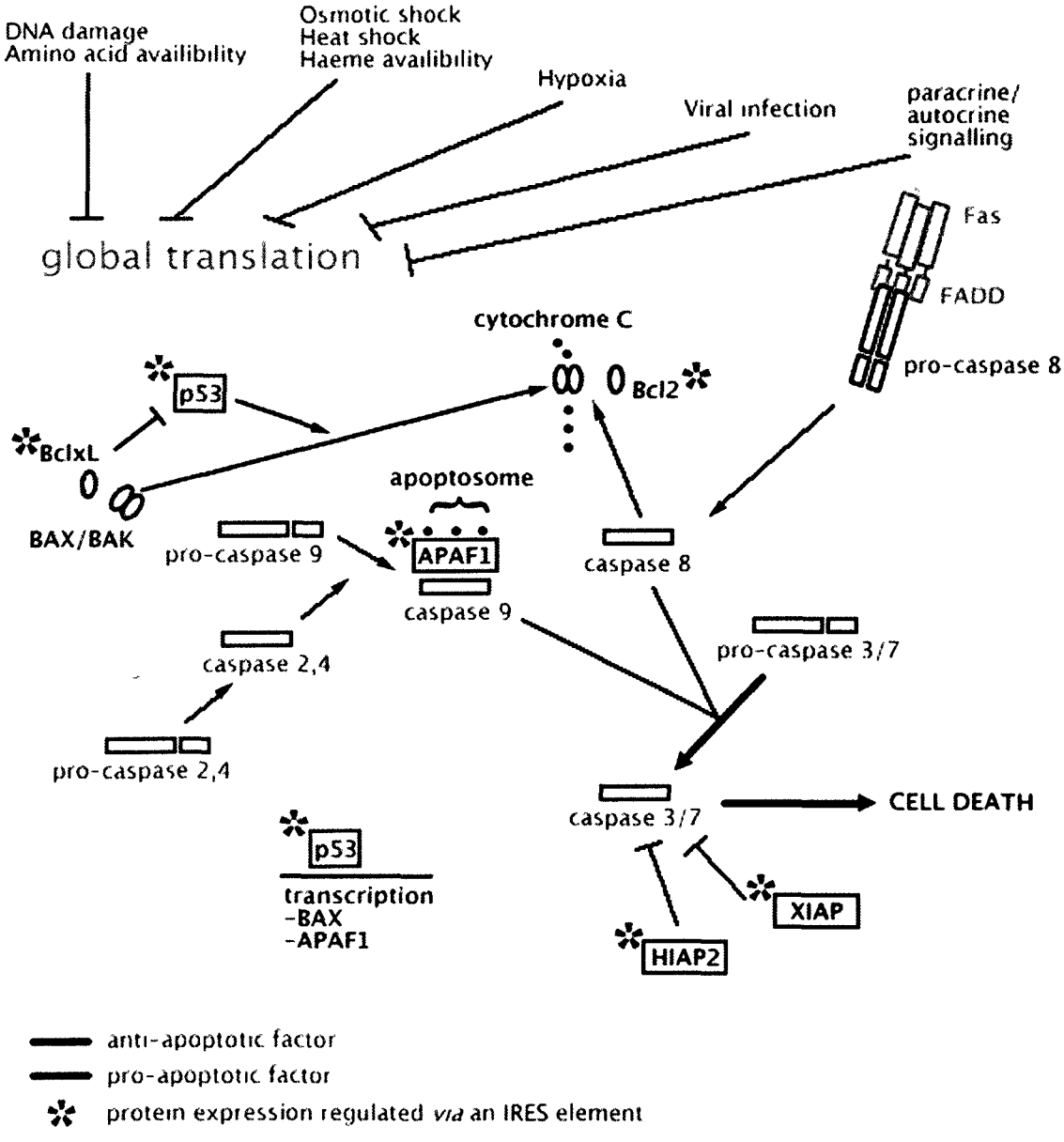
DNA damage
Amino acid availibility
Osmotic shock
Heat shock
Haeme availibility
Hypoxia
Viral infection
paracrine/
autocrine
signalling
global translation
Fas
FADD
pro-caspase 8
cytochrome C
p53
Bcl2
BclxL
BAX/BAK
apoptosome
pro-caspase 9
APAF1
caspase 8
caspase 9
caspase 2,4
pro-caspase 3/7
pro-caspase 2,4
caspase 3/7
CELL DEATH
p53
transcription
-BAX
-APAF1
XIAP
HIAP2
anti-apoptotic factor
pro-apoptotic factor
protein expression regulated *via* an IRES element

last few years in elucidating this poorly understood mechanism and how it may be favoured over canonical models of translation during cell stress and apoptosis.

Translational control is a homeostatic response to cellular stress

The cell has evolved exquisitely sensitive control points to regulate expression of its proteome. Regulation of protein translation, the penultimate control point of gene expression, plays a critical role in cellular homeostasis. Perturbations in the *status quo* upon exposure to physical or biochemical stressors occur during normal cell growth and differentiation, or as a result of disease. These cellular stresses lead to changes in protein levels and alter the efficiency of protein folding. The cellular response to stress is made up of numerous molecular signalling pathways that together determine whether the cell survives, and continues to proliferate, or undergoes programmed cell death. Translational control in eukaryotes has evolved to alter protein expression in specific cellular compartments at specific times. In contrast to the relatively slow process of de novo mRNA synthesis, processing, and transport, spatial and temporal control of protein translation allows for a rapid response to inter- and intra-cellular stress signals.

Canonical eukaryotic translation initiation

Although the elongation and termination steps in protein translation are themselves highly regulated, initiation – the rate-limiting step in protein translation – is arguably the most important and certainly the best studied component of the translation apparatus. However, the mechanism by which translation is initiated on some mRNAs can change drastically upon

perturbations in cellular homeostasis. To appreciate how this change occurs at the molecular level, it is necessary to have a general understanding of the current mechanistic dogma of eukaryotic translation initiation.

The majority of mature (i.e. capped and polyadenylated) eukaryotic mRNAs initiate translation via a cap-dependent ribosomal scanning mechanism under normal physiological conditions (Figure 1.3). The 7-methyl-guanosine (m7G) cap structure located at the 5' end of an mRNA interacts with the cap-binding protein initiation factor eIF4E together with a large adaptor protein (eIF4G) and an RNA helicase (eIF4A). This cap-binding complex (eIF4F) provides an anchored scaffold for the ATP-dependent recruitment of the 43S pre-initiation complex (consisting of the 40S small ribosomal subunit, "charged" methionyl-tRNA and several other initiation factors).[2] The resulting 48S pre-initiation complex is then believed to "scan" along the 5' untranslated region (UTR) toward the 3' end until it reaches an initiation codon (usually AUG) in an optimal context (typically GCCRCCAUGG, where R is any purine), at which point the 60S ribosomal subunit joins to form the 80S ribosome and peptide synthesis begins.[3] Notably, both the formation of the initiation complex and scanning of the message for an initiation codon require large amounts of ATP to drive the initiation phase of translation.[2]

Although the mechanisms are less well-understood, it is important to realize that the 3' end of the mRNA plays an important role in translation initiation whereby 3'UTR binding proteins (e.g. polyA binding protein, PABP) promote circularization of the mRNA through binding with eIF4G at the 5' cap. The result is a dramatic increase in the efficiency of

Figure 1.3

Canonical eukaryotic translation initiation. Translation initiation is highly regulated in eukaryotes and requires the concerted participation of numerous eukaryotic initiation factors (eIFs are depicted here as numbered shapes) at the 7-methyl-guanosine (m7G) structure located at the 5' end of a messenger RNA (mRNA). Note that interaction with the 3'UTR via polyA binding protein (PABP) enhances initiation rates. First, the cap-binding complex, eIF4F, (consisting of eIF4E, 4G and 4A) binds to the m7G mRNA cap in an ATP-dependent reaction. eIF4G provides a scaffold for the binding of the 43S pre-initiation complex that consists of the small 40S ribosomal subunit, the eIF2-bound charged initiator tRNA, the adaptor protein eIF3 and several other eIFs. The resulting 48S pre-initiation complex then scans in a 5' to 3' direction until an initiation codon (AUG) in the optimal context is encountered. The GTPase-activating protein eIF5 then catalyzes the activation of eIF2 resulting in the release of uncharged GDP-eIF2 which can be re-charged by eIF2B for use in a subsequent initiation event. eIF5B activity then facilitates the concurrent binding of the large 60S ribosomal subunit and dissociation of the remaining initiation factors. The assembled ribosome is now competent to proceed with the elongation step of protein translation.

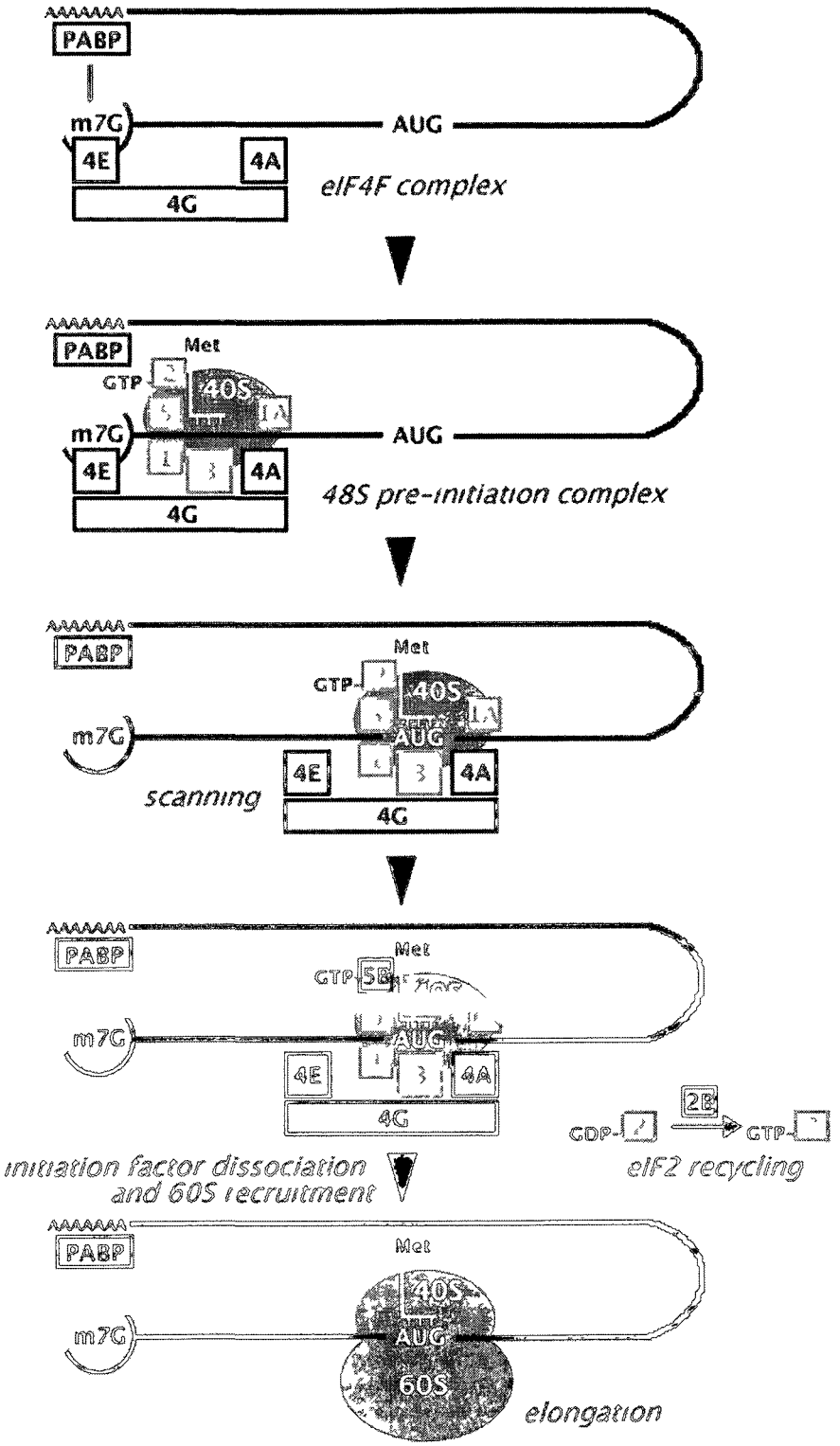
PABP
m7G
AUG
4E
4A
4G
eIF4F complex
Met
GTP
40S
48S pre-initiation complex
scanning
5B
initiation factor dissociation
and 60S recruitment
2B
GDP
GTP
eIF2 recycling
60S
elongation

translation that likely occurs due to the ability of terminating ribosomes to be recycled, allowing multiple rounds of translation on the same mRNA.[2]

Distinct mechanisms impair cap-dependent translation initiation during cell stress

eIF2 phosphorylation

While the local abundance of functional eIF2 (which catalyzes transfer of methionyl-tRNA to the 43S pre-initiation complex) and eIF4F complexes ensures efficient translation of mRNAs, the availability of these initiation factors during cell stress such as hypoxia[4] or viral infection[5] is restricted. Thus, during times of cellular stress, global rates of cap-dependent protein translation are reduced in an effort by the cell to conserve energy and precious resources.

For instance, in the specific case of hypoxic stress, early global translational arrest (70% reduction) is mediated by the phosphorylation of eIF2 which acts as a competitive inhibitor of the GTP-exchange factor eIF2B. This leads to the inability of eIF2 to be recycled and therefore formation of the pre-initiation complex is severely inhibited (Figure 1.4). While eIF2 phosphorylation is a hallmark of early hypoxia, the effect is transient with its dephosphorylation and re-activation occurring within 4 hours of a hypoxic insult.[4]

Figure 1.4

Changes in expression and/or function of translation initiation factors during cellular stress favours IRES-mediated translation initiation of some mRNAs. Detailed explanations are provided in the text. (**A**) Under normal physiological conditions eIF4EBP is phosphorylated, and eIF4F complex is available for cap-dependent initiation of translation. Circularization of the mRNA via polyA binding protein (PABP) can increase the efficiency of translation, while miRNA:Ago2 complexes can repress translation by competing with eIF4E for the m7G cap structure. (**B**) Cellular stress can impair cap-dependent translation by several mechanisms via: phosphorylation of eIF2 (1.), sequestration of eIF4E by eIF4E binding protein 1 (eIF4E-BP1) (2.), Proteolysis of eIF4G (4G*) resulting in a fragment that retains eIF4A and eIF3 binding sites (3.), modulation of protein interactions that bridge the 5' and 3'UTRs (4.). (**C**) A hypothetical model of potential factors required for ribosomal recruitment by an IRES. It is possible that the minimum complex consists of eIF4G or p97 fragments and/or eIF3 and eIF4A. Additional ITAFs appear to be required for cellular IRES activity (examples are listed), and these could function either as RNA chaperones or as adaptor proteins mediating direct recruitment of ribosomes. Many ITAFs can interact with both the 5' and 3'UTRs, suggesting that mRNA circularization may be involved in IRES-mediated translation initiation.

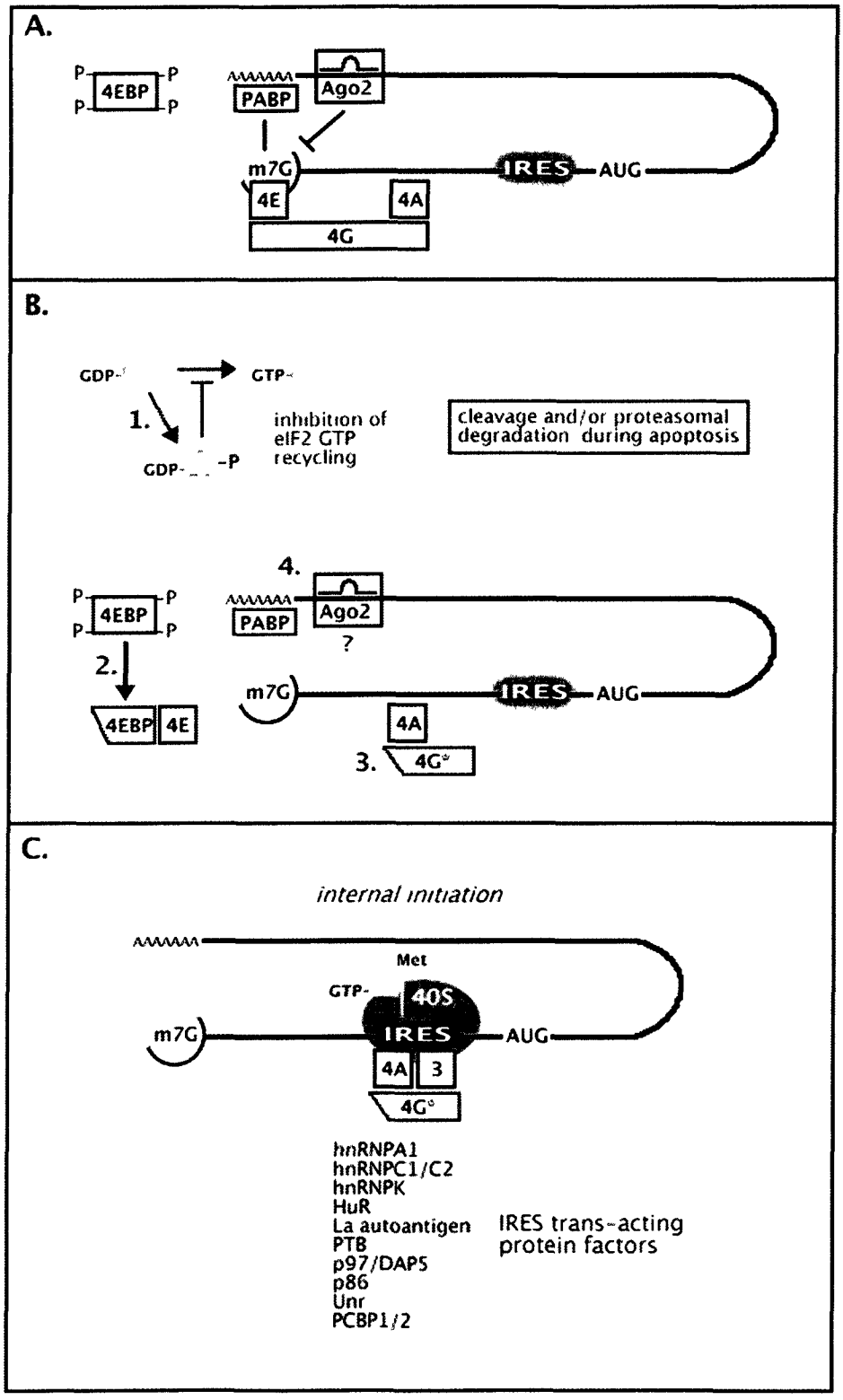
A.
4EBP
PABP
Ago2
m7G
IRES
AUG
4E
4A
4G
B.
GDP
GTP
1.
inhibition of eIF2 GTP recycling
cleavage and/or proteasomal degradation during apoptosis
4.
2.
?
3.
C.
internal initiation
Met
GTP
40S
hnRNPA1
hnRNPC1/C2
hnRNPK
HuR
La autoantigen
PTB
p97/DAP5
p86
Unr
PCBP1/2
IRES trans-acting protein factors

Availability of the cap-binding complex eIF4F

Sequestered eIF4E

Under sustained hypoxic stress, the integrity of the eIF4F cap-binding complex becomes increasingly compromised through dephosphorylation and activation of eIF4E binding protein (eIF4E-BP1), sequestering eIF4E and preventing it's association with the 5' cap structure on mRNA (Figure 1.4B). The reduced availability of eIF4F accounts for the observed continued inhibition of global translation (50% reduction) under prolonged hypoxia.[4]

Chronic hypoxia/anoxia triggers apoptosis and activation of caspases via the intrinsic mitochondrial pathway. One would therefore expect that eIF4E would be subject to proteolytic cleavage by active caspases. Indeed, while eIF4E does not appear to be modified by proteolysis during apoptosis, its regulator eIF4E-BP1 is cleaved by caspases during etoposide-induced apoptosis.[6] Importantly, the major cleavage fragment retains intact phosphorylation and eIF4E binding sites but exhibits a *reduced* phosphorylation status.[6] The hypophosporylated caspase cleavage fragment readily sequesters eIF4E and therefore attenuates cap-dependent translation initiation.

eIF4G proteolysis

In addition to alterations in eIF4E activity, caspase-dependent proteolytic cleavage of the scaffold protein eIF4G renders the eIF4F complex unable to associate with the 5' cap structure (Figure 1.4B). Recent evidence points to the existence of at least three eIF4G

family members (eIF4GI, eIF4GII and p97/DAP5). These functional homologues appear to enhance global protein synthesis in a non-redundant manner.

Specifically, they may selectively regulate translation of mRNA populations in the cell under different physiological conditions. This has been proven to be the case for eIF4GII, which preferentially regulates protein synthesis during cytokine-induced differentiation of hematopoietic cells.[7] p97/DAP5 also appears to play a critical role as a translational enhancer in unstressed cells.[8, 9]

In the context of apoptosis, caspase-dependent cleavage of both eIF4G isoforms (I and II) in cells treated with the apoptosis-inducing agents cycloheximide and cisplatin has been observed, along with a concomitant reduction in cap-dependent protein translation.[10,11] p97/DAP5 is also processed during apoptosis to yield an 86 kilodalton fragment (p86).[12] Several reports implicate these caspase-cleaved fragments in the translational regulation of mRNAs harbouring IRES elements; providing evidence for an intriguing model in which cleavage of eIF4G proteins mediates a switch from cap-dependent to cap-independent mechanisms of translation during apoptosis.[13-16]

microRNA at the cap

microRNAs (miRNAs) are small RNAs that have garnered much attention of late due to their seemingly critical role in a variety of cellular processes including apoptosis.[17] miRNAs mediate translation repression by binding to sites in the 3'UTR of an mRNA with partial complementarity. One possible mechanism of this repression has been recently elucidated by Kiriakidou et al., who showed that the miRNA-associated protein argonaute 2 (Ago2)

interacts directly with the 7-methyl-guanosine cap structure of its associated mRNA, competing with eIF4E binding and thus repressing cap-dependent translation (Figure 1.4A).[18] Notably, both cap-dependent and cap-independent (IRES) translation would be predicted to be repressed if such a "miRNA-locked" coil structure exists due to: 1) the inability of ribosomes to efficiently elongate and terminate on such a structure, and/or 2) because of the inability of canonical initiation factors or IRES trans-acting protein factors (ITAFs) to effectively interact with the 5' and 3'UTRs under these circumstances.

Consistent with this supposition, a recent study looked at internal translation in a capped, bicistronic reporter vector with two open reading frames (ORFs) and 3' miRNA binding sites.[19] Hepatitis C virus (HCV) or cricket paralysis virus (CrPV) IRES sequence elements were inserted between the two ORFs such that the upstream ORF is translated through a cap-dependent mechanism, while the downstream ORF is translated via the viral IRES. When cap-dependent translation of the upstream ORF was repressed by introduction of exogenous miRNA, translation of the downstream ORF was also repressed. Importantly however, internal initiation of translation *did* occur, but elongation of the nascent peptide was not efficient resulting in premature termination. Although the authors interpreted this as evidence that miRNAs repress translation at a point downstream of initiation, their results are entirely consistent with the model of the 3'UTR:Ago2:miRNA complex interacting with the 5' cap structure. Similarly, capped, HCV and CrPV IRES reporter vectors with let-7 miRNA binding sites showed a similar repression of both cap-dependent and IRES-dependent translation in transfected HeLa cells.[20]

That said, several groups have reported that IRES-mediated translation is insensitive to miRNA-mediated repression.[18, 21, 22] It is critical to note that all of these studies used an uncapped (or a modified cap that doesn't bind Ago2:miRNA) vector containing the Encephalomyocarditis virus (EMCV) IRES. Therefore, it would be expected that these reporter RNAs cannot form a 3'UTR:Ago2:miRNA locked complex, thus accounting for the lack of miRNA-mediated repression observed. It is thus critical that capped RNA vectors harbouring IRES elements other than EMCV be used to address the question of whether IRES-mediated translation is indeed sensitive to miRNA-induced repression.

Interestingly, cellular stress can relieve miRNA-mediated translational repression.[23] Whether or not argonaute proteins are subject to degradation during apoptosis is unknown. It is intriguing to speculate that the cellular stress response is required to unlock these miRNA:Ago2:cap complexes. The result would be a naked 5' cap in an environment of phosphorylated eIF2 and/or decreased eIF4F availability, thus precluding cap-dependent translation and allowing cap-independent mechanisms to spring into action.

Alternative mechanisms of translation initiation persist during cellular stress

As discussed in the introduction, cellular stress can trigger the apoptotic response and the principle of homeostasis dictates that the cell must respond by either attenuating or amplifying the apoptotic cascade. The end result will be a return to normal cellular homeostasis *or* the ordered destruction of the cell. How then can the cell carry out the decision to live or die if the proteins that mediate a response to the insult cannot be efficiently synthesized under these circumstances?

Under conditions of cellular stress, cap-dependent translation is impaired due to diminished levels of ATP, cap-binding complex, and functional eIF2.[24] Paradoxically, de novo protein synthesis is required for the cell to respond and 1) produce anti-apoptotic proteins to allow possible recovery from an insult or 2) produce pro-apoptotic proteins that will sustain the path to cellular suicide.[25]

The translation of several pro- and anti-apoptotic messages persists during cell stress because they employ alternative translation initiation mechanisms, such as ribosome shunting, re-initiation (bypass or leaky scanning), and internal ribosome entry.[26] Unlike the former two, the latter is mediated by an internal ribosome entry site (IRES), occurs independently of the 5' cap-binding complex, and could be maintained under conditions where cap-dependent initiation is compromised.[27]

IRES-mediated translation initiation was first described in picornaviruses almost 20 years ago.[28] IRES have since been identified in a number of naturally uncapped viral transcripts where they serve to usurp the host translational machinery in favour of viral protein production. In recent years, IRES have also been discovered in a number of cellular mRNAs.

Key players in apoptosis are regulated by IRES-mediated translation

The list of IRES within cellular mRNAs has been steadily growing since the identification of IRES activity within the 5'UTR of the protein chaperone BiP more than 15 years ago.[29] There are now more than 60 identified cellular IRES elements, and Translation State Array

analyses‡ (TSAA) by several research groups indicate that at least 10% of the human transcriptome could harbour IRES elements.[30] Intriguingly, many proteins encoded by IRES-containing mRNAs have pro- or anti-apoptotic functions in the cell (Figure 1.2). A more thorough list of the messages which harbour an IRES element can be found elsewhere.[24,31] Here, we will concentrate on recent advances in the discovery and mechanistic analysis of IRES elements whose function may be critical in apoptosis and oncogenesis.

Controversy – Do cellular IRES exist?

Unlike viral IRES however, the biological significance and even the existence of cellular IRES has been questioned in recent years with the realization that the classical "bicistronic assay" commonly used to test for IRES activity within 5'UTR sequences is prone to artefacts.[32] Published claims of IRES activity within a handful of mRNAs have since proven to be the result of cryptic promoter activity within the putative IRES sequence and/or spurious splicing of the commonly used Renilla/Firefly luciferase bicistronic vector.[30,33] More rigourous controls have been a welcome addition to the field, and they have confirmed that the vast majority of previously identified cellular IRES are indeed real; although some IRES may not be as "potent" as previously thought.[33]

Mechanism – Accessory proteins regulate IRES activity

Recruitment of the ribosome to viral IRES is, with exception, dependent on secondary and tertiary RNA structure.[31, 34] Conversely, mechanisms by which cellular IRES elements

‡ The translational efficiency of the transcriptome between two populations of cells can be determined using TSAA. The technique probes two polyribosome-associated mRNA populations fractionated by density gradient centrifugation with DNA microarrays.

mediate ribosome recruitment are unclear. Indeed, their requirement for any of the canonical eukaryotic initiation factors (eIFs) is unknown. Viral IRES do require some canonical initiation factors. For example, eIF3 interaction with the HCV IRES is required for internal initiation[35]. Also, EMCV IRES activity is enhanced in the presence of eIF4A.[36]

Regarding cellular IRES, it appears that during apoptosis, eIF4G cleavage fragments retain eIF3 and eIF4A binding sites and are necessary for optimal activity of several IRES.[37] This suggests that eIF3 and eIF4A may be necessary for optimum activity of cellular IRES but do not appear to be essential. On the other hand, it is possible that eIFs participate in maintaining both canonical and basal levels of IRES-mediated translation under normal physiological conditions but are dispensable during stress. In addition, the complex translational regulation of eIF4G isoforms suggests that some IRES could be regulated in a manner that is dependent on the interaction of eIF4E with the 5' cap structure – a so-called capped IRES.[38]

Recent studies support the hypothesis that non-canonical translation initiation factors regulate cellular IRES activity (Figure 1.4). These IRES trans-acting factors (ITAFs) are proposed to function as RNA chaperones, allowing for direct binding of the 40S ribosomal subunit through modification of RNA secondary and/or tertiary structure. Alternatively, ITAFs could function in a similar fashion to canonical, cap-dependent initiation factors; namely as adaptor proteins that facilitate RNA-ribosome interaction.

As yet, there appears to be no universal ITAF that modifies the activity of all IRES. However, the latest TSAA study performed in the context of TRAIL-induced apoptosis in MCF-7 cells revealed that pyrimidine-tract binding protein (PTB) positively regulates the

activity of several IRES.[39] Importantly, expression of PTB is increased under these conditions, and IRES activity associated with the binding of PTB appears to be dependent on a $(CCU)_n$ sequence motif.[40] Discovery of additional ITAF binding motifs within cellular IRES may facilitate the prediction of ITAF-IRES interactions. That said, binding of any ITAF to its cognate IRES does not predict function. In fact, ITAFs add an additional level of complexity to IRES-mediated translational control. Emerging evidence indicates that many ITAFs are nucleo-cytoplasmic shuttling proteins. For example, hnRNP A1 was recently found to act as an ITAF by repressing XIAP IRES activity during osmotic shock.[41] Interestingly, this repression is not brought about by a change in hnRNP A1 affinity for the IRES, rather the protein shuttles from the nucleus to the cytoplasm during osmotic shock, effectively increasing the repression of the XIAP IRES via a *localized* increase in ITAF concentration.

Stress, IRES-mediated translation and human disease

X-linked dyskeratosis congenita (X-DC)

The physiological relevance of IRES-mediated translation has recently been confirmed in the genetic context of X-linked dyskeratosis congenita (X-DC), a rare disorder resulting from a defect in the gene (DKC1) encoding a pseudouridine synthetase. Surprisingly, the resulting deregulation of rRNA modification leads to a phenotype in which translation of IRES-containing messages is exclusively impaired. Using a TSAA approach, Yoon and colleagues discovered that while global translation is unaffected in both DKC1 mutant mouse

embryonic cells and X-DC patient cells, cap-independent translation of the anti-apoptotic proteins XIAP and Bcl-xL, and the tumour suppressor protein $p27^{kip1}$ is severely impaired.[42]

Notably, the deregulation of XIAP and Bcl-xL protein translation could explain the increased apoptosis of hemapoietic progenitors and subsequent bone marrow failure that is observed in X-DC patients.[43] Further, while DKC1 mutant ($DKC1^{m}$) and p27 heterozygous mutant ($p27^{+/-}$) mouse thymocytes showed no differences in cellular proliferation, the number of cells in S phase of the cell cycle doubled in $DKC1^{m}$:$p27^{+/-}$ cells. Again, this observation parallels the susceptibility to cancer observed in human X-DC patients. The intriguing possibility that IRES-mediated translation could contribute to oncogenesis sets the stage for the next section that looks at the role of IRES under stress in the hypoxic environment of a tumour.

Hypoxia, endoplasmic reticulum stress and the progression of cancer

Low oxygen tension within the core of solid cancerous tumours can accelerate the progression of the disease to a more malignant phenotype.[44] It is hypothesized that transient and chronic hypoxia triggers the ER stress response that in turn favours IRES-mediated translation initiation.

Specifically, IRES-regulated transcripts such as HIF-1α[45], VEGF[46], and VCIP[47] are preferentially translated under these conditions. HIF-1α is a transcription factor whose downstream targets include genes that promote cell survival. Similarly, VEGF and VCIP are pro-angiogenic factors. Notably, ER stress also induces the IRES-dependent up-regulation of the caspase inhibitor HIAP2 in a cell culture model.[13] It is important to note that, coupled

with the deregulation of pro-apoptotic signalling pathways in cancer (e.g. as a result of p53 mutations), IRES-dependent up-regulation of proteins such as HIF-1α, VEGF, VCIP and others may, at least in part, be responsible for increased tumour invasiveness and metastatic potential.

IRES-mediated translation of p53 family members

p53, a classical harbinger of apoptosis, has recently been added to the list of genes capable of translation by an IRES-dependent mechanism. p53 biology has been intensely studied owing to its central role in the cell as a tumour suppressor. It has been reported to be mutated in 50% of all human cancers and its inactivation is a major contributor to oncogenesis.[48]

p53 is a central regulator of cell cycle progression and therefore its expression and activity must be able to quickly respond to changes in homeostasis. Indeed, p53 protein levels increase rapidly during etoposide-induced DNA damage.[49] Consistent with this rapid response, p53 mRNA levels are largely unaffected under cell stress while p53 protein stability increases[50] and its translation is enhanced.[51] In addition, both the 5' and 3'UTRs have been implicated in post-transcriptional control of p53 in the context of ionizing radiation.[52-54]

The existence of an alternative translation initiation site within the coding region of p53 mRNA adds an additional level of co-translational control of p53 function. This second AUG is located 40 amino acids downstream of the first initiation codon. Translation of this downstream ORF results in an N-terminal p53 isoform described in the literature as p53/47 or ΔNp53.[55, 56] Interestingly, while p53/47 is able to form complexes with full-length p53, it

lacks a transactivation domain and therefore functions in a dominant negative manner, preventing p53-mediated cell cycle arrest.[56] Based on these previous findings, it is perhaps not surprising that IRES activity was recently identified within the 5'UTR of p53 mRNA, and that this activity increases following treatment with etoposide, a DNA damage-inducing agent, in MCF-7 cells (a breast cancer cell line with normal p53 function).[57] Consistent with an IRES-mediated mechanism of translation, induction of p53 protein after etoposide treatment was insensitive to rapamycin, a drug which inhibits cap-dependent translation though inhibition of eIF4E-BP1 phosphorylation and subsequent reduction of eIF4E cap-binding activity.[57] The addition of a proteosome inhibitor resulted in only a 40% reduction in the increase in p53 protein levels following etoposide treatment, suggesting that protein stability cannot be solely responsible for the total increase in protein and that enhanced protein translation must account for the remainder.

Another recent study offers independent verification of IRES activity within the p53 5'UTR. Ray and colleagues also provide evidence for a second IRES within the coding sequence of the full-length p53 message that initiates translation of the N-terminally truncated p53/47 isoform (Figure 1.5).[58] Both groups used a renilla/firefly luciferase bicistronic vector and failed to detect aberrant splicing or cryptic promoter activity within any of the constructs, thus confirming that p53mRNA likely harbours two bona fide IRES elements.

Importantly, Ray and colleagues show that the p53 and p53/47 IRES are differentially regulated during cell cycle progression, with p53 IRES activity increasing at the G2/M checkpoint, and p53/47 IRES activity increasing at the G1/S checkpoint.[58] This implies that

IRES-mediated translation provides for precise control of p53 protein levels during times when cap-dependent translation is impaired (e.g. G2/M transition) by altering the stoichiometry of full-length p53 and p53/47. Further, it would be expected that the G2/M arrest seen following DNA damage would increase IRES-mediated translation of full-length p53, providing the push needed to initiate apoptosis.

Figure 1.5

Translation of p53 mRNA uses alternate initiation codons and is regulated by cap-dependent and IRES-dependent mechanisms. Cap-dependent translation from the 1st AUG yields full-length p53 protein. During G2/M cell cycle transition, or possibly during G2 arrest as a result of DNA damage, cap-dependent translation is impaired and translation of p53 may be regulated by an IRES located within the first 70 nucleotides of the p53 5'UTR. p53 protein itself, in addition to rpL26 and nucleolin, may act as an ITAF, stimulating or repressing IRES-mediated translation of p53. Efficient cap-dependent translation of full-length p53 during the G1/S transition may favour the activation of a second IRES within the p53 coding region that controls translation initiation at the 2nd AUG and production of the N-terminally truncated p53/47 protein. p53/47 can act in a dominant negative manner with full length p53 protein, thus representing a negative feedback loop that suppresses apoptotic signals during cell proliferation. Alternatively, evidence indicates that the p53/47 IRES could control internal translation initiation from both the 1st and 2nd initiation codons.

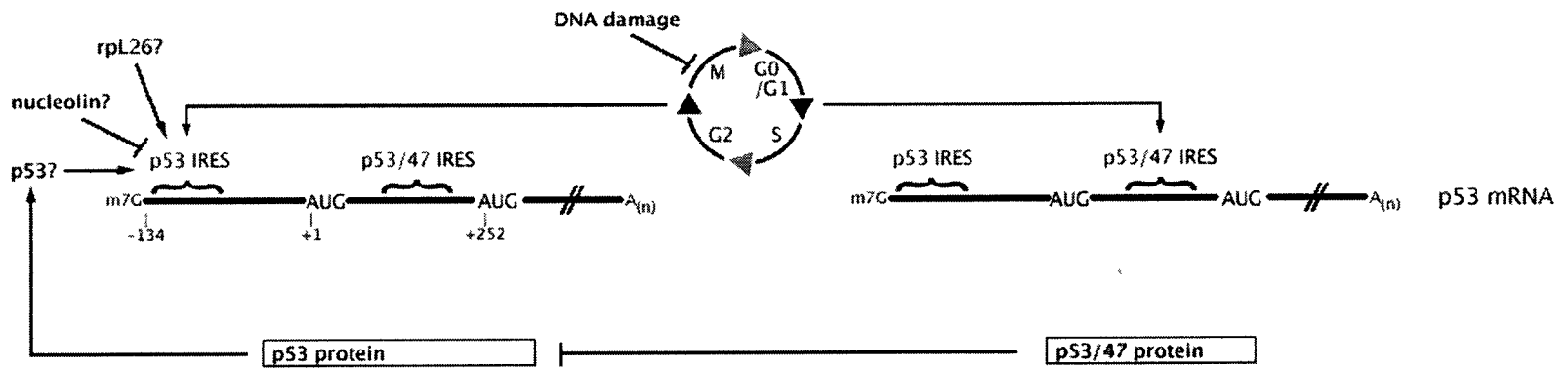
DNA damage
rpL26?
nucleolin?
p53?
M
G0
/G1
G2
S
p53 IRES
p53/47 IRES
m7G
AUG
AUG
A(n)
-134
+1
+252
p53 IRES
p53/47 IRES
m7G
AUG
AUG
A(n)
p53 mRNA
p53 protein
p53/47 protein

The apparent complexity of p53 translational control was revealed in a study which investigated p53 and p53/47 expression in various cancer cell lines (BT474, BT549, MLS-1765) under different apoptotic stress conditions (DNA damage, ER stress and serum starvation).[59] p53/47 protein levels were differentially induced, suggesting that its IRES may be regulated by cell and stress-specific p53/47 ITAFs.

The study also highlights conflicting results that often arise in the IRES field. While Candeias et al. provide ample data to confirm the existence and physiological importance of the p53/47 IRES, the authors conclude that the p53 IRES is not involved in the translational induction of full-length p53 during the response to DNA damage.[59] This conclusion appears to be based on data from HT1299 cells (a p53 null colorectal cell line) transfected with plasmids expressing full-length p53 mRNA without the UTRs. Exposure to the DNA damaging agent doxorubicin or the ER stress inducing drug tunicamycin, caused a modest (1.4 fold) increase in p53 protein levels in the absence of protease inhibitor. The authors interpret this UTR-independent increase in protein levels as evidence that the induction is due to a cap-dependent mechanism. However, it is likely that this increase of full-length p53 is simply due to increased protein half-life as found in previous studies.[50, 57] Indeed, in the same figure it is clear that endogenous p53 protein levels in other cell lines are induced more than 2-fold, suggesting that the UTRs, and likely the IRES participate in this induction following DNA damage or ER stress (c.f. Figure 1A in reference 59).

A more rigorous experiment was presented with p53 overexpressing cells (no UTRs) versus endogenous p53-expressing cells treated with doxorubicin or tunicamycin and labelled with ^{35}S-methionine in the presence of a proteosome inhibitor. Newly synthesised

full-length p53 was immunoprecipitated and an increase in de novo protein synthesis was observed in both the p53 ORF-expressing and endogenous p53-expressing cell lines. The authors interpret these data as evidence that the UTRs are not required for induction of p53 protein following DNA damage or ER stress. Close inspection of the data as presented (albeit without error bars) reveals that endogenous p53 levels are increased at least 25-fold after doxorubicin treatment and 8-fold after tunicamycin treatment (c.f. Figure 2B in reference 59) . This is in contrast to the UTR-independent, overexpressing p53 cell line that showed a respective 6- and 2-fold increase after doxorubicin and tunicamycin treatment (relative to DMSO control). Although there does appear to be a significant increase in protein synthesis in cells expressing p53 RNA lacking UTRs, there is certainly a UTR-dependent increase in translation (at least 4-fold) as well.

Even before the identification of a p53 IRES, previous reports have supported a 5'UTR dependent regulation of p53 translation. Mosner and colleagues showed that the translation of p53 mRNA is negatively regulated via its 5'UTR by p53 protein itself.[52] More recently it has been demonstrated that the ribosomal protein L26 specifically induces p53 in trans.[54] The L26-mediated activity was mapped to a region within the first 70 nucleotides of the p53 5'UTR – the region which we now know contains an IRES. Further, the same study identified nucleolin as a 5'UTR-dependent repressor of p53 translation. Although ITAF function was not formally ascribed to these p53 5'UTR-interacting proteins, it is likely that their modulation of p53 translation is IRES-dependent.

The induction of p53 translation in the absence of its UTRs could be explained if one considers the possibility that the IRES directing the translation of p53/47 (located within the

coding region of the p53 mRNA) could also modulate translation of the upstream initiation codon, namely that of full-length p53 (Figure 1.5). A similar bi-directional IRES has recently been reported downstream of the first translation initiation codon in the HIV-2 genome that regulates no less than three isoforms of Gag protein.[57]

More work needs to be done in order to tease apart the role that these IRES play (if any) in regulating p53-dependent apoptotic pathways and tumourogenesis. Can the loss of IRES-dependent p53 translation increase tumourogenicity? Is IRES-dependent p53 translation affected in tumours with a wildtype p53 genotype? Are other p53 family members (p63, p73) regulated via IRES?

Perspectives and outlook

In the last several years, translational control has emerged as a central player in cell growth, differentiation and apoptosis. During these normal cellular processes, or in many pathophysiological situations, the cell will mount a response to changing environmental conditions. As we have discussed in this review, the stress response is characterized by a reduction in cap-dependent translation of non-essential transcripts. We have reviewed several mechanisms by which this global decrease in translation may occur, however the relative contribution of these specific mechanisms toward translation arrest during apoptosis or within the complex framework of human disease is still not entirely clear.

IRES-dependent translation initiation appears to provide the cell with the ability to synthesize specific proteins that can influence the decision to either recover from the stress or to proceed with apoptosis. The importance of this mechanism of translational control has

been recently demonstrated in the rare congenital disorder X-DC, which draws a direct link between the specific impairment of IRES-mediated translation and the complex, tissue-specific disease phenotype (susceptibility to cancerous growth in thymocytes, but increased apoptosis in hematopoietic cells). The observed tissue-specificity of IRES activity in X-DC and in cell culture models points to a role for ITAFs in regulating the strength of an IRES. The role that IRES-mediated translation may play in tumourogenesis is only just being uncovered. IRES-mediated translation of p53 family members and evidence that tumour-associated hypoxia and/or ER stress can activate anti-apoptotic IRES, suggest that changes in IRES function during tumourogenesis could push the cell towards a more malignant phenotype.

Researchers continue to identify ITAFs and their respective IRES, however future work will most certainly shed light on how they are co-regulated in the context of specific stresses. The advent of systems approaches has allowed the identification of IRES elements on a genomic scale within specific cellular contexts (e.g. TSAA). Genome-level siRNA screens may hold promise for the identification of novel ITAFs and could allow for the classification of common ITAF-IRES relationships. In addition, this approach may also identify the role of canonical eIFs in IRES-dependent translation. Many questions about the basic mechanism of IRES-mediated translation will be answered with these approaches. Does stress-induced modification of ribosomal proteins favour IRES-dependent translation initiation? Are there common sequence and/or structural elements that confer IRES activity or do IRES preferentially behave as individuals? Is there a minimum cohort of ITAFs that is

required for basal IRES activity? Are canonical eIFs involved in IRES translation and, if yes, what is their role?

IRES-mediated translation has been postulated to provide the cell with a high degree of spatial and temporal control that is often needed to mount an appropriate response to upstream stress signals. Recent work reviewed in this article has begun supporting this hypothesis in physiological relevant models of human disease. It is only a matter of time before we are able to exploit this knowledge with the design of novel therapeutics specifically targeting IRES-mediated translation of mRNAs that are involved in the control of apoptosis.

Acknowledgements

We thank the members of our laboratory for helpful discussions. Work performed in the laboratory of M.H. is supported by grants from the Canadian Institutes of Health Research (CIHR), Premier's Research Excellence Award, Canada Foundation for Innovation, and Ontario Research and Development Challenge Fund. T.E.G. is the recipient of a CIHR doctoral award. M.H. is a CIHR New Investigator.

References

1. A. Masud, A. Mohapatra, S. A. Lakhani, A. Ferrandino, R. Hakem and R. A. Flavell, *The Journal of biological chemistry*, 2007, **282**, 14132-14139.

2. T. V. Pestova, J. R. Lorsch and C. U. T. Hellen, in *Translational Control in Biology and Medicine*, ed. N. S. Michael B. Mathews, John W.B. Hershey, Cold Spring Harbor Publishing, Cold Spring Harbor, New York, 2007, pp. 87-128.

3. M. Kozak, *Nucleic Acids Res*, 1981, **9**, 5233-5252.

4. M. Koritzinsky, M. G. Magagnin, T. van den Beucken, R. Seigneuric, K. Savelkouls, J. Dostie, S. Pyronnet, R. J. Kaufman, S. A. Weppler, J. W. Voncken, P. Lambin, C. Koumenis, N. Sonenberg and B. G. Wouters, *The EMBO journal*, 2006, **25**, 1114-1125.

5. M. Bushell and P. Sarnow, *The Journal of cell biology*, 2002, **158**, 395-399.

6. A. R. Tee and C. G. Proud, *Molecular and cellular biology*, 2002, **22**, 1674-1683.

7. S. Caron, M. Charon, E. Cramer, N. Sonenberg and I. Dusanter-Fourt, *Molecular and cellular biology*, 2004, **24**, 4920-4928.

8. S. H. Lee and F. McCormick, *The EMBO journal*, 2006, **25**, 4008-4019.

9. M. Nousch, V. Reed, R. J. Bryson-Richardson, P. D. Currie and T. Preiss, *RNA*, 2007, **13**, 374-384.

10. M. Bushell, D. Poncet, W. E. Marissen, H. Flotow, R. E. Lloyd, M. J. Clemens and S. J. Morley, *Cell Death Differ*, 2000, **7**, 628-636.

11. W. E. Marissen, A. Gradi, N. Sonenberg and R. E. Lloyd, *Cell Death Differ*, 2000, **7**, 1234-1243.

12. S. Henis-Korenblit, N. L. Strumpf, D. Goldstaub and A. Kimchi, *Molecular and cellular biology*, 2000, **20**, 496-506.

13. D. Warnakulasuriyarachchi, S. Cerquozzi, H. H. Cheung and M. Holcik, *The Journal of biological chemistry*, 2004, **279**, 17148-17157.

14. S. Henis-Korenblit, G. Shani, T. Sines, L. Marash, G. Shohat and A. Kimchi, *Proc Natl Acad Sci U S A*, 2002, **99**, 5400-5405.

15. T. A. Nevins, Z. M. Harder, R. G. Korneluk and M. Holcik, *The Journal of biological chemistry*, 2003, **278**, 3572-3579.

16. P. Hundsdoerfer, C. Thoma and M. W. Hentze, *Proceedings of the National Academy of Sciences of the United States of America*, 2005, **102**, 13421-13426.

17. H. W. Hwang and J. T. Mendell, *British journal of cancer*, 2007, **96 Suppl**, R40-44.

18. M. Kiriakidou, G. S. Tan, S. Lamprinaki, M. De Planell-Saguer, P. T. Nelson and Z. Mourelatos, *Cell*, 2007, **129**, 1141-1151.

19. C. P. Petersen, M. E. Bordeleau, J. Pelletier and P. A. Sharp, *Molecular cell*, 2006, **21**, 533-542.

20. J. R. Lytle, T. A. Yario and J. A. Steitz, *Proc Natl Acad Sci U S A*, 2007, **104**, 9667-9672.

21. D. T. Humphreys, B. J. Westman, D. I. Martin and T. Preiss, *Proc Natl Acad Sci U S A*, 2005, **102**, 16961-16966.

22. R. S. Pillai, S. N. Bhattacharyya, C. G. Artus, T. Zoller, N. Cougot, E. Basyuk, E. Bertrand and W. Filipowicz, *Science*, 2005, **309**, 1573-1576.

23. S. N. Bhattacharyya, R. Habermacher, U. Martine, E. I. Closs and W. Filipowicz, *Cell*, 2006, **125**, 1111-1124.

24. M. Holcik and N. Sonenberg, *Nat Rev Mol Cell Biol*, 2005, **6**, 318-327.

25. N. H. Ungureanu, M. Cloutier, S. M. Lewis, N. de Silva, J. D. Blais, J. C. Bell and M. Holcik, *Journal of Biological Chemistry*, 2006, **281**, 15155-15163.

26. C. U. Hellen and P. Sarnow, *Genes & development*, 2001, **15**, 1593-1612.

27. K. A. Spriggs, M. Bushell, S. A. Mitchell and A. E. Willis, *Cell death and differentiation*, 2005, **12**, 585-591.

28. J. Pelletier and N. Sonenberg, *Nature*, 1988, **334**, 320-325.

29. D. G. Macejak and P. Sarnow, *Nature*, 1991, **353**, 90-94.

30. T. E. Graber, S. M. Lewis and M. Holcik, *Current Genomics*, 2006, **7**, 205-215.

31. S. D. Baird, M. Turcotte, R. G. Korneluk and M. Holcik, *RNA*, 2006, **12**, 1755-1785.

32. M. Holcik, T. Graber, S. M. Lewis, C. A. Lefebvre, E. Lacasse and S. Baird, *RNA*, 2005, **11**, 1605-1609.

33. A. G. Bert, R. Grepin, M. A. Vadas and G. J. Goodall, *RNA*, 2006, **12**, 1074-1083.

34. J. S. Pfingsten, D. A. Costantino and J. S. Kieft, *J Mol Biol*, 2007, **370**, 856-869.

35. G. A. Otto and J. D. Puglisi, *Cell*, 2004, **119**, 369-380.

36. I. B. Lomakin, C. U. Hellen and T. V. Pestova, *Molecular and cellular biology*, 2000, **20**, 6019-6029.

37. P. Hundsdoerfer, C. Thoma and M. W. Hentze, *Proc Natl Acad Sci U S A*, 2005, **102**, 13421-13426.

38. M. P. Byrd, M. Zamora and R. E. Lloyd, *The Journal of biological chemistry*, 2005, **280**, 18610-18622.

39. M. Bushell, M. Stoneley, Y. W. Kong, T. L. Hamilton, K. A. Spriggs, H. C. Dobbyn, X. Qin, P. Sarnow and A. E. Willis, *Molecular cell*, 2006, **23**, 401-412.

40. S. A. Mitchell, K. A. Spriggs, M. Bushell, J. R. Evans, M. Stoneley, J. P. Le Quesne, R. V. Spriggs and A. E. Willis, *Genes & development*, 2005, **19**, 1556-1571.

41. S. M. Lewis, A. Veyrier, N. Hosszu Ungureanu, S. Bonnal, S. Vagner and M. Holcik, *Molecular biology of the cell*, 2007, **18**, 1302-1311.

42. A. Yoon, G. Peng, Y. Brandenburg, O. Zollo, W. Xu, E. Rego and D. Ruggero, *Science*, 2006, **312**, 902-906.

43. I. Dokal, *Current opinion in hematology*, 1996, **3**, 453-460.

44. M. Hockel and P. Vaupel, *Journal of the National Cancer Institute*, 2001, **93**, 266-276.

45. K. J. Lang, A. Kappel and G. J. Goodall, *Molecular biology of the cell*, 2002, **13**, 1792-1801.

46. I. Huez, L. Creancier, S. Audigier, M. C. Gensac, A. C. Prats and H. Prats, *Molecular and cellular biology*, 1998, **18**, 6178-6190.

47. J. D. Blais, C. L. Addison, R. Edge, T. Falls, H. Zhao, K. Wary, C. Koumenis, H. P. Harding, D. Ron, M. Holcik and J. C. Bell, *Molecular and cellular biology*, 2006, **26**, 9517-9532.

48. B. Vogelstein, D. Lane and A. J. Levine, *Nature*, 2000, **408**, 307-310.

49. A. J. Giaccia and M. B. Kastan, *Genes & development*, 1998, **12**, 2973-2983.

50. Y. Haupt, R. Maya, A. Kazaz and M. Oren, *Nature*, 1997, **387**, 296-299.

51. M. B. Kastan, O. Onyekwere, D. Sidransky, B. Vogelstein and R. W. Craig, *Cancer research*, 1991, **51**, 6304-6311.

52. J. Mosner, T. Mummenbrauer, C. Bauer, G. Sczakiel, F. Grosse and W. Deppert, *The EMBO journal*, 1995, **14**, 4442-4449.

53. L. Fu and S. Benchimol, *The EMBO journal*, 1997, **16**, 4117-4125.

54. M. Takagi, M. J. Absalon, K. G. McLure and M. B. Kastan, *Cell*, 2005, **123**, 49-63.

55. T. Stiewe, *Nature reviews*, 2007, **7**, 165-168.

56. S. Courtois, G. Verhaegh, S. North, M. G. Luciani, P. Lassus, U. Hibner, M. Oren and P. Hainaut, *Oncogene*, 2002, **21**, 6722-6728.

57. D. Q. Yang, M. J. Halaby and Y. Zhang, *Oncogene*, 2006, **25**, 4613-4619.

58. P. S. Ray, R. Grover and S. Das, *EMBO reports*, 2006, **7**, 404-410.

59. M. M. Candeias, D. J. Powell, E. Roubalova, S. Apcher, K. Bourougaa, B. Vojtesek, H. Bruzzoni-Giovanelli and R. Fahraeus, *Oncogene*, 2006, **25**, 6936-6947.

CHAPTER 2

The eIF4G homolog DAP5/p97 supports the translation of select mRNAs during endoplasmic reticulum stress

Preamble

"The eIF4G homolog DAP5/p97 supports the translation of select mRNAs during endoplasmic reticulum stress" was first published as a research article in the periodical Nucleic Acids Research (volume 36, January 2008). The article identifies p97 as an ITAF targeting translation of its own mRNA. This positive feedback loop provides the cell with increased expression of full-length p97 during ER stress that causes its caspase-mediated cleavage into the p86 fragment. The article also highlights the specific requirement of p86 for cIAP1 IRES activity and provides evidence for the in vivo interaction of cIAP1 mRNA with both p97 and p86.

Author list: Stephen M. Lewis, Sonia Cerquozzi, **Tyson E. Graber**, Nicoleta Hosszu Ungureanu, Meghan Andrews, and Martin Holcik

Author contributions: SML, TEG, MH wrote the article. TEG designed and performed experiments presented in Figures 2.1, 2.3B ("HIAP2" IRES assay). TEG provided technical support and advised on experimental design for experiments presented in Figures 2.2, 2.4A

Abstract

DAP5/p97 is a member of the eIF4G family of translation initiation factors that has been suggested to play an important role in the translation of select messenger RNA molecules. We have shown previously that the caspase-cleaved form of DAP5/p97, termed p86, is required for the induction of the endoplasmic reticulum (ER)-stress responsive internal ribosome entry site (IRES) of the caspase inhibitor HIAP2. We show here that expression of DAP5/p97 is enhanced during ER stress by selective recruitment of DAP5/p97 mRNA into polysomes via the DAP5/p97 IRES. Importantly, enhanced translation mediated by the DAP5/p97 IRES is dependent on DAP5/p97 itself, thus providing a positive feedback loop. In addition, we show that activation of DAP5/p97 and HIAP2 IRES during ER stress requires DAP5/p97. Significantly, the induction of DAP5/p97 during ER stress is caspase-independent whereas the induction of HIAP2 requires proteolytic processing of DAP5/p97. Thus, DAP5/p97 is a translational activator that selectively modulates translation of specific mRNAs during conditions of cellular stress in both a caspase-dependent and caspase-independent manner.

Introduction

Selective translation of messenger RNAs (mRNAs) has emerged as an important mechanism that regulates gene expression, particularly in response to various physiological and pathophysiological conditions that require rapid changes in gene expression profiles. mRNAs that employ selective translation utilize various regulatory elements, most often located within their 5' untranslated regions (UTRs), which allow preferential translation. For

example, the 5'UTR of the transcription factor ATF4 contains two short upstream open reading frames that render translation of the ATF4 reading frame inefficient.[1,2] However, translation of ATF4 is specifically increased under conditions of increased eIF2α phosphorylation, such as during endoplasmic reticulum stress (ER) and the unfolded protein response, although the rate of global protein synthesis is reduced.[3] Another stress-induced mode of translation initiation takes advantage of internal ribosome entry site (IRES) elements located within 5'UTRs, that permit cap-independent translation.[4] IRES were originally discovered in picornaviruses, where they initiate translation of naturally uncapped viral RNAs.[5,6] Interestingly, cellular IRES are found largely in mRNAs that encode proteins with important roles in differentiation, cell growth and proliferation, and the regulation of apoptosis, suggesting that the selective modulation of IRES-mediated translation is critical for the regulation of cell death and survival.[4,7]

The precise molecular mechanism of cellular IRES-mediated translation is not fully understood. Several studies have shown that most, if not all, cellular IRES require various auxilliary proteins termed ITAFs (IRES trans-acting factors) for efficient IRES-mediated translation.[8,9] While the requirement for ITAFs is not the same for all cellular IRES, it is generally believed that these factors may function as RNA chaperones that aid in the remodelling of proper IRES conformation and therefore allow access of the ribosome.[4] Alternatively, ITAFs may also directly recruit the ribosome to an IRES through interaction with ribosomal subunits. The requirement for canonical initiation factors in IRES-mediated translation is even less understood. Several studies have suggested that members of the eIF4G family may be required for cellular IRES-mediated translation, in particular during

conditions of cellular stress and compromised global protein synthesis. It was shown that caspase-cleaved fragments of two family members, eIF4GI and DAP5/p97, can specifically enhance translation mediated by several cellular IRES, including those of Apaf-1, c-myc, HIAP2, XIAP, and DAP5/p97 mRNAs.[10-13] Furthermore, using a HeLa cell-free translation system, the full-length DAP5/p97 was shown to support translation mediated by the c-myc, HIAP2, and XIAP IRES elements in eIF4G-depleted extracts.[14] More recently, DAP5/p97 was suggested to control cell proliferation by regulating the translation of cell cycle proteins such as $p27^{Kip1}$.[15]

In this study we have investigated the role of DAP5/p97 in modulating selective translation of IRES-containing mRNAs during ER stress. We show that DAP5/p97 is necessary for specific activation of at least two cellular IRES elements during pharmacologically induced ER stress. We find that expression of DAP5/p97 and an inhibitor of apoptosis protein HIAP2 are enhanced during ER stress; their mRNAs are selectively recruited to the polysomes via IRES elements located in their respective 5'UTRs. We further find that this process is dependent on DAP5/p97, as reducing the levels of endogenous DAP5/p97 by RNA interference abrogated the IRES-mediated translation of both DAP5/p97 and HIAP2 during ER stress. Moreover, we find that proteolytic cleavage of DAP5/p97 to the DAP5/p86 isoform is not required for the translational induction of DAP5/p97 during ER stress. Thus, a positive feedback loop exists in which ER stress results in elevated levels of DAP5/p97 that, in turn, activate translation of specific mRNAs such as HIAP2 and DAP5/ p97 itself under conditions of reduced cap-dependent translation.

Materials and Methods

Cell culture and reagents. Human embryonic kidney (293T), or human cervical carcinoma (HeLa) cells were maintained in standard conditions in Dulbecco's modified Eagle's medium (DMEM; Wisent Inc.) supplemented with heat inactivated 10% fetal calf serum (FCS), 2 mM L-glutamine and 1% antibiotics (100 U/ml penicillin-streptomycin). Transient transfections were performed using LipofectAMINE 2000 reagent (Invitrogen, Carlsbad, CA) according to the manufacturer's protocol. Briefly, cells were seeded at a density of 6 x 10^5 cells/well in 6-well plates and were transfected 24 h later in serum-free OPTI-MEM medium (Invitrogen, Carlsbad, CA) with 2 μg of DNA per well. siRNA transfections were performed using RNAifect according to the protocol provided by the manufacturer (Qiagen, Chatsworth, CA). Briefly, cells were seeded at a density of 5 × 10^5 cells/well in 6-well plates and were transfected 24 h later in serum-free DMEM with a 20 nM final concentration of DAP5/p97 siRNA or a non-silencing control siRNA (Qiagen, Chatsworth, CA). The target sequences of the DAP5/p97 siRNA oligonucleotides are as follows: #1- aatgtgggtgtagagtctaaa ;#2- aagcactagacgaaggaa ; #3- aaccagagtcagggactctta ; #4- aaggaccgcatgttggagatt. Cells were collected for analysis 24, 48, or 72 h post-transfection. For the ER stress experiments, cells were treated with tunicamycin at indicated doses or DMSO for 24 h and then collected for analysis as described below. Caspase inhibition during ER stress was achieved by pre-incubating cells with 100 μM Z-VAD-FMK (Calbiochem, San Diego, CA) for 6 h, followed by co-incubation with 8.5 μM tunicamycin and 100 μM Z-VAD-FMK for an additional 24 h. The bicistronic vectors pβgal/(-162)/CAT (containing the XIAP IRES and hence referred to

as pβgal/XIAP/CAT in the manuscript), pβgal/p97/CAT (containing the eukaryotic initiation factor DAP5/p97 IRES), and pβgal/HIAP2/CAT (containing the HIAP2 IRES) were described previously.[10,11,15,16] The expression vectors for FLAG-DAP5/p97 and FLAG-p86 were described previously.[11]

Cell viability. 293T cells were transiently transfected in 6-well plates with either DAP5/p97 siRNA or non-targeting (scr) siRNA as described above. For rescue experiments, cells were additionally transfected with expression vectors encoding either GFP or DAP5/p97 cDNAs. 24 h post-transfection the cells were harvested and cell viability was determined using a cell viability analyzer (Vi-Cell; Beckman Coulter, Fullerton, CA) for each treatment. All data are shown as an average ±SD of three independent experiments performed in triplicate. Western blots were performed on parallel samples to determine the levels of DAP5/p97 and GAPDH expression.

β-galactosidase and CAT analysis. Transiently transfected cells were washed twice in 1 ml PBS and harvested in 300 μl CAT ELISA kit lysis buffer according to the protocol provided by the manufacturer (Roche Molecular Biochemicals, Indianapolis, IN). β-galactosidase (β-gal) enzymatic activity was determined by spectrophotometric assay using *o*-nitrophenyl-β-D-Galactopyranoside as previously described.[17] CAT levels were determined using the CAT ELISA kit according to the protocol provided by the manufacturer (Roche Molecular Biochemicals, Indianapolis, IN). The relative IRES activity was determined as a ratio of

CAT/β-Gal. All data are shown as an average ±SD of three independent experiments performed in triplicate.

Western blot analysis. Cells were harvested in ice-cold PBS and cell extracts were prepared in RIPA buffer (1 % Nonidet P-40, 1% sodium deoxycholate, 0.1% SDS, 150 mM NaCl, 10 mM sodium phosphate [pH 7.2], 2 mM EDTA, 0.1 mM phenylmethylsulphonyl fluoride) containing 10 μg /ml each of aprotinin, pepstatin A and leupeptin (all from Sigma). The lysates were then centrifuged at 14,000 x g for 10 min and supernatants were collected. Protein concentration in the supernatants was determined by protein assay kit (Bradford Assay, Bio-Rad, Richmond, CA). Equal amounts of protein samples were separated by 10% SDS-PAGE, transferred to PVDF membrane and analyzed by western blotting. The antibodies used were as follows: mouse monoclonal anti-GAPDH (Advanced ImmunoChemical Inc., Long Beach, CA), mouse monoclonal anti-HIAP2 (R&D), mouse monoclonal anti-GRP78/BiP (Transduction Laboratories, San Jose, CA), rabbit polyclonal anti-cleaved PARP (Cell Signaling Technologies, Danvers, MA). Rabbit polyclonal antibody to DAP5/p97 was raised against the synthetic peptide EFLGKTPGQNAQKWIPAR (amino acids 37-53) and purified (Open Biosystems, Huntsville, AL). All antibodies were used at the manufacturer's suggested dilutions and conditions followed by secondary antibody (horseradish peroxidase-conjugated sheep anti-mouse or anti-rabbit IgG; Amersham Biosciences, Picataway, NJ). Antibody complexes were detected using the ECL Plus and ECL western blotting detection systems (Amersham Biosciences, Picataway, NJ). For the purposes of quantification of protein expression, parallel western blots were performed as

described above but the secondary antibody used was Alexa Fluor 680 goat anti-mouse, anti-rat, or anti-rabbit IgG (LI-Cor Inc, Lincoln, NE). Antibody complexes were then detected and quantified using the Odyssey Infrared Imaging system (LI-Cor Inc, Lincoln, NE). All quantification data are shown as an average ±SD of three independent experiments.

Quantitative RT-PCR. Total RNA was isolated from tunicamycin-treated or control cells that were previously transfected with the pβgal/p97/CAT or pβgal/HIAP2/CAT reporter plasmids using the Absolutely RNA miniprep kit (Stratagene, la Jolla CA) as directed by the manufacturer's instructions. For quantitative RT-PCR, reverse transcription was carried out using the First-Strand cDNA Synthesis kit (Amersham Biosciences, Piscataway, NJ) with oligo $d(T)_{18}$ primers. The quantitative PCR was performed using the QuantiTect SYBR green PCR kit (Qiagen) and analyzed on an ABI Prism 7000 sequence detection system using the ABI Prism 7000 SDS Software. Quantitative PCRs were carried out to detect βgal (5'-ACTATCCCGACCGCCTTACT-3'; 5'-CTGTAGCGGCTGATGTTGAA-3') and CAT (5'-GCGTGTTACGGTGAAAACCT-3'; 5'-GGGCGAAGAAGTTGTCCATA-3') as described previously.[18]

Analysis of polysome-associated mRNAs. Polysomes from treated and untreated cells were collected using sucrose-gradient centrifugation as described previously.[19] RNA was isolated from individual fractions using the Absolutely RNA miniprep kit (Stratagene, la Jolla, CA) according to the manufacturer's instructions. Indicated fractions (polysomes and 40S/60S/80S) were pooled and cDNA was generated for each pool using an oligo $d(T)_{18}$ primer and

the Bulk 1st Strand Syntesis kit according to the protocol provided by the manufacturer (Amersham Biosciences). cDNA was then used as a template for quantitative PCR using the QuantiTect SYBR Green PCR kit (Qiagen) and analyzed on an ABI Prism 7000 detection system as described above. Quantitative PCR reaction were carried out to detect BiP (forward: TGC AGC AGG ACA TCA AGT TC; reverse: AGT TCC AGC GTC TTT GGT TG), DAP5/p97 (forward: CTC TTA TCC CAG CTG CAA GG; reverse: CCC AGA GGT GGT GTT TGA GT), NF90 (forward: CCG TGA TGT TCC CTG TTT CT; reverse: CGT GTG TTG GCA CAA ACT TC), HIAP2 (forward: TGG CCT TTC ATT CGT ATC AAG A; reverse: TCT GGA GAT GAT CCA TGG GTA GA), Actin (forward: CTG GAA CGG TGA AGG TGA CA; reverse: AAG GGA CTT CCT GTA ACA ATG CA), and ATF4 (forward: CCT ACG TTG CCA TGA TCC CT. reverse: CTT CTG GCG GTA CCT AGT GG).

Analysis of global protein synthesis. HEK293T cells were seeded at 2.5 x 10^5 cells per well in a 6-well plate. Twenty-four hours later, cells were transfected with 0.5 μg/well siRNA (scrambled control or DAP5/p97 siRNA) as described above. Twenty-four hours post-transfection the media was replaced with methionine/cysteine-free minimal essential medium (Invitrogen) in which L-cysteine was added to a final concentration of 63mg/L and the cells were incubated at 37°C for 15 minutes. Cells were metabolically labelled by incubating at 37°C for 20 minutes in labelling media supplemented with 100 μCi/ml [^{35}S]-Methionine (GE Healthsciences). Cells were then washed in ice-cold PBS and harvested for 20 min at 4°C in RIPA buffer containing 10 μg /ml each of aprotinin, pepstatin A and leupeptin. The lysates were then centrifuged at 14,000xg for 10 min and supernatants were collected. Protein

concentration in the supernatant was determined by protein assay kit (Bradford Assay, Bio-Rad), and equal amounts of protein samples (20 μg) were separated by 10% SDS-PAGE. The total proteins were visualized by Coomasie brilliant blue (R-250) staining and the ^{35}S incorporation was visualized by autoradiography.

Co-precipitation of mRNA:protein complexes. The co-precipitation of mRNA:protein complexes was performed essentially as described.[20] Briefly, HEK293T cells were transfected with pCI, FLAG-DAP5/p97, or FLAG-DAP5/p86, and cytoplasmic lysates were harvested 24 h later by incubating 5×10^6 cells on ice for 5 minutes in 750 μl of cytoplasmic lysis buffer (20 mM Tris-Cl [pH 7.4], 100 mM KCl, 5 mM $MgCl_2$, 0.3% IGEPAL CA-630, RNasin [Promega], 1 mM PMSF, and protease inhibitors), then clarified by centrifugation at 10,000 × g for 10 minutes. 375 μl of cytoplasmic extract was incubated with 50 μl of a 50 % (v/v) suspension of anti-FLAG-coated agarose beads (Sigma) for 1 h at 4°C, and then the beads were then washed 5 times in NT2 buffer (50 mM Tris-Cl [pH 7.4], 150 mM NaCl, 1 mM $MgCl_2$, and 0.05% NP-40). Contaminating DNA was removed from the sample by incubating the beads in 100 μl of NT2 buffer supplemented with 2 μl DNase I (Invitrogen) for 40 minutes at 30°C. The beads were washed twice in NT2 buffer, and bound proteins were digested by incubating the beads in 100 μl NT2 buffer containing 0.1% SDS and supplemented with 0.5 mg/ml Proteinase K for 10 minutes at 55°C. RNA was then extracted using phenol:chloroform and precipitated in the presence of Glycoblue (Ambion, Austin, TX). Precipitated mRNA was detected by RT-PCR and visualized on a 1.5% agarose gel by ethidium bromide staining.

Results

Endoplasmic reticulum stress enhances translation of DAP5/p97

Induction of ER stress by various triggers results in enhanced translation of the inhibitor of apoptosis (IAP) protein HIAP2 in various cell types.[11,21] In addition, induction of ER stress leads to caspase-dependent cleavage of the DAP5/p97 protein, a member of the eIF4G family of initiation factors, to generate a p86 isoform that specifically enhances translation of HIAP2 via an IRES element located within the 5'UTR of HIAP2 mRNA.[11] While investigating the role of DAP5/p97 in ER stress, we have noticed that the levels of DAP5/ p97 are also elevated following induction of ER stress by tunicamycin (an inhibitor of protein glycosylation) or thapsigargin (an inhibitor of ER calcium pump) (Figure 2.1 and data not shown). The induction of DAP5/p97 expression by tunicamycin was dose-dependent and paralleled the expression pattern of known ER stress-inducible genes GRP78/Bip and HIAP2 (Figure 1A). Examination of DAP5/p97 and HIAP2 mRNA levels from treated and untreated samples by quantitative RT-PCR revealed that the levels of mRNA did not change following drug treatment (Figure 2C and Warnakulasuriyarachchi et al[11]). These data indicate that the observed changes in DAP5/p97 protein levels are likely due to translational up-regulation.

To confirm that DAP5/p97 translation is indeed enhanced during ER stress, we examined the association of DAP5/p97 mRNA with polysomes in DMSO and tunicamycin-treated cells. Enhancement of DAP5/p97 expression at the translational level should result in

Figure 2.1

ER stress causes induction of eukaryotic initiation factor DAP5/p97 expression. **(A)** Western blot analysis of endogenous DAP5/p97 and HIAP2 proteins in 293T cell lysates treated with DMSO (Ctrl) or indicated doses of tunicamycin (Tm). The induction of ER stress that was confirmed by western blot analysis for the ER chaperone BiP, and the membrane was probed with anti-GAPDH as a loading control. **(B)** The densitometric analysis of DAP5/p97 and HIAP2 protein expression (relative to GAPDH) from three independent experiments (average ±SD).

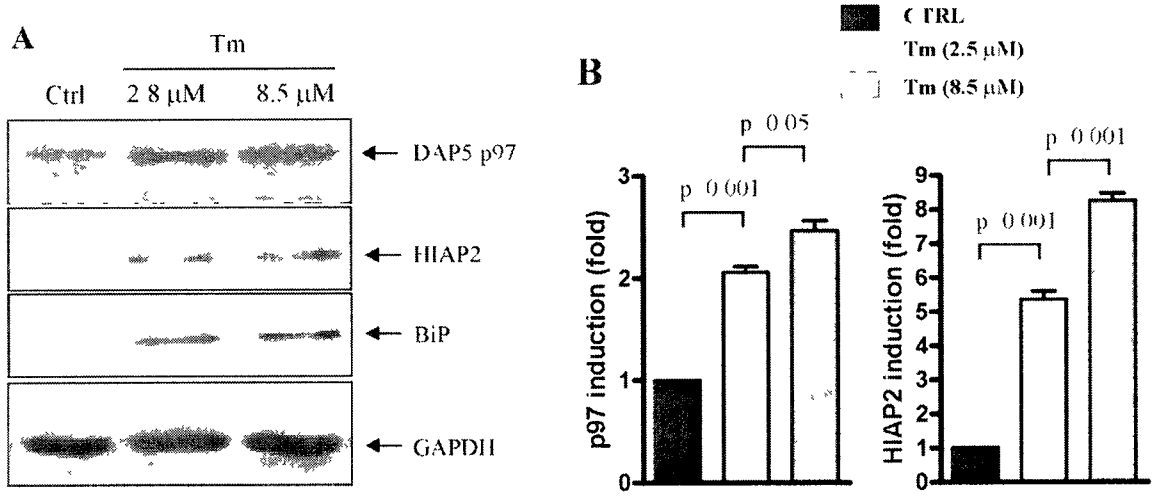
A
Tm
Ctrl
2 8 μM
8.5 μM
DAP5 p97
HIAP2
BiP
GAPDH
B
CTRL
Tm (2.5 μM)
Tm (8.5 μM)
p 0 05
p 0 001
p 0 001
p 0 001
p97 induction (fold)
HIAP2 induction (fold)
0
1
2
3
0
1
2
3
4
5
6
7
8
9

Figure 2.2

DAP5/p97 and HIAP2 mRNAs remain associated with polysomes during ER stress. (A) Polysome profiles from tunicamycin (Tm; 8.5 μM) or DMSO-treated cells were generated as described in Materials and Methods. **(B)** The polysomal distribution of actin and BiP mRNAs (shown as percentage of total RNA) was used to confirm the induction of ER stress and validate the qRT-PCR approach. Mean ±SEM of two independent experiments performed in triplicates is shown. The images of agarose gels on the right are representative of results from RT-PCR reactions that were run in parallel. **(C)** The levels of DAP5/p97 and HIAP2 mRNAs that remain associated with polysomes in Tm-treated cells (relative to actin) were determined as in **(B)**. The polysomal association of ATF4, which is known to be translated during ER stress, was used as positive control; NF90, which is not known to be translated during ER stress, was used as negative control. Average ±SD of two independent experiments performed in triplicate. DMSO treated samples were set as 100.

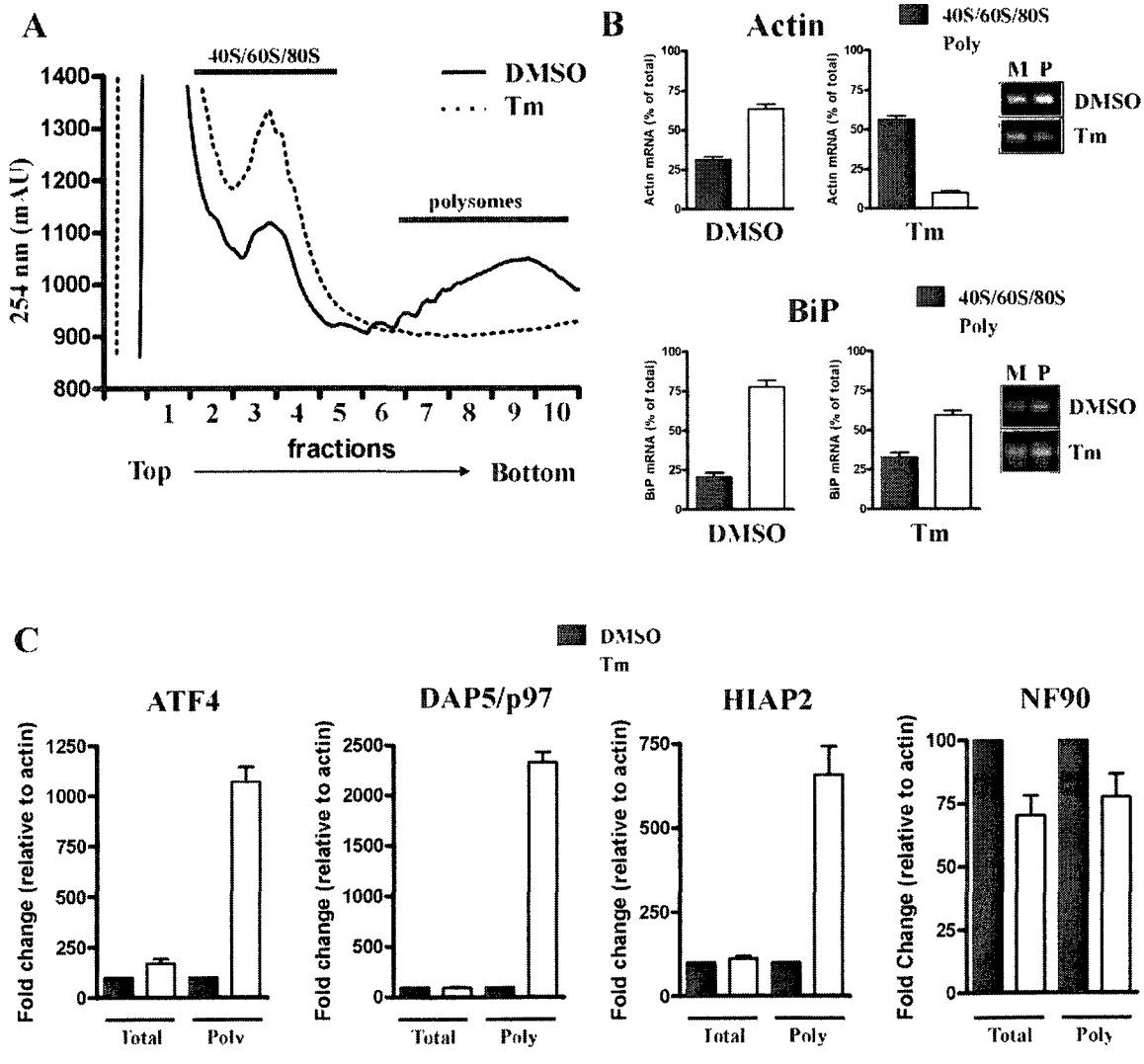
A
40S/60S/80S
DMSO
Tm
polysomes
254 nm (mAU)
1400
1300
1200
1100
1000
900
800
1 2 3 4 5 6 7 8 9 10
fractions
Top
Bottom
B
Actin
40S/60S/80S
Poly
Actin mRNA (% of total)
DMSO
Tm
M P
BiP
BiP mRNA (% of total)
C
DMSO
Tm
ATF4
DAP5/p97
HIAP2
NF90
Fold change (relative to actin)
Fold Change (relative to actin)
Total
Poly

recruitment of DAP5/p97 mRNA into the polysomal fraction. Polysomal mRNA was isolated from total cellular mRNA by sucrose gradient centrifugation. The typical optical density profile of the sucrose gradient recorded at 254 nm is shown in Figure 2.2A. The top fractions (fractions 2–5) represent free mRNAs and ribosomal complexes (40S, 60S and 80S) and were pooled together for future mRNA analysis. Conversely, the bottom fractions (fraction 6–10) represent mRNA molecules associated with polysomes. We observed that treatment of cells with tunicamycin resulted in a significant inhibition of proteins synthesis as demonstrated by a considerable decrease in the polysome peak and concomitant accumulation of free mRNAs and an increase in the monosome peak (Figure 2.2A). We performed control experiments to verify that tunicamycin-induced ER stress results in an inhibition of general protein synthesis (as evidenced by the distribution of actin mRNA) while supporting selective translation of ER stress-inducible genes (as evidenced by the distribution of BiP mRNA).[22] Indeed, examination of the distribution of actin mRNA showed that 70% of total actin mRNA is associated with polysomes in DMSO-treated cells, whereas only 10% of total actin mRNA remains in polysomes during tunicamycin-induced ER stress (Figure 2.2B). In contrast, the mRNA of BiP, a known ER stress-inducible gene, remains associated with polysomes in tunicamycin-treated cells (Figure 2.2B).

Next, we analyzed the polysomal association of DAP5/p97 mRNA in DMSO and tunicamycin-treated cells. We observed that there was a significant increase in the amount of DAP5/p97 mRNA associated with polysomes in tunicamycin-treated cells (relative to actin mRNA) (Figure 2.2C). We did not observed any increase in the amount of total DAP5/p97 mRNA, indicating that enhanced transcription does not contribute to the observed increase in

polysome-associated DAP5/p97 mRNA. As a control, we analyzed the expression of ATF4, which is known to increase in response to ER stress by both increased transcription and translation.[23] As expected, we observed an increase in total ATF4 mRNA as well as polysomal-associated ATF4 mRNA (Figure 2.2C). Similar to DAP5/p97 mRNA, HIAP2 mRNA was also found to be mobilized into polysomes in ER-stressed cells without a concomitant increase in total HIAP2 mRNA levels (Figure 2.2C). In contrast, mRNA levels of NF90 [24], a transcription factor that is not known to be induced during ER stress and was chosen randomly as a control, decreased in both total and polysome fractions.

These observations are consistent with the notion that pharmacologically induced ER stress results in a significant increase in the translation of DAP5/p97 and HIAP2 due to the selective recruitment of their mRNAs into polysomes.

Translational induction of DAP5/p97 during ER stress is mediated by its IRES

The data described above confirm that the translation of DAP5/p97 and HIAP2 is selectively enhanced during ER stress. We have previously established the regulatory mechanism for the translational control of HIAP2 in response to ER stress.[11] The 5'UTR of HIAP2 encodes a short upstream open reading frame (uORF) that mediates repression of HIAP2 expression.[25] Adjacent and overlapping with the uORF is an inducible IRES element that allows for selective translational induction of HIAP2 during pharmacologically induced ER stress [11] and also in cells treated with etoposide or sodium arsenite.[26] The key step in the translational up-regulation of HIAP2 during ER stress is caspase-dependent cleavage of DAP5/p97, which generates the p86 fragment that specifically enhances IRES-mediated translation of HIAP2 .

[11] In addition, DAP5/p86 was shown to be involved in translation of other IRES elements such as those found in the Apaf-1 and DAP5/p97 mRNAs.[10,12] We therefore wished to examine if translational induction of DAP5/p97 during ER stress is mediated by its IRES element. To assess DAP5/p97 IRES activity, we used the previously described bicistronic reporter plasmids containing the IRES elements ofDAP5/p97, HIAP2 (positive control) and XIAP (negative control).[10,11,16] HEK293T cells were transiently transfected with bicistronic reporter constructs and the IRES activity was determined in control (DMSO treated) or tunicamycin-treated cells 24 h later. We observed dose-dependent induction of DAP5/p97 and HIAP2 IRES activity by tunicamycin treatment (Figure 2.3B). In contrast, the activity of the XIAP IRES remained unchanged in tunicamycin-treated cells, as reported previously.[11] To eliminate the possibility that the observed IRES activity in tunicamycin-treated cells is due to the presence of cryptic promoters or spurious splicing events, we assessed the levels and integrity of the reporter mRNA by quantitative RT-PCR analysis as described.[18] Total RNA was isolated from cells treated with either DMSO or tunicamycin that were previously transfected with the bicistronic plasmids. cDNA was produced by reverse transcription and was used as a template for quantitative PCR analysis using primers that amplify a portion of the β-Gal coding region and a portion of the CAT coding region. As shown in Figure 2.3C, the ratio of the CAT and β-Gal cistrons remained unchanged in cells treated with tunicamycin as compared to cells treated with DMSO. These data confirm that the integrity of the bicistronic RNA transcript produced from the reporter plasmids is not affected by tunicamycin. We therefore conclude that translational induction of p97 during tunicamycin-induced ER stress is mediated by the IRES elements in their respective mRNAs.

Figure 2.3

The activity of the DAP5/p97 IRES element is enhanced during ER stress. (**A**) Schematic diagram depicting the bicistronic reporter constructs harbouring the IRES elements of DAP5/p97, HIAP2, and XIAP used in this study. (**B**) HEK293T cells were transiently transfected with the indicated bicistronic constructs and the effect of tunicamycin (Tm) treatment or DMSO treatment on IRES-mediated translation was determined by measuring the β−Gal and CAT levels as described in Materials and Methods. Relative IRES activity (CAT/β−Gal) was determined for three independent experiments performed in triplicate. Average ±SD. The activity of each construct in DMSO-treated cells was set as 1. (**C**) Quantitative RT-PCR analysis of β−Gal and CAT cistron RNA was used to test for cryptic promoter activity and spurious splicing of the DAP5/p97 IRES and HIAP2 IRES-containing bicistronic RNAs. Values are expressed as CAT relative to β−Gal ($2^{-[Ct(CAT) - Ct(\beta Gal)]}$). Average ±SD of three independent experiments performed in triplicate.

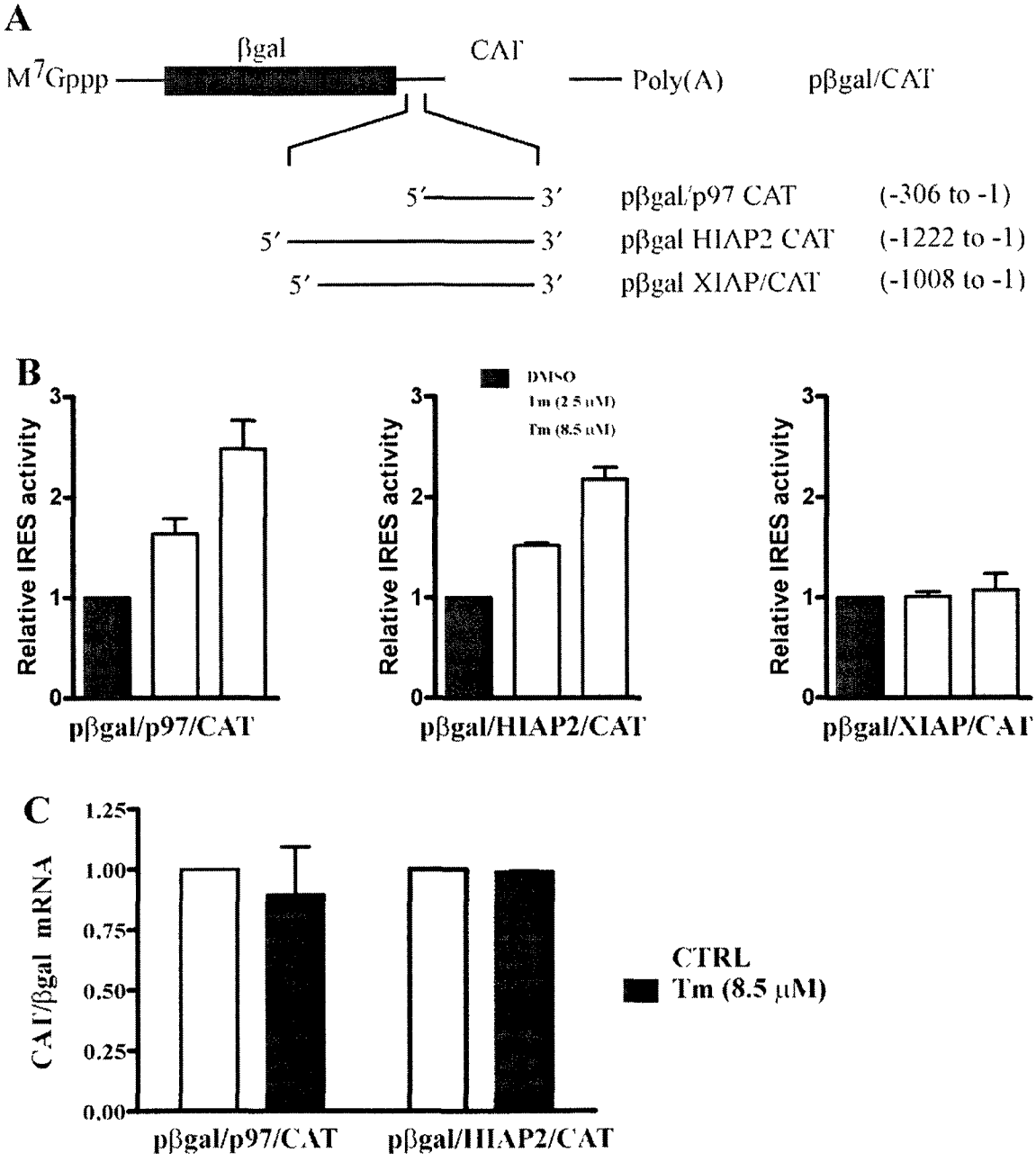
A
βgal
CAT
M7Gppp
Poly(A)
pβgal/CAT
5′ 3′
pβgal/p97 CAT
(-306 to -1)
5′ 3′
pβgal HIAP2 CAT
(-1222 to -1)
5′ 3′
pβgal XIAP/CAT
(-1008 to -1)
B
DMSO
Tm (2.5 μM)
Tm (8.5 μM)
Relative IRES activity
0
1
2
3
pβgal/p97/CAT
pβgal/HIAP2/CAT
pβgal/XIAP/CAT
C
CAT/βgal mRNA
0.00
0.25
0.50
0.75
1.00
1.25
pβgal/p97/CAT
pβgal/HIAP2/CAT
CTRL
Tm (8.5 μM)

IRES-mediated translation of DAP5/p97 and HIAP2 is dependent on DAP5/p97

We have shown that the enhanced translation of DAP5/p97 and HIAP2 during tunicamycin-induced ER stress (as evidenced by the selective recruitment of DAP5/p97 and HIAP2 mRNAs to polysomes) is mediated by their respective IRES elements. DAP5/p97 is a translation initiation factor belonging to the eIF4G family that has been shown previously to stimulate the translation of several IRES elements.[10–12,14] We therefore wished to examine the activity of the DAP5/p97 IRES and HIAP2 IRES in cells depleted of DAP5/p97 to determine if the activities of the DAP5/p97 IRES and HIAP2 IRES are dependent on the presence of DAP5/p97 in tunicamycin-treated cells. Cells were transfected with DAP5/p97 siRNA or non-silencing control siRNAs and the extent of DAP5/p97 knockdown was determined in DMSO and tunicamycin-treated cells. We observed that all four DAP5/p97 siRNAs, individually or in combination, significantly reduced expression of DAP5/p97 (Figure 2.4A and data not shown).

First, we investigated the effect of DAP5/97 downregulation on global protein synthesis by metabolic labelling and by examining polysome profiles from DAP5/p97 siRNA and control siRNA-treated cells. We found that reduced expression of DAP5/p97 had no significant effect on global protein synthesis (Figure 2.4A). In contrast, the activities of the DAP5/p97 IRES and HIAP2 IRES were severely impaired in control as well as tunicamycin

Figure 2.4

DAP5/p97 knockdown impairs IRES translation and reduces cell viability. (A) HEK293T cells were transiently transfected with the indicated siRNA molecules and the levels of DAP5/p97 protein were determined by western blot analysis 24 h later. Polysome profiles were generated from control (scr) or DAP5/p97 siRNA-transfected cells as described in Materials and Methods section. Metabolic labelling of control and DAP5/p97 siRNA-transfected cells was performed using ^{35}S-Met as described in Materials and Methods section and is shown on the right. **(B)** IRES activity of the DAP5/p97 and HIAP2 5'UTRs was determined in control or DAP5/p97 siRNA-transfected cells treated with DMSO or 8.5 μM Tm using the bicistronic reporter plasmids described in Figure 2.3A. Average ±SD of three independent experiments performed in triplicate. Samples from DMSO-treated cells transfected with scrambled siRNA were set as 1. The levels of BiP, HIAP2, and GAPDH proteins were determined by western blot analysis and are shown on the right. **(C)** Cell viability of control (scr) or DAP5/p97 siRNA-transfected cells was determined 24 h post-transfection by counting viable cells using the Vi-Cell cell viability analyzer (Beckman Coulter). Average ±SD of three independent experiments performed in triplicate. For rescue experiments, the indicated plasmids were transfected into the cells at the time of siRNA transfection. The extent of DAP5/97 expression and/or knockdown was assessed by western blot analysis of parallel samples.

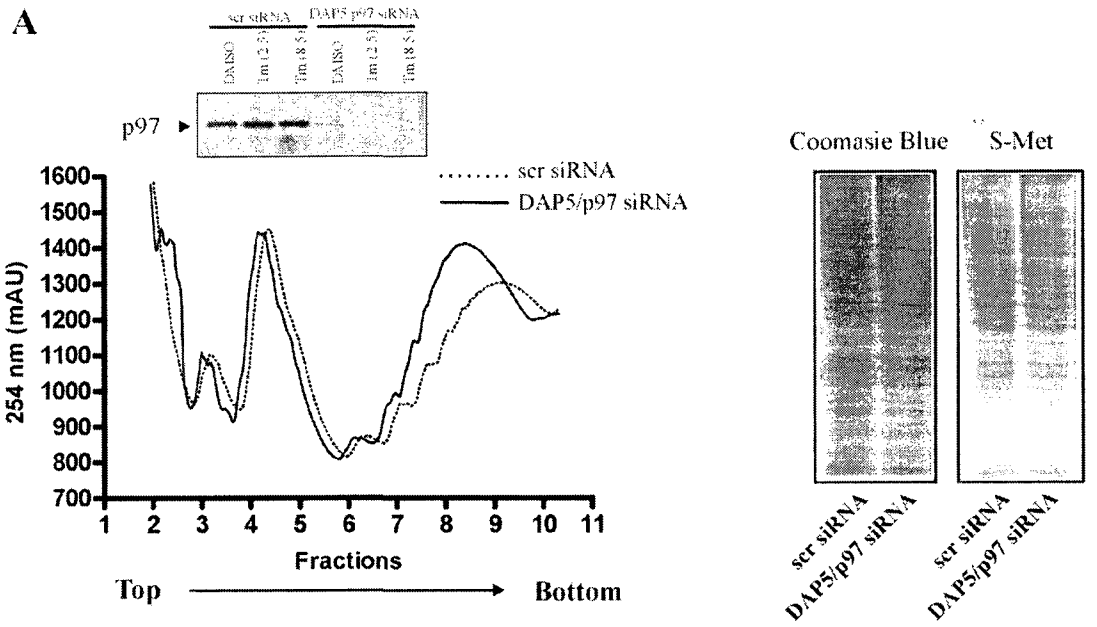
A
scr siRNA
DAP5/p97 siRNA
DMSO
Tm (2.5)
Tm (8.5)
p97
scr siRNA
DAP5/p97 siRNA
254 nm (mAU)
Fractions
Top
Bottom
Coomasie Blue
S-Met
scr siRNA
DAP5/p97 siRNA

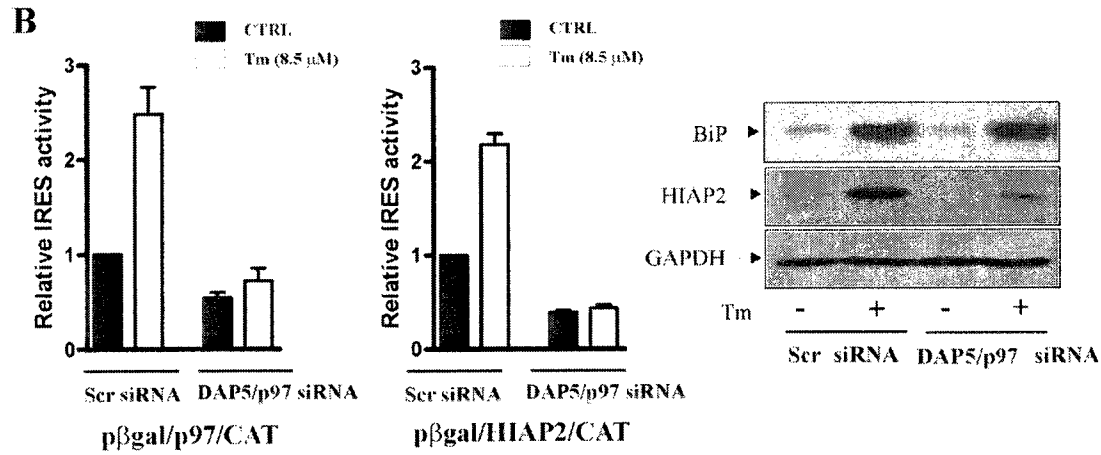
B
CTRL
Tm (8.5 μM)
Relative IRES activity
Scr siRNA
DAP5/p97 siRNA
pβgal/p97/CAT
pβgal/HIAP2/CAT
BiP
HIAP2
GAPDH
Tm
Scr siRNA
DAP5/p97 siRNA

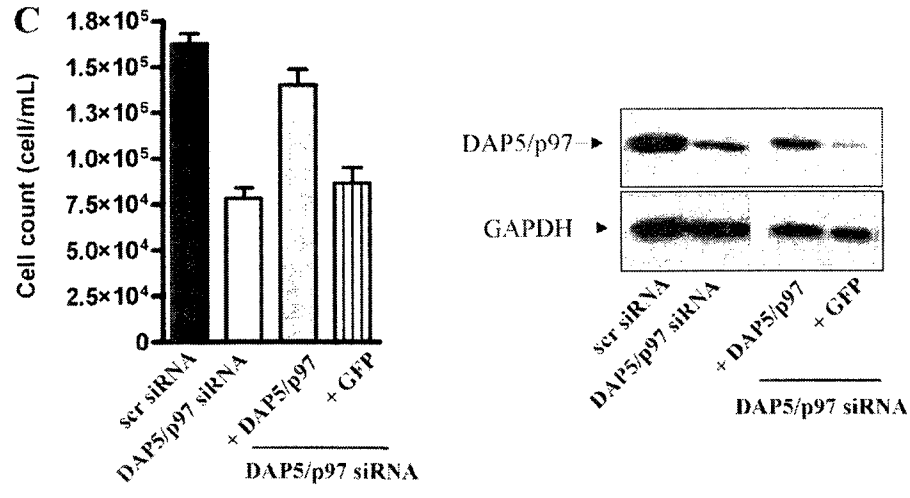
C
Cell count (cell/mL)
scr siRNA
DAP5/p97 siRNA
+ DAP5/p97
+ GFP
DAP5/p97 siRNA
DAP5/p97
GAPDH
scr siRNA
DAP5/p97 siRNA
+ DAP5/p97
+ GFP
DAP5/p97 siRNA

treated cells transfected with p97 siRNA (Figure 2.4B). Furthermore, transfection of cells with DAP5/ p97 siRNA, but not the control non-silencing siRNA, significantly reduced the levels of endogenous HIAP2 protein in response to ER stress (Figure 2.4B). Therefore, DAP5/p97 is necessary for IRES-mediated translational induction of HIAP2 and p97 in response to ER stress.

We have shown previously that DAP5/p97-mediated induction of HIAP2 expression increases the resistance of cells to ER stress.[11] We therefore wished to determine if downregulation of DAP5/p97 levels sensitizes cells to tunicamycin treatment. Surprisingly, we noted that transfection of cells with DAP5/p97 siRNA resulted in a significant loss of cell viability (Figure 2.4C), precluding us from assessing the tunicamycin sensitivity of the cells. The loss of viability was specific to DAP5/p97 downregulation, as non-silencing siRNA did not affect cell survival. Furthermore, we were able to rescue cell viability of DAP5/p97 siRNA-transfected cells by elevating the levels of DAP5/p97 using an overexpression plasmid (Figure 2.4C). Taken together, our data suggest that loss of p97 is not compatible with cell survival, likely by impinging on the translation of specific cellular mRNAs.

Translational induction of DAP5/p97 during ER stress is caspase-independent

Caspase cleavage of DAP5/p97 to the p86 isoform has been shown to be important for the activation of several IRES elements.[10–12] Moreover, the DAP5/p86 isoform potently induces HIAP2 IRES activity, and caspase activity is required for the induction of HIAP2 IRES activity during ER stress.[11] A recent report has shown that DAP5/p97 can affect IRES activity independent of caspase cleavage, suggesting that DAP5/p97 may be able to affect

IRES activity independently of proteolytic cleavage to the DAP5/p86 isoform.[27] As we have found that DAP5/p97 is absolutely required for the induction of DAP5/p97 IRES activity during ER stress, we therefore wished to determine if caspase activity is required for the translational induction of DAP5/p97 during ER stress. Cells were pre-treated with the pan-caspase inhibitor Z-VAD-FMK or DMSO for 6 h and then incubated with 8.5 μM tunicamycin in the presence or absence of 100 μM Z-VAD-FMK for an additional 24 h. Protein extracts were harvested and the levels of BiP, p97, GAPDH and cleaved PARP were assayed by western blot analysis. Surprisingly, we found that translational induction of DAP5/p97 during ER stress occurs in both the presence and absence of caspase activity (Figure 2.5A, lanes 2 and 4). These results indicate that translational induction of DAP5/p97 during ER stress occurs in a caspase-independent manner.

To further confirm the function of full-length DAP5/p97 in DAP5/p97 IRES activation, we cotransfected HEK293T cells with a DAP5/p97-overexpressing plasmid and either the DAP5/p97 IRES or the HIAP2 IRES-containing bicistronic reporter plasmids. We found that while overexpression of DAP5/p97 had no effect on the activity of the HIAP2 IRES (Figure 2.5B and Warnakulasuriyarachchi et al[11]) it resulted in significantly enhanced activity of the DAP5/p97 IRES (Figure 2.5B). Thus, full-length DAP5/p97 is sufficient to drive the translation mediated by its own IRES element.

We next sought to determine how full-length DAP5/p97 is able to modulate the activity of the DAP5/p97 IRES but not the HIAP2 IRES. We hypothesized that full-length DAP5/p97 may be able to bind to DAP5/p97 IRES-containing mRNA but not to HIAP2 IRES-containing mRNA, whereas DAP5/p86 may bind to both p97 and HIAP2 mRNAs.

Figure 2.5

Translational induction of DAP5/p97 during ER stress is caspase independent. (**A**) HEK293T cells were pre-treated with 100 μM Z-VAD-FMK or DMSO for 6 h and were then incubated with 8.5 μM tunicamycin or DMSO in the presence or absence of 100 μM Z-VAD-FMK for an additional 24 h. Protein extracts were harvested, separated by 10% SDS-PAGE, transferred to PVDF membrane, and the levels of BiP, p97, GAPDH, and cleaved PARP were determined by western blot analysis. (**B**) IRES activity of the DAP5/p97 and HIAP2 5'UTRs was determined in DAP5/p97-overexpressing or control plasmid transfected cells using the bicistronic reporter plasmids described in Figure 2.3A. Average ±SD of three independent experiments performed in triplicate. Samples from the control plasmid transfected cells were set as 1. (**C**) Both DAP5/p97 and HIAP2 mRNA associate with full-length DAP5/p97. HEK293T cells were transfected with pCI, FLAG-DAP5/p97, or FLAG-DAP5/p86, and mRNA:protein complexes were co-precipitated using anti-FLAG coated agarose beads as described in Materials and Methods section. cDNA was produced from precipitated mRNA by reverse transcription (RT) using an oligo $d(T)_{18}$ primer, which was subsequently amplified by PCR using gene-specific oligonucleotide primers for DAP5/p97, HIAP2, and GAPDH. The resulting products were separated on a 1.5% agarose gel and visualized by ethidium bromide staining.

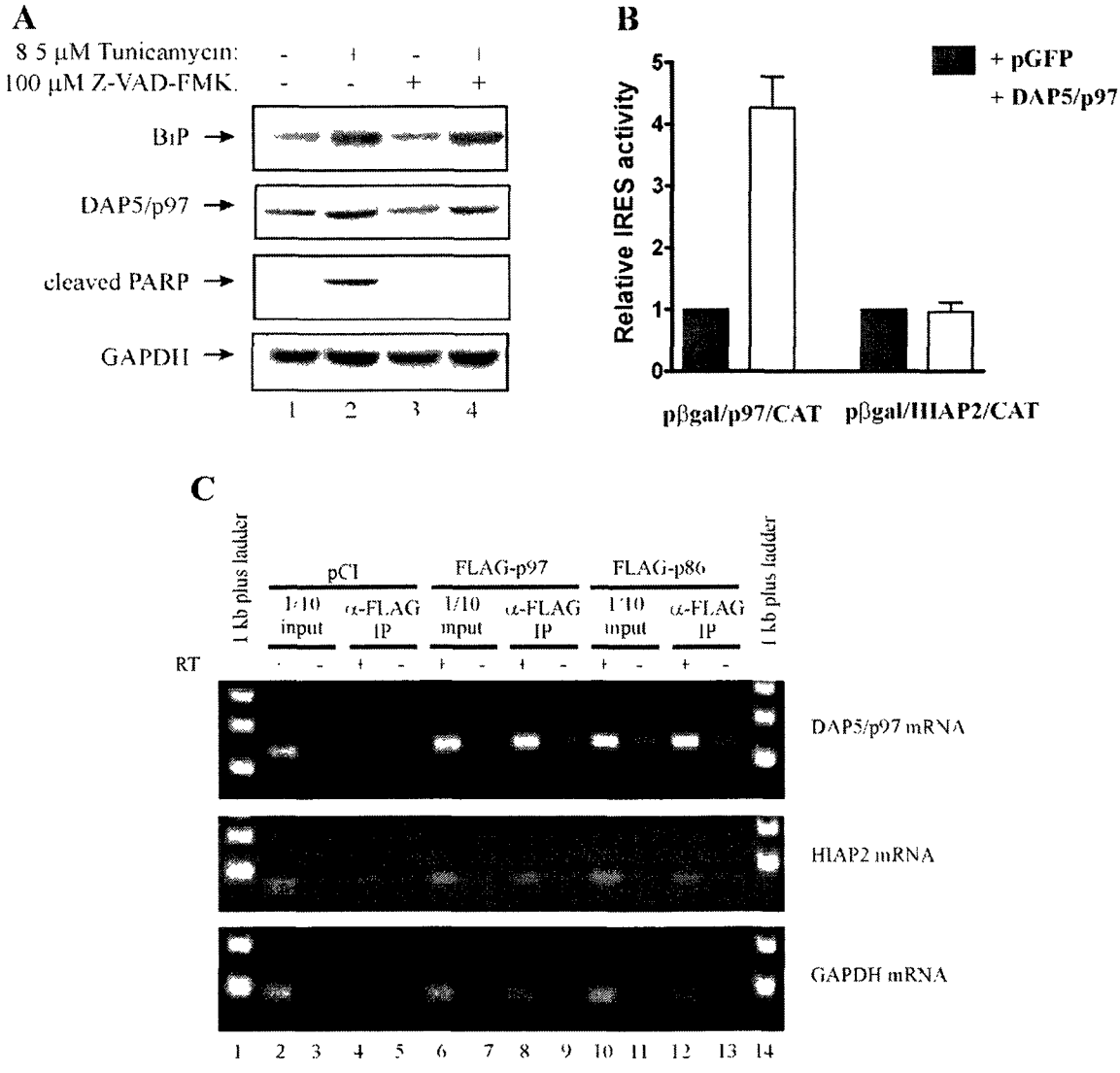
A
8.5 μM Tunicamycin: - + - +
100 μM Z-VAD-FMK: - - + +
BiP
DAP5/p97
cleaved PARP
GAPDH
1 2 3 4
B
+ pGFP
+ DAP5/p97
Relative IRES activity
0 1 2 3 4 5
pβgal/p97/CAT
pβgal/HIAP2/CAT
C
1 kb plus ladder
pCI
FLAG-p97
FLAG-p86
1/10 input
α-FLAG IP
RT
DAP5/p97 mRNA
HIAP2 mRNA
GAPDH mRNA
1 2 3 4 5 6 7 8 9 10 11 12 13 14

To test this hypothesis, we co-precipitated mRNAs associated with either full-length DAP5/p97 or the DAP5/p86 caspase-cleavage product of p97. HEK293T cells were transfected with plasmids expressing FLAG-DAP5/p97, FLAG-DAP5/p86 or the empty pCI vector. Cytoplasmic extracts were harvested 24 h later, mRNA:protein complexes were co-precipitated using anti-FLAG-coated agarose beads and the co-precipitated mRNA was isolated by phenol:chloroform extraction and amplified by RT-PCR. As expected we were able to co-precipitate both DAP5/p97 and HIAP2 mRNA with DAP5/p86 (Figure 2.5C, lane 12). Surprisingly, we found that both DAP5/p97 and HIAP2 mRNA were co-precipitated with full-length DAP5/p97 (Figure 2.5C, lane 8). We could only weakly co-precipitate GAPDH mRNA with full-length DAP5/97 and not at all with DAP5/p86 (Figure 2.5C, lanes 8 and 12), indicating some degree of specificity of DAP5/p97 and DAP5/p86 for mRNA ligands. These data indicate that both full-length DAP5/p97 and the DAP5/p86 isoform can bind to IRES-containing mRNAs and therefore suggest that factors other than the ability of these proteins to associate with their mRNA ligands (such as protein–protein interactions) control the effect of full-length DAP5/p97, as well as the DAP5/p86 isoform, on IRES activity.

Discussion

In this work, we demonstrate that a member of the eIF4G translation initiation factor family, DAP5/p97, is necessary for the specific activation of at least two cellular IRES elements during pharmacologically induced ER stress. We find that DAP5/p97 and HIAP2 protein levels are enhanced during ER stress; their mRNAs are selectively recruited to the polysomes

via IRES elements located within their respective 5'UTRs. We further find that this process is dependent on DAP5/p97, as reducing the levels of endogenous DAP5/p97 by RNA interference abrogated both the translation and IRES activity of DAP5/p97 and HIAP2 during ER stress. Thus, in a positive feedback loop the triggering of ER stress results in elevated levels of DAP5/p97 that, in turn, activate translation of specific mRNAs such as HIAP2 and DAP5/p97 itself under conditions of reduced cap-dependent translation. Moreover, while cleavage of p97 to the DAP5/p86 isoform is required for the induction of HIAP2 IRES activity during ER stress [11], the translational induction of DAP5/p97 during ER stress is mediated by DAP5/p97 itself in a caspase-independent manner. The pivotal role of DAP5/p97 is further strengthened by our observation that siRNA-mediated reduction of DAP5/p97 results in cell death.

DAP5/p97 was identified by several groups by virtue of its homology to eIF4G [28], as a target of the APOBEC-1 editing enzyme that is heavily edited in the liver [29] and in a functional screening assay to identify modulators of interferon-induced apoptosis.[30] DAP5/p97 shares significant homology to eIF4G; however, this homology is restricted to the central and C-terminal portions of eIF4G.[31] Like eIF4G, DAP5/p97 can interact with eIF3, eIF4A and Mnk-1.[29,32,33] Unlike eIF4G, however, DAP5/p97 lacks the amino-terminal portion that includes the eIF4E and PABP-binding domains. Therefore, it is believed that DAP5/p97 cannot support cap-dependent translation initiation. Consistent with this idea, overexpression of DAP5/p97 was found to repress both cap-dependent and EMCV IRES-dependent translation, presumably by sequestering eIF3 and eIF4A in inactive complexes.[28,29] In contrast, however, DAP5/p97-null ES cells have normal levels of global protein synthesis

and show no differences in the activities of several IRES.[34] Furthermore, many studies have shown that the caspase-cleaved fragment of DAP5/p97 (termed DAP5/p86), but not the full-length DAP5/p97, is capable of specifically enhancing the translation mediated by the Apaf-1, c-myc, XIAP, and HIAP2 IRES elements.[10–13] Thus a model has emerged in which DAP5/p97 is activated by caspase cleavage and the resulting DAP5/p86 fragment functions as a specific translation initiation factor for cellular IRES, in particular during conditions of pathophysiological stress.[4,7,11,31]

However, several recent publications have challenged this model. It was shown that the addition of exogenous DAP5/p97 can stimulate the activity of the XIAP, c-myc, DAP5/p97 and HIAP2 IRES elements in a HeLa-based cell-free translation system depleted of eIF4G.[14] More recently, it was shown that DAP5/p97 can function as an activator of translation in vivo and this function of DAP5/p97 does not necessarily require proteolytic processing.[27,35] In these experiments, DAP5/p97 was found to be associated with polysomes, overexpression of DAP5/p97 resulted in the activation of cap-dependent reporter mRNA translation and global protein synthesis and siRNA-mediated knockdown of DAP5/p97 led to a reduction of global protein synthesis. These observations are all consistent with the role of DAP5/p97 as an activator of translation. In addition, reduced DAP5/p97 levels result in a reduction in cell viability and embryonic lethality in both zebrafish and mouse.[27,34,35] Our data confirm the observation that DAP5/p97 knockdown is not compatible with cell survival. However, in contrast to the data of Lee and McCormick[15] we find that a reduction in DAP5/p97 levels does not affect global protein synthesis (Figure 2.4A). The likely explanation for this discrepancy is that, while Lee and McCormick assessed protein synthesis 48 h post-

DAP5/p97 knockdown, in our experiments polysome profiling was performed 24 h after siRNA treatment because we observed a significant loss of cell viability after this timepoint. It should also be noted that DAP5/p97-null ES cells do not display a defect in global protein synthesis [15,34] suggesting that the role of DAP5/97 in the regulation of global translation may be cell-type specific.

We and others have shown previously that overexpression of the p86 fragment of DAP5/p97 is sufficient to activate the DAP5/p97 and HIAP2 IRES elements.[10–12] Here we have extended these observations by demonstrating that both DAP5/p97 and HIAP2 IRES-mediated translation are dependent on DAP5/p97, since the knockdown of p97 significantly reduces translation of DAP5/p97 itself and HIAP2 during ER stress by precluding activation of their respective IRES elements. However, in contrast to the requirement of caspase-mediated cleavage of DAP5/p97 to the p86 isoform for induction of HIAP2 IRES activity [11], we find that the translational induction of DAP5/p97 following ER stress does not require caspase activity. Since DAP5/p97 is absolutely required for the translational induction of DAP5/p97 during ER stress, we conclude that DAP5/p97 enhances the activity of its IRES in a caspase-independent manner. These data support the hypothesis that DAP5/p97 can function as a translational activator in the absence of proteolytic processing. It is possible that other post-translational modifications of DAP5/p97 during ER stress control its ability to modulate IRES activity. Indeed, phosphorylation of DAP5/p97 at threonine 508 was identified by a large-scale proteomics study[36] and it has been suggested that phosphorylation of DAP5/p97 controls its activity in response to growth factor signalling.[27] Further

investigations of the signalling pathways that modulate DAP5/p97 activity during cellular stress or following growth factor stimulation should prove to be enlightening.

We sought to mechanistically determine how full-length DAP5/p97 differentiates between distinct mRNA molecules such as DAP5/p97 and HIAP2. Our data indicate that both full-length DAP5/p97 and the truncated p86 fragment are capable of binding DAP5/p97 and HIAP2 endogenous mRNAs equally well. Thus, the simple model whereby DAP5/p97 associates with a particular pool of cellular mRNAs while its DAP5/p86 truncated isoform associates with a different cohort of mRNAs is unlikely. Our observations raise the possibility that full-length DAP5/p97 preassembles with several mRNAs, but is only able to enhance IRES-dependent translation following a particular post-translational modification, which may be different depending on the target mRNA molecule. For example, caspase cleavage of DAP5/p97 to generate the DAP5/p86 isoform enhances both DAP5/p97 and HIAP2 IRES activity, whereas other post-translational modifications (such as phosphorylation) may be sufficient to allow full-length DAP5/p97 to enhance the activity of its own IRES.

In summary, our data provide direct evidence that DAP5/p97 can function as a translational activator of at least two IRES-containing cellular mRNAs during conditions of pathophysiological stress. Together with previously published observations[35], these findings support the hypothesis that DAP5/p97 controls translation of select, rather than all, mRNAs. Importantly, the fact that the DAP5/p97 IRES itself is activated by DAP5/p97 during ER stress suggests the existence of a positive feedback loop that ensures elevated levels of

DAP5/p97 to support IRES-dependent translation of select mRNAs during conditions of reduced global protein synthesis.

Acknowledgements

We thank members of the Apoptosis Research Centre for helpful discussions and critical comments. This work was supported by grants from the Canadian Institutes of Health Research (CIHR MOP # 74740), Premier's Research Excellence Award, Canada Foundation for Innovation and Ontario Research and Development Challenge Fund. M.H. is a CIHR New Investigator. Funding to pay the Open Access publication charges for this article was provided by CIHR. *Conflict of interest statement.* None declared.

References

1. Vattem, K.M. and Wek, R.C. (2004) Reinitiation involving upstream ORFs regulates ATF4 mRNA translation in mammalian cells. *Proc Natl Acad Sci USA*, **101**, 11269-11274.

2. Lu, P.D., Harding, H.P. and Ron, D. (2004) Translation reinitiation at alternative open reading frames regulates gene expression in an integrated stress response. *J Cell Biol*, **167**, 27-33.

3. Kaufman, R.J. (2004) Regulation of mRNA translation by protein folding in the endoplasmic reticulum. *Trends Biochem Sci*, **29**, 152-158.

4. Holcik, M. and Sonenberg, N. (2005) Translational control in stress and apoptosis. *Nat Rev Mol Cell Biol*, **6**, 318-327.

5. Pelletier, J. and Sonenberg, N. (1988) Internal initiation of translation of eukaryotic mRNA directed by a sequence derived from poliovirus RNA. *Nature*, **334**, 320-325.

6. Jang, S.K., Krausslich, H.G., Nicklin, M.J., Duke, G.M., Palmenberg, A.C. and Wimmer, E. (1988) A segment of the 5' nontranslated region of encephalomyocarditis virus RNA directs internal entry of ribosomes during in vitro translation. *J Virol*, **62**,

2636-2643.

7. Holcik, M., Sonenberg, N. and Korneluk, R.G. (2000) Internal ribosome initiation of translation and the control of cell death. *Trends in Genetics*, **16**, 469-473.

8. Stoneley, M. and Willis, A.E. (2004) Cellular internal ribosome entry segments: structures, trans-acting factors and regulation of gene expression. *Oncogene*, **23**, 3200-3207.

9. Lewis, S.M. and Holcik, M. (2005) IRES in distress: translational regulation of the inhibitor of apoptosis proteins XIAP and HIAP2 during cell stress. *Cell Death Differ*, **12**, 547-553.

10. Nevins, T.A., Harder, Z.M., Korneluk, R.G. and Holcik, M. (2003) Distinct Regulation of Internal Ribosome Entry Site-mediated Translation following Cellular Stress Is Mediated by Apoptotic Fragments of eIF4G Translation Initiation Factor Family Members eIF4GI and p97/DAP5/NAT1. *J. Biol. Chem.*, **278**, 3572-3579.

11. Warnakulasuriyarachchi, D., Cerquozzi, S., Cheung, H.H. and Holcik, M. (2004) Translational induction of the inhibitor of apoptosis protein HIAP2 during endoplasmic reticulum stress attenuates cell death and is mediated via an inducible internal ribosome entry site element. *J Biol Chem*, **279**, 17148-17157.

12. Henis-Korenblit, S., Shani, G., Sines, T., Marash, L., Shohat, G. and Kimchi, A. (2002) The caspase-cleaved DAP5 protein supports internal ribosome entry site-mediated translation of death proteins. *Proc Natl Acad Sci USA*, **99**, 5400-5405.

13. Henis-Korenblit, S., Strumpf, N.L., Goldstaub, D. and Kimchi, A. (2000) A Novel Form of DAP5 Protein Accumulates in Apoptotic Cells as a Result of Caspase Cleavage and Internal Ribosome Entry Site-Mediated Translation. *Mol Cell Biol*, **20**, 496-506.

14. Hundsdoerfer, P., Thoma, C. and Hentze, M.W. (2005) Eukaryotic translation initiation factor 4GI and p97 promote cellular internal ribosome entry sequence-driven translation. *Proc Natl Acad Sci U S A*, **102**, 13421-13426.

15. Lee, S.H. and McCormick, F. (2006) p97/DAP5 is a ribosome-associated factor that facilitates protein synthesis and cell proliferation by modulating the synthesis of cell cycle proteins. *EMBO J.*, **25**, 4008-4019.

16. Holcik, M., Lefebvre, C.A., Yeh, C., Chow, T. and Korneluk, R.G. (1999) A new internal-ribosome-entry-site motif potentiates XIAP-mediated cytoprotection. *Nature*

Cell Biology, **1**, 190-192.

17. MacGregor, G.R., Nolan, G.P., Fiering, S., Roederer, M. and Herzenberg, L.A. (1991) In Murray, E. J. and Walker, J. M. (eds.), *Methods in Molecular Biology*. Humana Press Inc., Clifton, N.J., Vol. 7, pp. 217-235.

18. Holcik, M., Graber, T., Lewis, S.M., Lefebvre, C.A., Lacasse, E. and Baird, S. (2005) Spurious splicing within the XIAP 5'UTR occurs in the Rluc/Fluc but not the {beta} gal/CAT bicistronic reporter system. *RNA*, **11**, 1605-1609.

19. Blais, J.D., Addison, C.L., Edge, R., Falls, T., Zhao, H., Wary, K., Koumenis, C., Harding, H.P., Ron, D., Holcik, M. *et al.* (2006) Perk-dependent translational regulation promotes tumor cell adaptation and angiogenesis in response to hypoxic stress. *Mol Cell Biol.*, **26**, 9517-9532. Epub 2006 Oct 9519.

20. Abdelmohsen, K., Pullmann, R., Jr., Lal, A., Kim, H.H., Galban, S., Yang, X., Blethrow, J.D., Walker, M., Shubert, J., Gillespie, D.A. *et al.* (2007) Phosphorylation of HuR by Chk2 regulates SIRT1 expression. *Mol Cell.*, **25**, 543-557.

21. Cheung, H.H., Lynn Kelly, N., Liston, P. and Korneluk, R.G. (2006) Involvement of caspase-2 and caspase-9 in endoplasmic reticulum stress-induced apoptosis: a role for the IAPs. *Exp Cell Res.*, **312**, 2347-2357. Epub 2006 Apr 2344.

22. Harding, H.P., Zhang, Y. and Ron, D. (1999) Protein translation and folding are coupled by an endoplasmic-reticulum-resident kinase. *Nature*, **397**, 271-274.

23. Harding, H.P., Novoa, I.I., Zhang, Y., Zeng, H., Wek, R., Schapira, M. and Ron, D. (2000) Regulated translation initiation controls stress-induced gene expression in mammalian cells. *Mol Cell*, **6**, 1099-1108.

24. Kao, P.N., Chen, L., Brock, G., Ng, J., Kenny, J., Smith, A.J. and Corthesy, B. (1994) Cloning and expression of cyclosporin A- and FK506-sensitive nuclear factor of activated T-cells: NF45 and NF90. *J Biol Chem.*, **269**, 20691-20699.

25. Warnakulasuriyarachchi, D., Ungureanu, N.H. and Holcik, M. (2003) The translation of an antiapoptotic protein HIAP2 is regulated by an upstream open reading frame. *Cell Death Differ*, **10**, 899-904.

26. Van Eden, M.E., Byrd, M.P., Sherrill, K.W. and Lloyd, R.E. (2004) Translation of cellular inhibitor of apoptosis protein 1 (c-IAP1) mRNA is IRES mediated and regulated during cell stress. *RNA*, **10**, 469-481.

27. Nousch, M., Reed, V., Bryson-Richardson, R.J., Currie, P.D. and Preiss, T. (2007) The eIF4G-homolog p97 can activate translation independent of caspase cleavage. *RNA*, **19**, 19.

28. Imataka, H., Olsen, H.S. and Sonenberg, N. (1997) A new translational regulator with homology to eukaryotic translation initiation factor 4G. *EMBO J*, **16**, 817-825.

29. Yamanaka, S., Poksay, K.S., Arnold, K.S. and Innerarity, T.L. (1997) A novel translational repressor mRNA is edited extensively in livers containing tumors caused by the transgene expression of the apoB mRNA-editing enzyme. *Genes Dev*, **11**, 321-333.

30. Levy-Strumpf, N., Deiss, L.P., Berissi, H. and Kimchi, A. (1997) DAP-5, a novel homolog of eukaryotic translation initiation factor 4G isolated as a putative modulator of gamma interferon-induced programmed cell death. *Mol Cell Biol*, **17**, 1615-1625.

31. Marash, L. and Kimchi, A. (2005) DAP5 and IRES-mediated translation during programmed cell death. *Cell Death Differ*, **8**, 8.

32. Imataka, H. and Sonenberg, N. (1997) Human eukaryotic translation initiation factor 4G (eIF4G) possesses two separate and independent binding sites for eIF4A. *Mol Cell Biol*, **17**, 6940-6947.

33. Pyronnet, S., Imataka, H., Gingras, A.C., Fukunaga, R., Hunter, T. and Sonenberg, N. (1999) Human eukaryotic translation initiation factor 4G (eIF4G) recruits mnk1 to phosphorylate eIF4E. *Embo J*, **18**, 270-279.

34. Yamanaka, S., Zhang, X.Y., Maeda, M., Miura, K., Wang, S., Farese, R.V., Jr., Iwao, H. and Innerarity, T.L. (2000) Essential role of NAT1/p97/DAP5 in embryonic differentiation and the retinoic acid pathway. *Embo J*, **19**, 5533-5541.

35. Lee, S.H. and McCormick, F. (2006) p97/DAP5 is a ribosome-associated factor that facilitates protein synthesis and cell proliferation by modulating the synthesis of cell cycle proteins. *Embo J*, **24**, 24.

36. Beausoleil, S.A., Jedrychowski, M., Schwartz, D., Elias, J.E., Villen, J., Li, J., Cohn, M.A., Cantley, L.C. and Gygi, S.P. (2004) Large-scale characterization of HeLa cell nuclear phosphoproteins. *Proc Natl Acad Sci U S A.*, **101**, 12130-12135.

CHAPTER 3

NF45 functions as an IRES trans-acting factor that is required for translation of cIAP1 during the unfolded protein response

Preamble

"NF45 functions as an IRES trans-acting factor that is required for translation of cIAP1 during the unfolded protein response" was first published as a research article in the periodical Cell Death and Differentiation (volume 17, April 2010). The article identifies additional cIAP1 ITAFs. One of these proteins, NF45, is identified as a novel RNA binding protein that is required for IRES-mediated translation of cIAP1 following endoplasmic reticulum stress.

Author list: Tyson E. Graber, Stephen D. Baird, Peter N. Kao, Michael B. Mathews and Martin Holcik

Author contributions: TEG wrote the article. TEG, SDB, MH designed experiments. TEG performed experiments presented in Figures 3.2-8. PNK, MBM provided reagents and contributed to discussions.

Abstract

Expression of the cellular inhibitor of apoptosis protein 1 (cIAP1) is unexpectedly repressed at the level of translation under normal physiological conditions in many cell lines. We have previously shown that the 5′ untranslated region of cIAP1 mRNA contains a stress-inducible internal ribosome entry site (IRES) that governs expression of cIAP1 protein. Although inactive in unstressed cells, the IRES supports cap-independent translation of cIAP1 in response to endoplasmic reticulum stress. To gain an insight into the mechanism of cIAP1 IRES function, we empirically derived the minimal free energy secondary structure of the cIAP1 IRES using enzymatic cleavage mapping. We subsequently used RNA affinity chromatography to identify several cellular proteins, including nuclear factor 45 (NF45) as cIAP1 IRES binding proteins. In this report we show that NF45 is a novel RNA binding protein that enhances IRES-dependent translation of endogenous cIAP1. Further, we show that NF45 is required for IRES-mediated induction of cIAP1 protein during the unfolded protein response. The data presented are consistent with a model in which translation of cIAP1 is governed, at least in part, by NF45, a novel cellular IRES trans-acting factor.

Introduction

Eukaryotes have evolved distinct mechanisms that allow them to control the expression of their proteome independent of the transcriptional apparatus. The ability to regulate translation ensures rapid and measured expression of specific proteins in time and space. Translational control allows for efficient reprogramming of gene expression during cell growth and differentiation[1,2] and provides a level of homeostatic control following exposure

to stresses such as viral infection,[3] endoplasmic reticulum (ER) stress,[4,5] hypoxia[6] or DNA damage.[7] Regulation of translation occurs primarily at the initiation step and targets several eukaryotic initiation factors that mediate recruitment of the ribosome to the mRNA before polypeptide synthesis.[8]

The 7-methyl-guanosine cap located at the 5′ end of mature mRNAs catalyzes the formation of a protein complex consisting of a cap binding protein (eIF4E), a scaffold protein (eIF4G) and an RNA helicase (eIF4A). Together, these proteins comprise the cap binding complex (eIF4F), which allows for the recruitment of the small ribosomal subunit (along with accessory factors) forming a preinitiation complex that is believed to proceed in a 5′–3′ direction along the 5′ untranslated region (UTR) until an optimal initiation codon is reached. It is at this point that the large ribosomal subunit joins to form the 80S ribosome and peptide synthesis commences.[8] This cap-dependent, ribosomal scanning mechanism of translation initiation works efficiently under normal physiological conditions; however, during times of cellular stress, decreased availability of ATP and the preinitiation complex significantly reduces overall protein synthesis rates.

To respond properly to various physiological stimuli, cells must be able to ensure expression of specific genes despite repressed global translation rates. One such mechanism uses an RNA sequence element located in the 5′ UTR that facilitates recruitment of the ribosome. First discovered in picornaviruses, the internal ribosome entry site (IRES) element is present in a number of eukaryotic mRNAs where it mediates cap-independent translation initiation under stress conditions.[9] The exact mechanism used by eukaryotic IRES elements to recruit the ribosome is the subject of intense investigation. Unlike some viral IRES, which

can function by direct recruitment of the ribosome, eukaryotic IRES appears to require accessory protein factors in addition to canonical initiation factors. Several of these IRES trans-acting factors (ITAFs) have been identified, including PTB,[10] hnRNP A1,[11] La[12] and hnRNPC1/C2.[13] Exactly how ITAFs function in modulating cellular IRES activity is not clear. ITAFs were suggested to function as adapter proteins acting as a bridge between the ribosome and RNA.[14] Alternatively, they may exert their effect as RNA chaperones, remodelling RNA into a conformation that is permissive to ribosome recruitment.[15]

Cellular inhibitor of apoptosis protein 1 (cIAP1) is a critical regulator of cell survival and nuclear factor-κB (NF-κB) signalling.[16, 17] We and others have shown that the expression of cIAP1 is regulated at the level of translation through an IRES located within its 5′ UTR that supports cap-independent translation.[5, 18, 19] Although this IRES is inactive in unstressed cells, drug-induced ER stress that leads to the unfolded protein response (UPR), DNA damage by etoposide treatment or cell-cycle arrest by sodium arsenite treatment causes an increase in cIAP1 IRES activity. Importantly, the concomitant increase in cIAP1 protein levels during the UPR delays the onset of apoptosis, consistent with the antiapoptotic role of cIAP1.

To better understand the regulation and function of cIAP1 IRES, we derived the minimum free energy secondary structure of the cIAP1 IRES using in vitro enzymatic cleavage mapping. Furthermore, we identified a specific cohort of cIAP1 IRES binding proteins including nuclear factor 45 (NF45). NF45 was first identified as an NFAT-related transcription factor that together with its binding partner NF90 regulates interleukin-2 transcription.[20] Here we ascribe a novel, post-transcriptional role for NF45. Specifically, we

found that NF45 enhances IRES-mediated translation of cIAP1 mRNA. Surprisingly, we found that NF45 alone possesses RNA binding activity, interacts specifically with the cIAP1 IRES in vitro and modulates cIAP1 IRES activity in vivo. More importantly, cells lacking NF45 failed to upregulate IRES-mediated translation of cIAP1 during the UPR. Our data show that NF45 is a novel RNA binding protein that interacts with the cIAP1 5′ UTR in a sequence and structure dependent manner and regulates expression of cIAP1 in response to stress.

Results

Minimum free energy secondary structure model of the cIAP1 IRES

We have mapped the cIAP1 IRES activity to nucleotides −150 to −80 (relative to AUG start codon) of the 1.2-kb-long cIAP1 5′ UTR.[18] In addition to the primary sequence, secondary and tertiary structures are important determinants of cellular IRES activity.[21] To determine whether the cIAP1 IRES shares common structural features with other cellular IRES and to better understand the role that RNA structure may have in the regulation of the cIAP1 IRES activity, we empirically determined the secondary structure of the cIAP1 IRES by primer extension analysis of nuclease-digested RNA fragments. The cIAP1 IRES was in vitro transcribed and subjected to digestion with RNase T1, T2 or V1. cDNA was then generated from the resulting RNA fragments by reverse transcription and resolved on a denaturing polyacrylamide gel (Figure 3.1). Using the digest pattern as folding constraints for the mfold structure prediction algorithm,[22] we obtained a minimum free energy model of the cIAP1 IRES structure (Figure 3.2a; Table 3.1).

Figure 3.1

RNase sensitive cut sites from nucleotides -150 to -1 of the cIAP1 5'UTR. Lanes 1-4 represent a DNA sequencing reaction of the UTR. Using the same labelled primer as the sequencing reaction, RNase digested in vitro transcribed RNA was reverse transcribed and run on the gel as described in Baird et al.[30] The following lanes show the results with decreasing amount of RNase used in the reactions for RNase T1 (lanes 6-9), RNase V1 (lanes 10-13) and RNase T2 (lanes 14-17). RNase cleavage will have occurred 3' of the upstream nucleotide relative to the band in the gel.

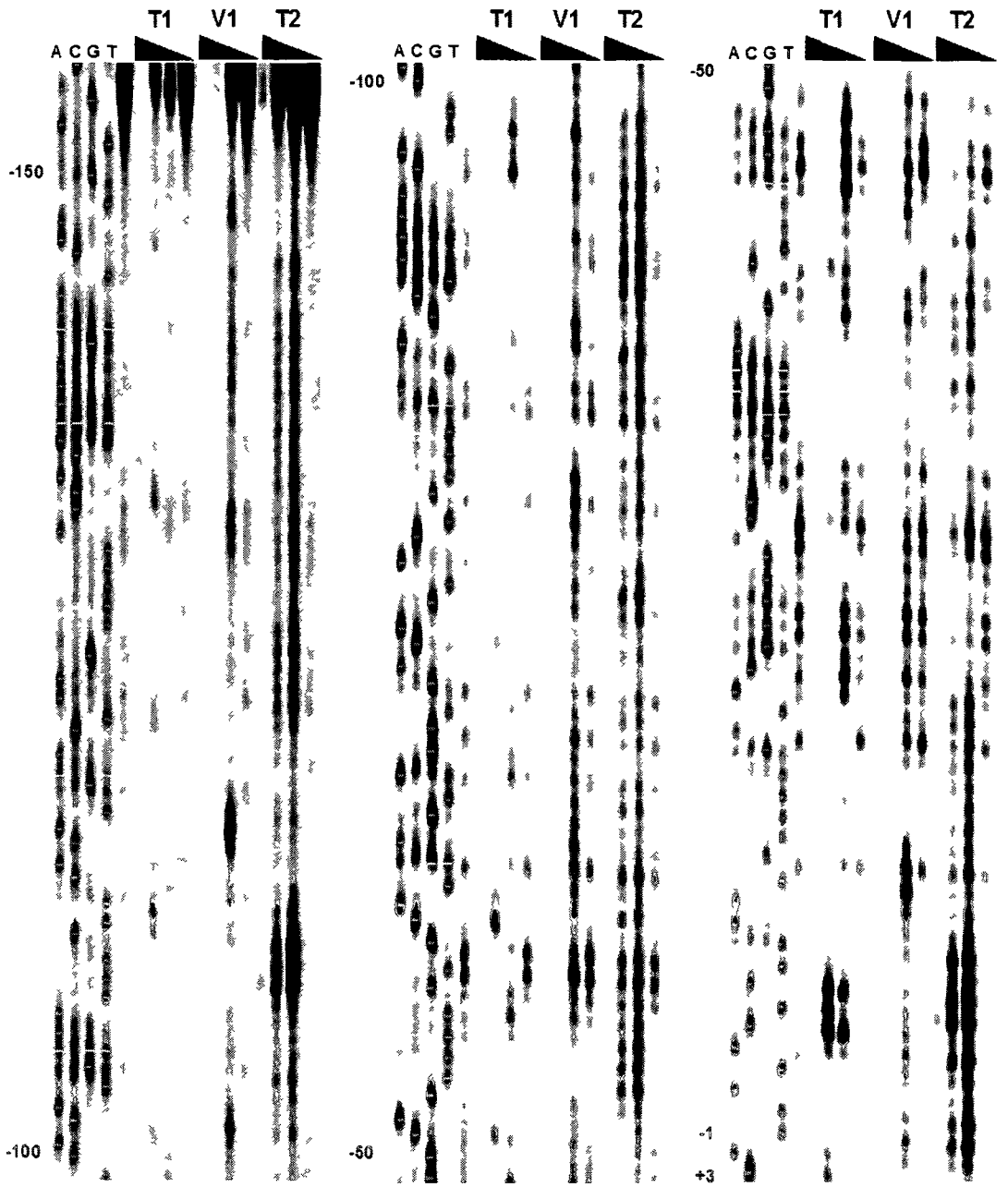
T1
V1
T2
A C G T
-150
-100
-100
-50
-50
-1
+3

Table 3.1
List of RNase sensitive cut sites for nucleotides -150 to -1 of the cIAP1 5'UTR.

Seq#	5'	3'	T1	V1	T2	Seq#	5'	3'	T1	V1	T2	Seq#	5'	3'	T1	V1	T2
-150	T	A				-99	A	T				-48	T	A			
-149	G	C		2		-98	A	T				-47	C	G			
-148	A	T		2		-97	T	A				-46	C	G			
-147	T	A				-96	G	C				-45	C	G			
-146	T	A				-95	T	A				-44	A	T			
-145	T	A				-94	T	A				-43	A	T			
-144	C	G				-93	T	A				-42	A	T			
-143	T	A				-92	T	A				-41	G	C	1		
-142	T	A				-91	A	T				-40	A	T			
-141	T	A				-90	G	C		1		-39	C	G			
-140	T	A				-89	C	G		1		-38	T	A			
-139	T	A				-88	T	A				-37	T	A			
-138	G	C				-87	A	T				-36	T	A			
-137	T	A				-86	T	A				-35	T	A			
-136	G	C				-85	C	G				-34	C	G			
-135	G	C	2	2	2	-84	A	T				-33	C	G			
-134	T	A		2		-83	A	T		1		-32	C	G			
-133	A	T		2		-82	A	T		1		-31	A	T			
-132	A	T				-81	C	G		1		-30	G	C			
-131	A	T				-80	A	T				-29	G	C			
-130	A	T				-79	G	C				-28	T	A			
-129	A	T			1	-78	T	A				-27	C	G			
-128	T	A			1	-77	A	T				-26	C	G			
-127	C	G				-76	C	G				-25	C	G			
-126	T	A			1	-75	T	A				-24	T	A			
-125	T	A			1	-74	G	C				-23	C	G			
-124	A	T				-73	T	A				-22	G	C	1		
-123	G	C				-72	C	G				-21	T	A			
-122	T	A				-71	A	T				-20	A	T			
-121	T	A				-70	C	G				-19	T	A			
-120	C	G		1		-69	C	G				-18	C	G			
-119	A	T		1		-68	T	A				-17	A	T			
-118	T	A		1		-67	A	T				-16	A	T			
-117	G	C				-66	C	G		2		-15	A	T			
-116	T	A				-65	T	A		2		-14	A	T			
-115	G	C				-64	C	G		2		-13	C	G			
-114	A	T	1		1	-63	A	T				-12	A	T		1	
-113	A	T			1	-62	T	A				-11	T	A		1	
-112	G	C			1	-61	G	C				-10	T	A			
-111	A	T			1	-60	C	G				-9	A	T			1
-110	A	T			1	-59	A	T				-8	A	T			
-109	A	T				-58	C	G	1			-7	G	C	1		
-108	T	A				-57	A	T			1	-6	A	T			
-107	T	A				-56	A	T			1	-5	G	C	1		
-106	T	A				-55	A	T			1	-4	T	A			1
-105	C	G				-54	A	T			1	-3	A	T			
-104	A	T				-53	C	G				-2	T	A			
-103	T	A				-52	T	A				-1	A	T			1
-102	G	C				-51	G	C				1	A	T			1
-101	T	A				-50	C	G				2	T	A			
-100	G	C				-49	C	G				3	G	C			

Figure 3.2

cIAP1 IRES structure model and identification of binding proteins. (**a**) The cIAP1 IRES RNA secondary structure model (nucleotides −150 to −1) with sites sensitive to RNase T1, T2 and V1 shown as shaded circles. (**b**) SYPRO Ruby-stained RNA affinity chromatography gel of proteins pulled down with a biotin-tagged cIAP1 IRES RNA probe (probe 1) from an HEK293T cytoplasmic lysate. (**c**) Peptides identified from excised bands by mass spectrometry were mapped to four unique proteins. (**d**) To confirm protein binding specificity, RNA affinity chromatography was repeated with a cIAP1 IRES (probe 1) or non-IRES (probe 2) RNA, followed by immunoblotting with antibodies specific for RHA, NF90, IGF2BP1 and NF45.

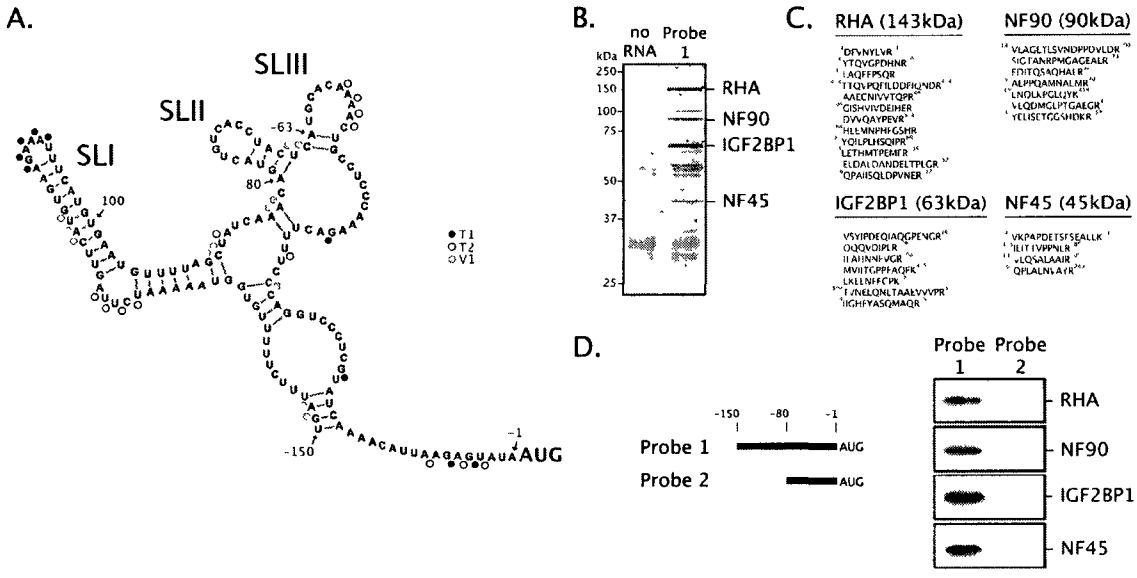
A.
SLI
SLII
SLIII
AUG
B.
no RNA
Probe 1
kDa
250
150
100
75
50
37
25
RHA
NF90
IGF2BP1
NF45
C.
RHA (143kDa)
NF90 (90kDa)
IGF2BP1 (63kDa)
NF45 (45kDa)
D.
Probe 1
Probe 2
Probe 1
Probe 2
RHA
NF90
IGF2BP1
NF45

A specific set of proteins interacts with the cIAP1 IRES

A cursory examination of the highly structured cIAP1 IRES reveals a partial likeness to the IRES of cricket paralysis virus (CrPV). Stem-loops I, II and III of the cIAP1 IRES (Figure 3.2a) bear a striking similarity to pseudoknots II and III of the CrPV IRES – motifs that mediate direct interaction with the 40S ribosomal subunit.[23] We therefore wished to determine if cIAP1 IRES RNA is capable of a direct interaction with the 40S ribosomal subunit. Although CrPV IRES was able to bind directly to the purified 40S in an electromobility shift assay we did not observe any binding with the cIAP1 IRES (data not shown). This suggests that additional cellular proteins are required for the recruitment of the cIAP1 IRES to the ribosome. To identify these proteins, we carried out RNA electromobility shift and UV cross-linking assays using a cytoplasmic extract from HEK293T cells and in vitro transcribed and radiolabelled RNA corresponding to the cIAP1 IRES. We observed specific protein–RNA complexes forming under both native (Figure 3.3a) and denaturing (Figure 3.3b) conditions, supporting the notion that specific proteins may regulate cIAP1 IRES activity.

To resolve and identify these proteins we used an RNA affinity chromatography strategy followed by identification of RNA-bound proteins by MALDI-TOF mass spectrometry. RNA encoding the cIAP1 IRES (nucleotides −150 to −1) or the non-IRES portion of the cIAP1 5′ UTR (nucleotides −80 to −1) was in vitro transcribed, 5′ end-labelled with biotin and conjugated to streptavidin-coated agarose beads. The labelled RNA was then incubated with a cytoplasmic HEK293T cell lysate and bound proteins were resolved by SDS-PAGE and visualized with SYPRO Ruby stain. A specific set of proteins was observed

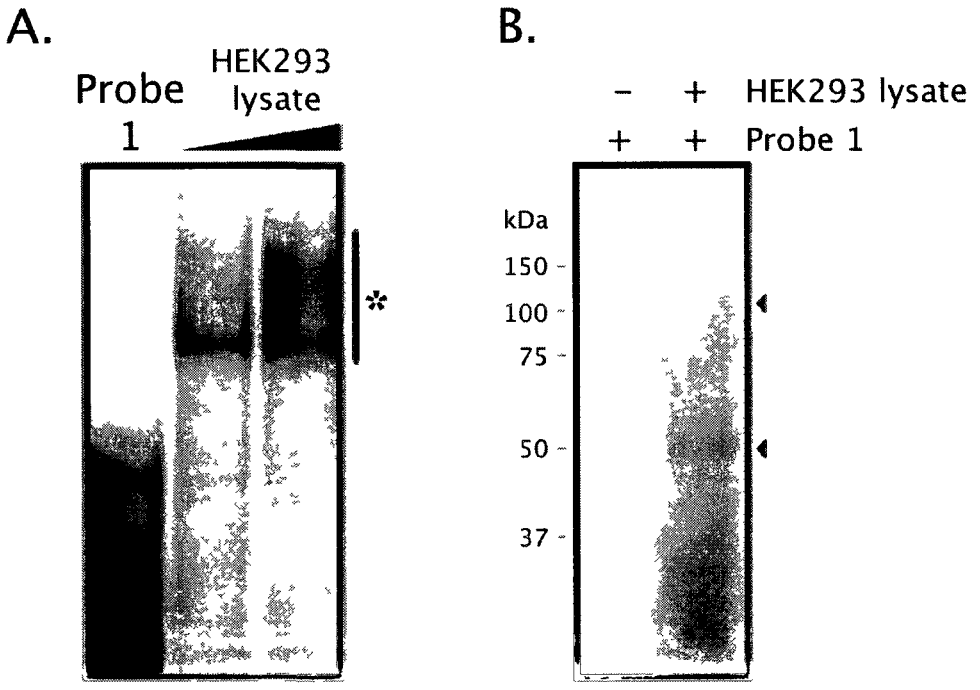
A.
Probe 1
HEK293 lysate
*
B.
- + HEK293 lysate
+ + Probe 1
kDa
150
100
75
50
37

binding to the cIAP1 IRES but not in a control reaction lacking an RNA matrix (Figure 3.2b). Proteins resolved by affinity chromatography were excised from the gel and submitted for analysis by MALDI-TOF mass spectrometry. Peptides were mapped with high confidence to four distinct proteins using the MASCOT database (Figure 3.2c). Specifically, we found that RNA Helicase A (RHA; UniProt accession: Q08211), insulin-like growth factor 2 mRNA binding protein 1 (IGF2BP1; UniProt accession: Q9NZI8), NF90 (UniProt accession: Q12906) and NF45 (UniProt accession: Q12905) interacted with the cIAP1 IRES.

To confirm that these proteins interact specifically with the cIAP1 IRES, we repeated the affinity chromatography experiment and transferred the bound proteins to a membrane followed by immunoblotting with antibodies specific for RHA, NF90, IGF2BP1 and NF45. Importantly, these four proteins were confirmed to interact with the cIAP1 IRES but not to the portion of the cIAP1 5′ UTR that does not exhibit IRES activity (probe 2), indicating that these interactions are specific to the cIAP1 IRES sequence and/or structure (Figure 3.2d). Furthermore, probing the affinity preparations with antibodies specific for the canonical RNA binding proteins hnRNP A1, HuR and TIA1 did not yield a positive signal, showing that only a subset of RNA binding proteins interact with the cIAP1 IRES (Lewis et al.[11]; data not shown).

NF45 enhances translation of endogenous cIAP1

We chose to focus our investigation of cIAP1 IRES binding proteins on NF45, as relatively little is known about this protein's function in translation. NF45 was initially implicated, along with its binding partner NF90, as an interleukin-2 transcription factor in Jurkat T cells.

[20] Complicating the study of NF45 function is its apparent co-regulation with NF90. A recent study by Guan et al.[24] and our own unpublished observations showed that removing NF45 triggers proteasomal degradation of NF90 and vice versa. The intimate relationship between NF45 and NF90 also extends to their apparent function in modulating protein translation, as the NF45–NF90 complex has been shown by Merrill et al.[25] to bind and inhibit human rhinovirus 2 (HRV2) IRES activity. Consistent with their finding, we found that U373MG glioblastoma cells express approximately 50% less NF45 and NF90 protein relative to HEK293T cells (Figure 3.4a). Curiously, we found that U373MG and HEK293T cells express similar levels of cIAP1 protein as determined by western blot (Figure 3.4a). However, when we assessed levels of newly synthesized cIAP1 protein by metabolic labelling and immunoprecipitation of cIAP1, we observed that translation of cIAP1 was reduced in U373MG cells relative to HEK293T cells (Figure 3.4b). We observed a similar reduction in cIAP1 translation after transiently knocking down NF45 in HEK293T cells using siRNA (Figure 3.5). Of note, although the inhibitory NF45/NF90 heterodimers are present in high abundance in HEK293T cells, both the abundance and the activity of this heterodimer are significantly lower in cell lines of glial origin.[26] Therefore, we chose U373MG glioblastoma cells as a model to address the function of NF45 in an NF90-independent manner.

We transiently transfected U373MG glioblastoma cells with a FLAG-tagged NF45 overexpression plasmid. Western blot analysis indicated a 1.5- to 2-fold enhancement of NF45 expression in transfected cells (Figure 3.4c, lower panels). To determine the effect of NF45 on de novo cIAP1 protein translation, U373MG cells overexpressing NF45 or GFP as

Figure 3.4

NF45 regulates cIAP1 mRNA translation. (**a**) Western blots illustrating differential expression of endogenous NF45 and NF90 in HEK293T and U373MG cells. (**b**) Metabolic labeling and immunoprecipitation of cIAP1 shows impaired translation of cIAP1 in U373MG relative to HEK293T cells. (**c**) NF45 increases de novo cIAP1 protein synthesis. Top panel: U373MG cells transiently expressing NF45 or GFP were pulse-labeled 24 h following transfection and newly synthesized cIAP1 and β-actin proteins were co-immunoprecipitated, resolved on SDS-PAGE and detected by autoradiography. Bottom panel: western blot of U373MG cells transiently transfected with a FLAG-tagged NF45 overexpression plasmid illustrating efficient expression of the transgene. (**d**) NF45 enhances cIAP1 protein translation but not transcription. Top panel: densitometric analysis of cIAP1 protein expression from experiments performed in panel c (*n=2, $P<0.001$; mean ±SD). Bottom Panel: quantitative RT-PCR of total cIAP1 mRNA levels in cells expressing GFP or NF45 (**n=3, $P=0.33$; mean ±SD). (**e**) NF45 enhances translation efficiency of cIAP1 mRNA as measured by polysome profiling of U373MG cells transiently expressing GFP or NF45. The efficiency of the separation was assessed by resolving ethidium-bromide-stained 28S and 18S rRNA from each fraction. Individual fractions were probed for cIAP1 or β-actin (control) mRNA expression by RT-PCR. PCR products were resolved by gel electrophoresis and densitometry was performed to determine the percent distribution of specific mRNAs across the gradient (n=3; mean ±SD). The amount of specific mRNA present in higher-order polysomes (P) relative to the translationally quiescent pool (M) produces the metric P/M, and quantifies the change in translational efficiency.

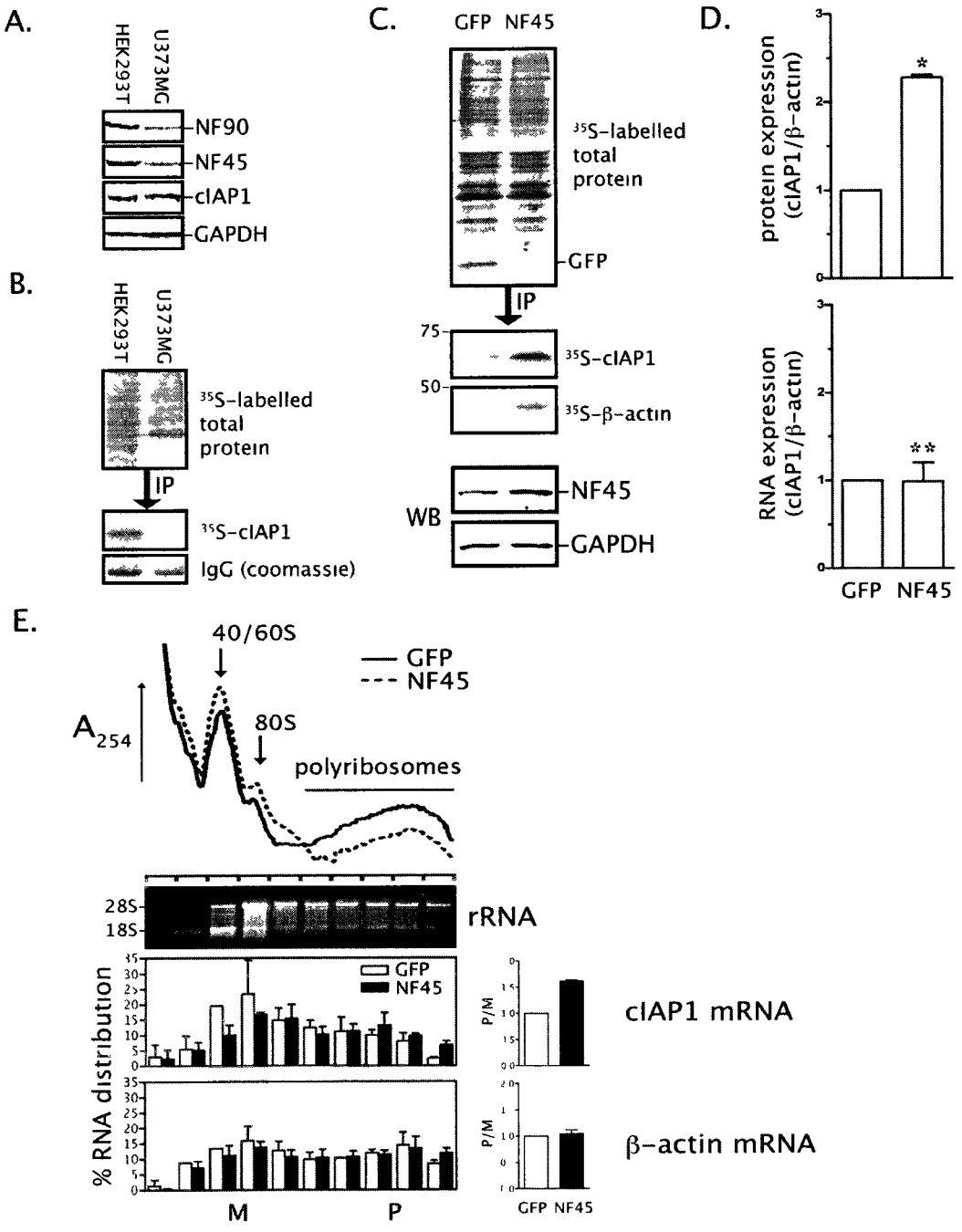
A.
HEK293T
U373MG
NF90
NF45
cIAP1
GAPDH
B.
HEK293T
U373MG
35S-labelled total protein
IP
35S-cIAP1
IgG (coomassie)
C.
GFP NF45
35S-labelled total protein
GFP
IP
75
50
35S-cIAP1
35S-β-actin
WB
NF45
GAPDH
D.
protein expression (cIAP1/β-actin)
RNA expression (cIAP1/β-actin)
GFP NF45
E.
40/60S
GFP
NF45
A254
80S
polyribosomes
28S
18S
rRNA
% RNA distribution
GFP
NF45
M
P
P/M
cIAP1 mRNA
β-actin mRNA
GFP NF45

Figure 3.5

Transient knockdown of NF45 in HEK293T cells impairs cIAP1 translation. HEK293T cells were transfected with a non-targeting siRNA (*C*) or siRNA targeted against NF45 (*D5*)[24] using Lipofectamine 2000 (Invitrogen). After 48 hours, cells were pulse-labelled with S^{35}-Methionine and newly synthesized cIAP1 and β-actin proteins were co-immunoprecipitated and resolved by SDS-PAGE. Lower panel shows a western blot from the lysates illustrating efficient knockdown of NF45.

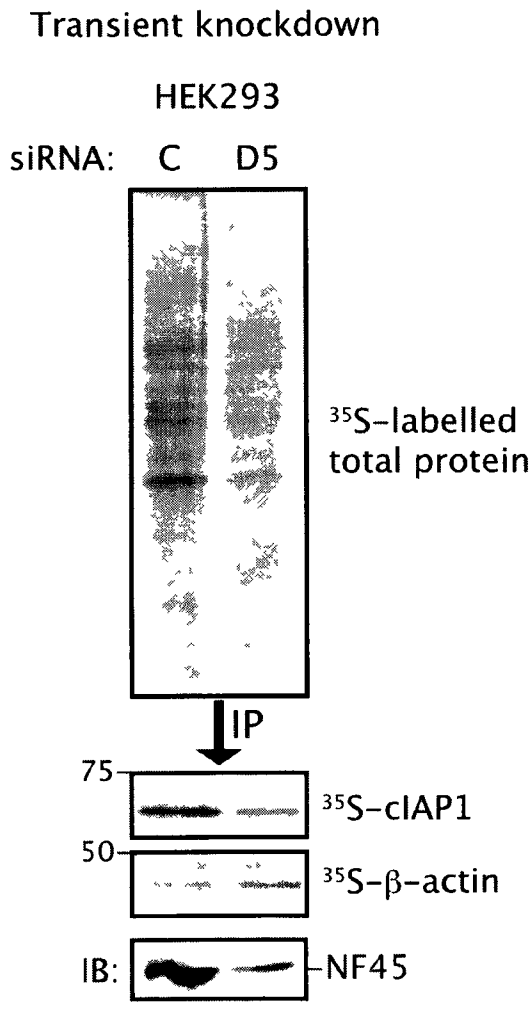
Transient knockdown
HEK293
siRNA: C D5
35S-labelled total protein
IP
75
35S-cIAP1
50
35S-β-actin
IB:
NF45

a control were pulse-labelled with ^{35}S-methionine for 25 min, followed by immunoprecipitation of cIAP1 and β-actin. Although the global translation rate did not appear to be significantly affected by NF45 overexpression, cIAP1 translation was enhanced approximately 2.5-fold relative to β-actin translation (Figure 3.4c and densitometric analysis in upper panel of d). NF45 was originally described in the literature as a transcription factor. Therefore, it was plausible that our observations could be the result of NF45 targeting cIAP1 at the transcriptional level. We therefore assessed the steady-state levels of cIAP1 mRNA in U373MG cells transiently transfected with NF45 overexpression plasmid by quantitative RT-PCR. Despite efficient expression of the NF45 relative to GFP-transfected cells (Figure 3.4c), no significant change was observed in cIAP1 mRNA levels (Figure 3.4d, lower panel).

To confirm that NF45 indeed affects the efficiency of cIAP1 mRNA translation, we assessed the polysomal distribution of cIAP1 mRNA in cells overexpressing GFP or NF45. A quantitative shift (1.5-fold increase in the polysome/monosome ratio of cIAP1 versus β-actin) into the higher-order polysome fractions was observed in NF45 overexpressing cells whereas no significant shift was observed in the β-actin mRNA pools, confirming that NF45 specifically enhances translation of cIAP1 mRNA (Figure 3.4e). Together, these data support a model in which NF45 enhances translation of endogenous cIAP1 mRNA.

NF45-dependent translation of cIAP1 is mediated by its IRES

We next sought to determine the mechanism by which NF45 alters the translational efficiency of cIAP1 mRNA. We initially identified NF45 interacting with the portion of the cIAP1 5′ UTR that confers IRES activity; therefore we hypothesized that NF45 modulates

cIAP1 IRES activity. We have previously established a bicistronic reporter system to test the IRES activity in which the cIAP1 5′ UTR is inserted downstream of a β-galactosidase (β-GAL) cistron and upstream of a chloramphenicol transferase (CAT) cistron.[27] The ratio of CAT expression to β-GAL activity yields a relative measure of IRES activity. The bicistronic vector was transiently co-transfected with a plasmid expressing full-length NF45 or GFP into U373MG cells. Cells transiently expressing NF45 exhibited a 240% increase in cIAP1 IRES activity relative to cells co-transfected with GFP (Figure 3.6a). Notably, this increase in cIAP1 IRES activity closely correlated with the increase in endogenous cIAP1 protein translation that we observed in our metabolic labelling/immunoprecipitation experiment (≈230%relative to GFP-expressing cells; Figure 3.4d, upper panel).

To confirm that NF45 acts in a UTR-specific manner, we compared a monocistronic expression vector in which the 5′ UTR of cIAP1 (nucleotides −1222 to −1) or the portion of the 5′ UTR to which NF45 does not bind (nucleotides −80 to −1) is inserted upstream of the CAT cistron. DNA transfection was normalized by co-transfection with a β-GAL expression plasmid. We observed a significant increase in translation of the downstream CAT reporter in NF45-overexpressing cells with the full-length 5′ UTR (Figure 3.6b, construct 1) but not the IRES-deleted 5′ UTR (Figure 3.6b, construct 2).

We next asked whether the ITAF activity of NF45 is specific to the cIAP1 IRES or whether it could modulate other cellular IRES. To address this question, we assessed the IRES activity of cIAP1, APAF1,[28] BclxL,[29] DAP5[30] and VCIP[31] in HeLa cell lines (HeLa cells express high levels of NF45 comparable to HEK293T) that stably express shRNA directed against NF45 (*d5* cells) or shRNA with no specific target (*c* cells). This NF45

Figure 3.6

NF45 regulates IRES-dependent cIAP1 translation. (**a**) U373MG cells were assayed 24 h following transient transfection of a bicistronic DNA reporter construct (schematic) containing the cIAP1 5′ UTR. IRES activity is expressed as the ratio of CAT expression over β-GAL activity. (**b**) U373MG cells were transiently transfected with GFP or NF45 together with a monocistronic CAT reporter plasmid with either the cIAP1 5′ UTR (1.) or a truncated UTR that does not bind NF45 (2.) inserted upstream of the CAT reporter. A β-GAL reporter was co-transfected to normalize CAT expression across samples. (*$P<0.05$,**$P<0.005$, n=3 mean ±SD).

A.

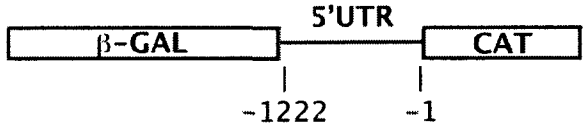
β-GAL
5'UTR
CAT
-1222
-1

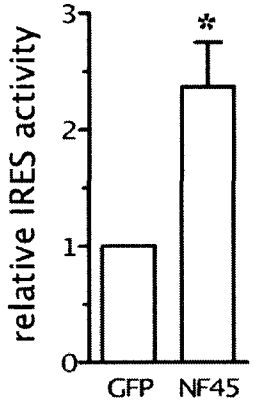
relative IRES activity
3
2
1
0
*
GFP
NF45

B.

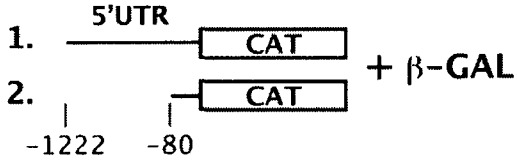
1.
5'UTR
CAT
+ β-GAL
2.
CAT
-1222
-80

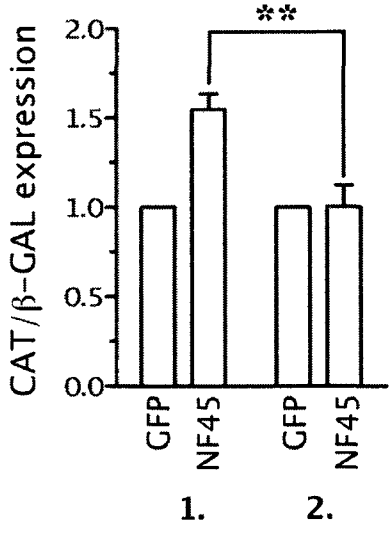
CAT/β-GAL expression
2.0
1.5
1.0
0.5
0.0
**
GFP
NF45
GFP
NF45
1.
2.

knockdown cell line has been previously characterized.[24] As expected, we found that cIAP1 IRES activity was significantly reduced in cells expressing low amounts of NF45 (*d5* versus *c* cells) (Figure 3.7a). Further, these data suggest that the mechanism of NF45-mediated regulation of cIAP1 IRES activity is conserved in glioblastoma and HeLa cells lineages. Importantly, we also found that there was no significant effect on either BclxL or APAF1 IRES activity, whereas we observed a small but consistent increase in DAP5 and VCIP IRES activity in the absence of NF45 (Figure 3.7a). These data confirm that NF45 functions to enhance translation in a UTR-dependent manner, specifically using the cIAP1 IRES element.

Translation of cIAP1 during the unfolded protein response requires NF45

Induction of cIAP1 following ER stress has been observed in our laboratory and others. We have previously shown that IRES-mediated translation of cIAP1 is enhanced following ER stress and that p86, the ER stress-induced cleavage product of p97/DAP5, can enhance cIAP1 IRES activity.[18] However, we were unable to observe direct binding of p86 to the cIAP1 IRES. This could be due to the transient interaction of p86 with the IRES, or an indirect interaction requiring an intermediary protein. Therefore, we asked whether NF45 could mediate ER stress induction of cIAP1 downstream of p86. To answer this question we again used the *d5* cell line that expresses low levels of NF45. We have previously shown that induction of ER stress with the calcium ATPase inhibitor thapsigargin leads to increased cIAP1 protein through enhanced IRES activity in HeLa cells.[18] We treated HeLa cell lines stably expressing control shRNA (*c*) or shRNA targeting NF45 (*d5*) with DMSO (D) vehicle or thapsigargin (T), for 24 h and assessed steady-state levels of cIAP1 by western blot

Figure 3.7

NF45 is required for IRES-mediated translation of cIAP1 during ER stress. (a) Knockdown of NF45 specifically impairs cIAP1 IRES activity. IRES activity in *d5* (NF45 shRNA) cells relative to *c* (nontargeting shRNA) cells was measured using a bicistronic assay for cIAP1, APAF1, BclxL, DAP5 and VCIP as detailed in Material and methods (n=3, mean ±SD). (**b**) NF45 is required for ER stress-mediated induction of cIAP1. *c* or *d5* cells were treated with DMSO (D) as a vehicle or 5 μM thapsigargin (T) to induce ER stress for 24 h. Western blots were performed with antibodies against the indicated proteins. (**c**) Rescue of *d5* cells with transient overexpression of NF45 but not NF90 enhances cIAP1 expression. *d5* cells were transiently transfected with an OMNI-tagged NF90 construct (O.NF90c) or a FLAG-tagged NF45 construct harbouring a silent mutation that renders it resistant to NF45 shRNA (F.NF45r). Cells were then treated with DMSO (D) or 5 μM thapsigargin (T) for 24 h. Western blots were performed with antibodies against the indicated proteins. Blots shown are representative of at least three experiments.

A.

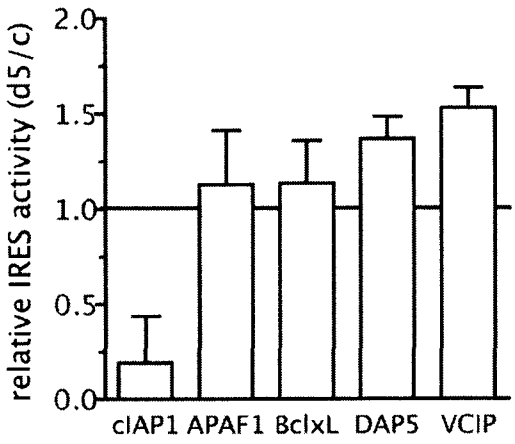
relative IRES activity (d5/c)
2.0
1.5
1.0
0.5
0.0
cIAP1
APAF1
BclxL
DAP5
VCIP

B.

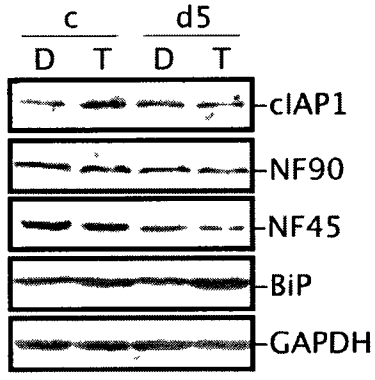
c
d5
D
T
D
T
cIAP1
NF90
NF45
BiP
GAPDH

C.

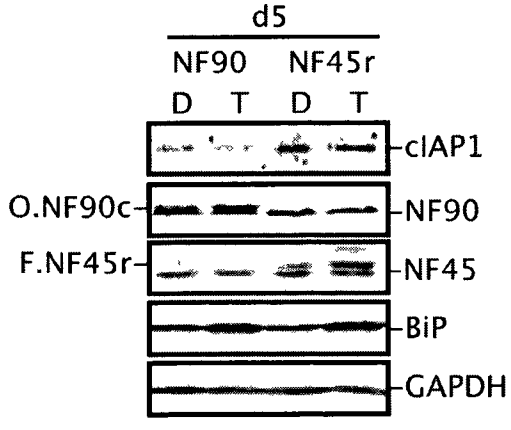
d5
NF90
NF45r
D
T
D
T
cIAP1
O.NF90c
NF90
F.NF45r
NF45
BiP
GAPDH

(Figure 3.7b). As expected, we observed an increase in cIAP1 protein levels relative to GAPDH in control cells. However, no such increase was observed in the cell line lacking NF45 (*d5*) despite the fact that these cells show no impairment in the UPR pathway as shown by the induction of the protein chaperone BiP.

The lack of NF45 in *d5* cells also results in decreased stability of its in vivo binding partner, NF90.[24] To determine whether NF45 by itself is sufficient to mediate an increase in cIAP1 translation or whether the phenomenon also requires NF90, we performed a rescue experiment by transiently transfecting *d5* cells before treatment with thapsigargin with either 1) an overexpression plasmid coding for an epitope-tagged NF90 (O.NF90c) or 2) an epitope-tagged version of NF45 that is resistant to NF45 shRNA (F.NF45r). We observed that despite increased levels of exogenous NF90 in transfected *d5* cells (Figure 3.7c) there was still no induction of cIAP1 after ER stress. In contrast, cells expressing shRNA-resistant NF45 exhibited an increase in endogenous cIAP1 expression, whereas there was no observable additive effect of both thapsigargin treatment and NF45 overexpression on cIAP1 expression. These data show that NF45 is physiologically relevant and that it is sufficient to regulate cIAP1 levels during the UPR.

NF45 is a novel RNA binding protein

NF45 possesses no experimentally verified RNA binding activity and circumstantial evidence points to NF45 interacting with RNA indirectly through NF90. Recent data suggest that NF45 is able to bind directly to dsDNA, specifically to purine-rich boxes within the SP-10 and interleukin-2 promoters.[32] As the affinity chromatography experiment may not

distinguish between direct and indirect protein–RNA interactions, we attempted to photo-crosslink *Escherichia coli* expressed and purified, full-length NF45 (Figure 3.8a) to the cIAP1 5′ UTR in vitro. Recombinant GST-NF45, but not GST alone directly interacted with the portion of the cIAP1 5′ UTR that exhibits IRES activity (Figure 3.8b, probe 3). Moreover, the NF45–RNA complex was not efficiently formed on an RNA probe corresponding to the non-IRES portion of the 5′ UTR (Figure 3.8b, probe 2), an observation that is consistent with the results of the affinity chromatography experiments (Figure 3.2d). As a portion of probes 2 and 3 overlap (nucleotides −80 to −63, comprising SLII), we can conclude that sequence and/or structure common to this region participate in the formation of the NF45–RNA complex.

To further delineate the NF45 binding site within the cIAP1 5′ UTR, we designed competitive DNA oligonucleotides spanning nucleotides −150 to −63 and hybridized them to a heat-denatured RNA probe before renaturation and incubation with recombinant NF45 to compete with the potential binding sites.Figure 3.8c shows that oligos 1, 2 and 3 successfully compete out NF45 binding whereas smaller oligos 2a/b and 3b fail to compete with binding. We observed partial competition with oligos 3a and 4. On the basis of these observations and analysis of the primary structure, we hypothesized that the base of stem-loop I is essential for direct interaction with NF45 (refer to SLI in Figure 3.2a). Specifically, the structure of stem-loop I is likely disrupted by oligos 1, 2, 3 and 3a but not by oligos 2a, 2b and 3b. Oligo 4, which targets the second stem-loop (SLII) in the cIAP1 IRES, also masks NF45 binding partially. We predict that this stem-loop may be required for optimal NF45–RNA complex formation.

Figure 3.8

NF45 interacts directly with the cIAP1 IRES. (**a**) Recombinant GST-NF45 used for in vitro binding studies was expressed in *E. coli* using IPTG, affinity purified and assessed by SDS-PAGE as shown. (**b**) Recombinant NF45 (300 ng) was UV cross-linked to a ^{32}P-labeled cIAP1 IRES RNA probe (nucleotides −150 to −63, probe 3) or a portion of the 5′ UTR with no IRES activity (nucleotides −80 to −1, probe 2). The RNA–protein complex was resolved by SDS-PAGE and detected by autoradiography. (**c**) Determination of NF45 binding sites on the cIAP1 IRES using masking DNA oligonucleotides. Experiments were performed as in (**b**) using RNA probe 3, except that the probe was first hybridized with each of eight competition DNA oligonucleotides (100-fold molar excess). The top panel shows a primary structure of the probe with the location of the masking oligos and the bottom panel illustrates oligo locations on the cIAP1 IRES secondary structure. (**d**) Confirmation of NF45 binding sites on the cIAP1 IRES by mutational analysis. Experiments were performed as in (**b**) with probe 3 ($3^{wildtype}$) or a mutant probe 3 with the bulge of SLI removed ($3^{\Delta CUUA}$). Alternatively, a probe corresponding to SLI of the cIAP1 IRES ($SLI^{wildtype}$) was used together with a sequence mutant that preserves the stem-loop structure (SLI^{s}), or a sequence mutant that also disrupts base pairing at the base of SLI (SLI^{ss}).

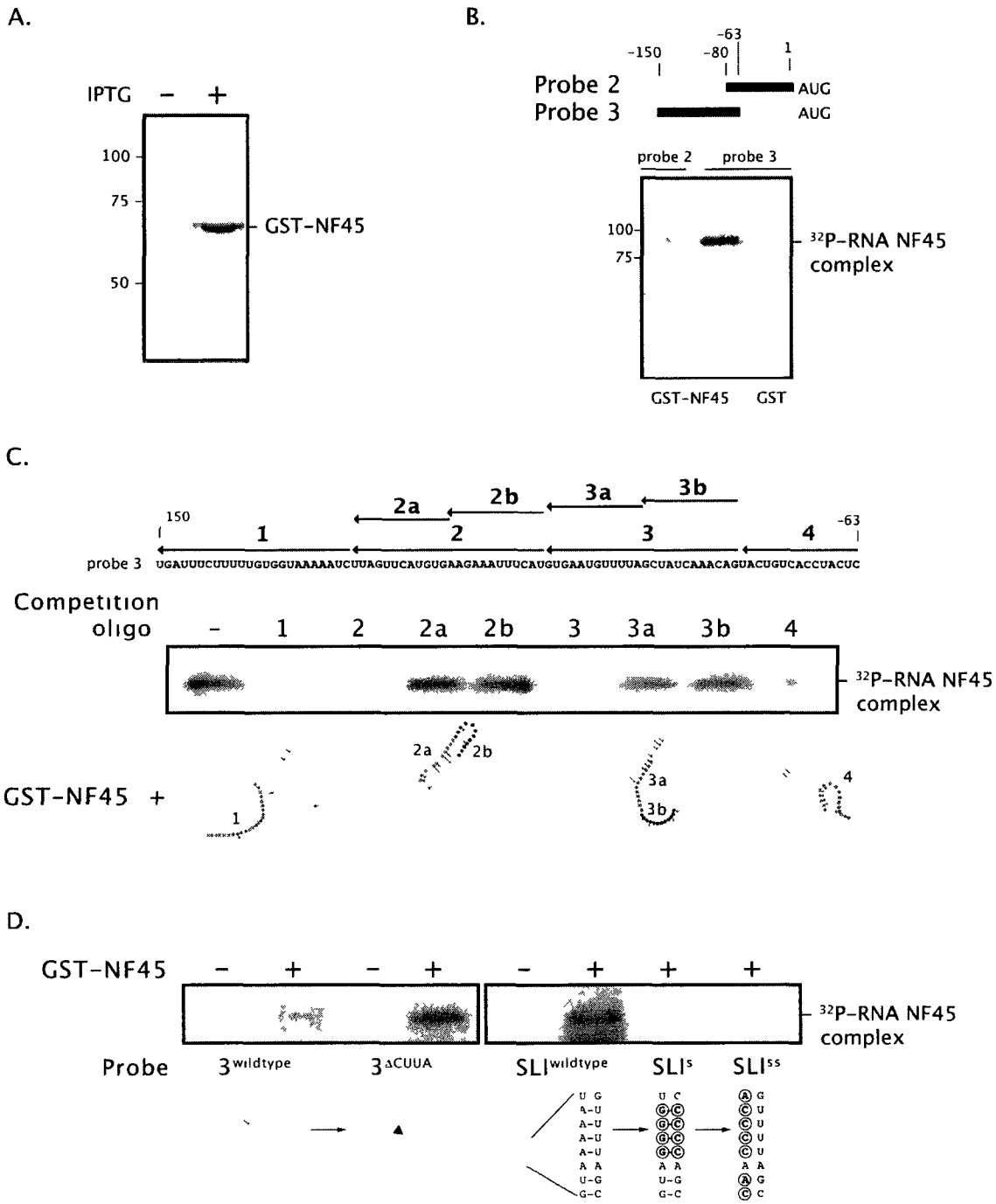
A.
IPTG – +
100
75
50
GST-NF45
B.
-63
-150
-80
1
Probe 2
Probe 3
AUG
AUG
probe 2
probe 3
100
75
32P-RNA NF45 complex
GST-NF45
GST
C.
150
-63
2a
2b
3a
3b
1
2
3
4
probe 3 UGAUUUCUUUUUGUGGUAAAAAUCUUAGUUCAUGUGAAGAAAUUUCAUGUGAAUGUUUUAGCUAUCAAACAGUACUGUCACCUACUC
Competition oligo
- 1 2 2a 2b 3 3a 3b 4
32P-RNA NF45 complex
GST-NF45 +
D.
GST-NF45
- + - + - + + +
32P-RNA NF45 complex
Probe
3wildtype
3ΔCUUA
SLIwildtype
SLIs
SLIss

In examining published nucleic acid motifs that interact with NF45 and/or NF90, we noted that the structure encapsidation signal RNA of hepatitis B virus (HBVε) resembles stem-loop I of the cIAP1 IRES including a prominent bulge. Shin et al.[33] showed that NF45/ NF90 interaction with HBVε RNA is dependent on the bulge of its stem-loop. We performed a similar experiment by deleting the CUUA nucleotide sequence that comprises the bulge within the cIAP1 IRES using site-directed mutagenesis to create Probe $3^{\Delta CUAA}$. Equivalent amounts of labelled RNA probe corresponding to the wildtype or CUUA mutant IRES were incubated with recombinant GST–NF45 or GST alone, followed by UV cross-linking and resolving the complex by SDS-PAGE. We found that the bulge in stem-loop I was not required for NF45 binding to the cIAP1 IRES (Figure 3.8d).

The results from our oligo competition experiment suggested that the AU-rich base of stem-loop I was important for binding to NF45. To directly confirm this hypothesis, we synthesized a new RNA probe corresponding to stem-loop I of the cIAP1 IRES (probe $SLI^{wildtype}$) as well as two mutant probes that could distinguish between sequence (SLI^{s}) and sequence+structure-dependent (SLI^{ss}) interactions. We found that NF45 interacts with the wildtype SLI RNA but not SLI^{s} or SL^{ss} mutants (Figure 3.8d). Together with the oligo masking data (specifically the lack of binding observed with oligo 2 that disrupts SL1 structure), we conclude that NF45 binds in a sequence and structure-specific manner to the AU stem-loop present in the cIAP1 IRES.

Discussion

Unlike cellular IRES, viral IRES exhibit conserved secondary structures that, with some exceptions, require minimal accessory factors to mediate recruitment of the ribosome.[21] This is in contrast to the limited homology shared by the published set of cellular IRES secondary structures.[34, 35] Indeed, the primary sequence and our empirically derived secondary structure of the cIAP1 IRES share no obvious similarity with the XIAP IRES and other published cellular IRES structures. Although cellular IRES comprise an evolutionarily divergent group, specific cellular RNA structure motifs have likely been co-opted by viruses at an early stage in evolution that allows them to compete for host ribosomes successfully. Meanwhile, the emerging need for eukaryotes to control protein synthesis in time and space may have lead to a greater dependence on ITAFs, which can modulate IRES activity of a diverse set of mRNAs in different physiological contexts. Indeed we found that cIAP1 IRES is unable to interact with the purified 40S ribosome in the absence of other protein factors.

In a search for protein factors that modulate translation of cIAP1 mRNA, we identified a cohort of RNA binding proteins, using the cIAP1 IRES as an RNA affinity probe. This complement of cIAP1 IRES binding proteins includes RNA helicase A, IGF2BP1, NF90 and NF45. The cIAP1 IRES is induced during ER stress, therefore we had initially attempted to compare protein–IRES interactions between cells treated with and without tunicamycin – a pharmacological inducer of ER stress. However, one-dimensional RNA affinity chromatography failed to reveal any differences in protein affinities and/or profiles following induction of ER stress (data not shown). This points to the possibility that the regulatory event that induces IRES activity during ER stress involves either post-

translational modifications or subcellular relocalization of cIAP1 ITAFs. Nevertheless, the protein complex that interacts with the cIAP1 IRES merits further investigation as all four of these proteins have been previously identified to interact with viral IRES elements, including those encoded by HRV2, hepatitis C virus (HCV) and bovine viral diarrhea virus (BVDV) genomes.[25, 36, 37] Importantly, no role for NF45 in translation of cellular mRNAs has been described. Interestingly, NF45/NF90 heterodimers were found to bind to the HRV2 IRES and inhibit translation of downstream cistrons.[26] It appears that inhibition of IRES activity by this binary complex is highly dependent on cell type. Merrill et al.[25] found that neuronal cells (including HEK293T) highly express both NF45 and NF90 that readily form heterodimers, and interact with the HRV2 IRES, leading to inhibition of downstream ORF expression. In contrast, cells from glial lineages were poor expressors of both NF45 and NF90 and showed impaired formation of functional inhibitory complexes. Complicating the study of NF45 or NF90 in isolation is the finding by Guan et al.[24] that targeting NF45 expression by RNA interference significantly decreases the stability of NF90 and vice versa. Therefore, we first looked at the function of NF45 in a glial cell line in which expression levels of NF45 and NF90 are limited.

In dissecting the individual function of NF45 in U373 glioblastoma cells, we have generated data in support of the hypothesis that NF45 is involved in the regulation of cellular IRES activity and by extension, cIAP1 protein levels. We have shown that NF45 is able to enhance translation of endogenous cIAP1 mRNA when transiently expressed in U373 glioblastoma cells. Importantly, NF45 overexpression did not significantly affect steady-state cIAP1 mRNA levels, suggesting that increased translation rates are not the result of

enhanced transcription or stability of cIAP1 mRNA. Indeed, we found that the cIAP1 mRNA pool was present in higher-order polysomes in cells expressing NF45, indicating that NF45 functions at the level of translation initiation. This report is the first to ascribe a direct role for NF45 in modulating the translation of a cellular mRNA, although circumstantial evidence of NF45 interacting with components of the canonical translational machinery (e.g., eIF2α/β/γ) exists in the literature.[38]

We identified NF45 interacting with the portion of the cIAP1 5′ UTR that confers IRES activity, therefore we surmised that the NF45-mediated changes in endogenous cIAP1 mRNA translation may be the result of NF45's ability to modulate cIAP1 IRES activity. To test this hypothesis we used a bicistronic expression vector previously used by our laboratory to assess cIAP1 IRES activity. Relative to cells expressing GFP, NF45-expressing cells exhibited a 240% increase in IRES activity indicating that NF45 modulates the translational efficiency of cIAP1 mRNA through its IRES. NF45 can therefore be categorized as a bona fide ITAF by virtue of its ability to modulate IRES activity.

To further delineate the specificity of NF45 ITAF activity we looked at the activity of several cellular IRES in HeLa cell lines that constitutively express shRNA targeting NF45 (*d5*) relative to cells that express a nontargeting shRNA (*c*). In these cells that have significantly reduced levels of NF45 expression, the activity of cIAP1 was significantly reduced, whereas other IRES (APAF-1, BclxL, DAP5, VCIP) exhibited no change or modest increase in activity (Figure 3.7a). These data point to the specificity of NF45 in modulating cIAP1 translation through its IRES.

We and others have shown that the cIAP1 IRES is induced as part of the UPR following ER stress. Therefore, the observed decrease in cIAP1 IRES activity in *d5* cells lead us to the hypothesis that these cells should be refractory to cIAP1 induction following ER stress. Indeed, after the treatment of cells with thapsigargin we observed an induction of cIAP1 in wildtype HeLa cells but not in cells stably expressing NF45 shRNA (Figure 3.7b). Interestingly, thapsigargin also failed to induce cIAP1 in our U373 glioblastoma cells (expressing low levels of NF45) despite robust induction of the ER stress marker BiP (data not shown). Furthermore, we were unable to rescue the phenotype of increased cIAP1 translation during the UPR with the introduction of ectopic NF90 in *d5* cells (Figure 3.7c). In contrast, reintroduction of RNAi-resistant NF45 into these cells induced endogenous levels of cIAP1 as expected (Figure 3.7c). These data suggest that the interaction of NF45 with its in vivo binding partner NF90 is not required for NF45 ITAF activity, although the data do not preclude the possibility that NF90 could act as a sink for NF45, thus reducing the effective ITAF activity of NF45 in the cell. The observation that overexpression of NF45 in the absence of ER stress can increase cIAP1 translation (in both *d5* and U373 cells) would argue for the 'sink' hypothesis, whereby NF45 ITAF activity is masked within a stable NF45/ NF90 heterodimer until a trigger (e.g. ER stress) releases it.

We next looked at physical interactions of NF45 with the cIAP1 IRES in vitro to shed light on the mechanism by which NF45 may be affecting cIAP1 IRES activity. Although there is no evidence in the current literature that NF45 interacts with RNA directly, the protein does contain two potential RNA binding domains, namely a DNA zinc-finger motif and an N-terminal RGG box motif. Importantly, we were able to resolve an NF45–IRES

complex following photo cross-linking of recombinant full-length NF45 and in vitro transcribed and labelled RNA corresponding to the cIAP1 IRES sequence. This shows that NF45 alone is sufficient to bind to the cIAP1 IRES in a sequence-dependent manner.

To determine the minimal NF45 binding site on the cIAP1 IRES, we used DNA oligonucleotide competitors to block potential binding sites within the IRES. From this data, we concluded that NF45 binding likely requires both sequence and structural motifs present in the base of the first stem-loop of the cIAP1 IRES. We confirmed this hypothesis by mutational analysis of stem-loop I. By mutating the AU-rich stem to a GC-rich stem, we were able to retain its structure but abrogate NF45 binding, suggesting that either the unstructured AAAA/UUUU stretch or the structured AU stem-loop was necessary (Figure 3.8d, mutant SLI^{s}). The efficient masking of binding with oligo 2 (that prevents formation of the AU stem-loop but preserves access to the single-stranded AAAA/UUUU sequence) from our oligo competition experiment allows us to conclude that primary sequence (i.e. AAAA/ UUUU) alone is not sufficient for binding of NF45, rather it is the base of the stem-loop formed by AU base pairs that are required. The lack of binding that we observed with a mutant that disrupts both sequence and structure in this region (SLI^{ss}) supports this conclusion. Further, stem-loop II of the IRES contains asymmetrical AU base pairs that may explain the partial binding with NF45 that we observed when using probes 2 and 3 that have stem-loop II in common (Figure 3.8b) and when masking with oligo 4 (Figure 3.8c). Intriguingly, the AU content of the UTRs that exhibited no change or increased IRES activity in NF45-deficient cells (Figure 3.7a) was significantly lower than that for cIAP1 (cIAP1,

70%; APAF1, 32%; BclxL, 46%; DAP5, 43%; VCIP, 34%). These observations suggest that the AU stem-loop motif is necessary for NF45 ITAF activity in the context of cIAP1.

Our interpretations agree with data from other groups who have investigated NF45 interactions with RNA. For example, using mutational analysis, Isken et al.[36] determined that the interaction of the NF45/NF90 proteins with HCV and BVDV 5′ and 3′ UTRs was dependent on both sequence and stem-loop structures. In another study NF45 and NF90 were found to interact with the HBVε RNA.[33] The authors showed that NF45/NF90 interaction with HBVε RNA is dependent on the bulge of its stem-loop.[33] We noticed that the HBVε structure resembles the first stem-loop of the cIAP1 IRES including a prominent bulge. On the basis of this, we hypothesized that this bulge would also be important for the NF45–cIAP1 IRES interaction. Surprisingly, we found that the bulge mutant (Figure 3.8d, mutant $3^{\Delta CUUA}$) showed no impairment in binding to NF45. This data imply that the NF45/NF90 heterodimer and NF45 alone have different sequence requirements for binding to RNA.

The specific domain(s) that is responsible for interaction of NF45 with the cIAP1 IRES remains unknown. A likely candidate is the conserved RGG box motif at the N terminus of the protein. RGG box motifs can serve as RNA binding domains and are present in many RNA binding proteins; therefore the potential importance of the RGG box motif in the context of NF45 and cIAP1 IRES interactions merits further investigation. The RGG box motifs in nucleolin and hnRNPU have been shown to disrupt RNA secondary structure in a nonspecific manner.[39, 40] For other proteins such as FMRP, the RGG box imparts a more specific RNA binding activity. Specifically, the RGG box within FMRP confers binding to planar RNA conformations referred to as G-quartet structures within mRNAs.[41, 42] The idea

that the cIAP1 IRES can adopt an inter- or intramolecular G-quartet structure that can have a role in translational regulation is an intriguing possibility. Whether the NF45 RGG box could participate in a manner analogous to FMRP is an open question that is currently under investigation.

The mechanism that the cIAP1–ITAF complex may use to modulate translation remains to be elucidated; however we have shown that NF45, a component of this complex, is able to interact directly with the cIAP1 IRES and positively affect its activity, resulting in increased translation of cIAP1 mRNA. Thus, NF45 is a novel RNA binding protein and ITAF that functions to upregulate cIAP1 translation during ER stress.

Materials and Methods

Cell culture, expression constructs and transfection. Human embryonic kidney (HEK293T) and human glioblastoma (U373MG) cells were maintained in standard conditions in serum- and antibiotic-supplemented Dulbecco's modified Eagle's medium (DMEM). *c* and *d5* HeLa cell lines were previously characterized[24].HeLa cells expressing shRNA were maintained under selective pressure with 400 μg/ml of G418 (Invitrogen, Burlington, ON, Canada). For transient knockdown of NF45, we transfected 293T cells with two rounds of 50 nM *d5* siRNA and Lipofectamine 2000 (Invitrogen) over a period of 96 h. The full-length NF45 ORF from an NF45 expression plasmid (pEF.NF45.HA; Kao et al.[20]) was re-cloned into a pcDNA3 backbone as an N-terminal FLAG-tagged vector (pcDNA3.F.NF45) and verified by sequencing. Transient transfections of U373MG cells

were performed using Amaxa nucleofector technology (Lonza, Germany; solution T, programme T-020). Transfection efficiency was verified by light microscopy, western blotting and RT-PCR. For *d5* rescue experiments, 2 μg O.NF90c[24] or F.NF45r (an RNAi-resistant version of F.NF45 in which a silent mutation was introduced by SDM) DNA was transfected using Lipofectamine 2000 (Invitrogen). Unless otherwise stated, all assays were performed 24 h after transfection.

RNA secondary structure determination. The cIAP1 IRES secondary structure was determined using enzymatic probing with RNases as described previously.[34] RNase cut sites were used as constraints in either mfold[22] or RNAStructure[43] to predict secondary structure models. The RNA secondary structure graphic was generated using jViz.Rna (Available at: http://jviz.cs.sfu.ca).

In vitro transcription. DNA templates for the synthesis of the cIAP1 RNA probes were generated from a cIAP1 5′ UTR-containing plasmid (probes 1–3) or synthesized oligonucleotides (for SLI probes) by PCR. The 5′ primers incorporated the T7 promoter sequence. For UV cross-linking experiments, we synthesized labeled RNA probes by in vitro transcription with T7 polymerase (MAXIscript kit; Applied Biosystems, Streetsville, ON, Canada) in the presence of [α-^{32}P]UTP (PerkinElmer, Woodbridge, ON, Canada) followed by gel purification of full-length transcripts. For RNA affinity chromatography, unlabeled RNA was synthesized using T7 polymerase (MEGAshortscript; Applied Biosystems).

RNA affinity chromatography. For preparation of cytoplasmic lysates, confluent HEK293T cells were resuspended in lysis buffer (10 mM Tris-HCl (pH 7.4), 1.5 mM MgCl2, 10 mM KCl, 0.5 mM DTT, 0.1 mM PMSF, 10 μg/ml leupeptin) and dounce-homogenized. Lysates were centrifuged at 10 000 × g for 10 min at 4°C, and the supernatant was retained. Protein concentration was determined using a modified Lowry Assay (DC Protein Assay; Bio-Rad, Mississauga, ON, Canada). In vitro synthesized cIAP1 RNA was 5′ end-labeled with biotin (5′ End Tag; Vector Laboratories, Burlington, ON, Canada), and conjugated to avidin-coated agarose beads (Sigma-Aldrich, Oakville, ON, Canada) for 2 h at 4°C in the presence of RNA binding buffer (10 mM Tris-HCl (pH 7.4), 150 mM KCl, 1.5 mM MgCl2, 0.5 mM DTT, 0.5 mM PMSF, 0.05% NP-40, 10 μg/ml leupeptin and 1 U/ml RNase inhibitor). The beads were then washed twice with RNA binding buffer and incubated with 200 μg of precleared HEK293T S10 extract and 30 μg of wheat germ tRNA (Sigma-Aldrich) for 30 min at room temperature followed by an additional 2 h at 4°C. The beads were then washed five times with RNA binding buffer and bound proteins were released by boiling in Laemmli buffer. Captured proteins were resolved on 10%SDS-PAGE and stained overnight with SYPRO Ruby (Invitrogen). Specific bands were excised and analyzed by MALDI-TOF mass spectrometry and peptide mass fingerprinting (Queen's University Protein Function Discovery Facility, Kingston, Canada).

Western blot analysis. Cells were lysed in RIPA buffer for 30 min at 4°C, followed by centrifugation at 10 000 × g to remove debris. Equal amounts of protein were resolved by 10% SDS-PAGE, transferred to PVDF membranes using a semidry transfer protocol and

probed with antibodies to RNA Helicase A (Center for Biomedical Inventions, University of Texas Southwestern at Dallas), NF90 (anti-DRBP76; BD Laboratories or anti-NF9044), IGF2BP1 (anti-IMP1; a gift from Dr. F Nielsen), NF45,[44] HuR (clone 3A2; Santa Cruz Biotechnology), TIA-1/TIAR (clone 3E6; a gift from Dr. P Anderson), hnRNP A1 (Santa Cruz Biotechnology, Santa Cruz, CA, USA), β-actin (Sigma-Aldrich) and GAPDH (BD Laboratories, Mississauga, ON, Canada). Membranes were then incubated with species-specific horseradish-peroxidase-conjugated secondary antibody (GE Biosciences, Baie d'Urfe, QC, Canada) followed by detection with ECL+ substrate (GE Biosciences). Alternatively, membranes were incubated with Alexa 680-conjugated (Invitrogen) or IR 800-conjugated (LI-COR Biotechnology, Lincoln, NE, USA) secondary antibody followed by detection using the Licor Odyssey Infrared scanner.

Metabolic labelling/immunoprecipitation. A total of 1.5 × 106 U373MG cells were nucleofected with 10 μg of GFP or NF45 DNA plasmid and seeded in 10 cm plates 24 h before assay. Cells were incubated with DMEM lacking methionine and cysteine and supplemented with 10% FCS (Invitrogen) for 15 min at 37°C. Cells were pulse-labeled with 0.1 mCi/ml ^{35}S-methionine and cysteine mix (EasyTag EXPRE^{35}S^{35}S Protein Labelling Mix; PerkinElmer) for 25 min at 37°C. Cells were washed, harvested in cold PBS and boiled in 50 μl of denaturing lysis buffer (50 mM Tris (pH 7.4), 5 mM EDTA, 1%SDS, 10 mM DTT, 1 mM PMSF, 2 μg/ml leupeptin, 15 U/ml DNaseI) for 5 min. Cold nondenaturing buffer (450 μl; 50 mM Tris (pH 7.4), 5 mM EDTA, 300 mM NaCl, 1%Triton X-100, 10 mM iodoacetamide, 1 mM PMSF, 2 μg/ml leupeptin) was then added and the lysate was passed

through a 25-gauge syringe needle 10 times. Following centrifugation to remove debris, we precleared the lysate before immunoprecipitation with Pansorbin cells for 2 h at 4°C (EMD Chemicals, Gibbstown, NJ, USA). Co-immunoprecipitation of cIAP1 and β-actin from the precleared lysates was performed at 4°C for 16 h using Protein G/Protein A-Agarose beads (EMD Chemicals) coated with antibodies specific for β-actin (Sigma-Aldrich) and cIAP145 at a titer of 1:500 and 1:150, respectively. The beads were then washed extensively with cold wash buffer (50 mM Tris (pH 7.4), 300 mM NaCl, 0.1% Triton X-100), resuspended in Laemmli buffer and boiled to elute bound proteins. Immunoprecipitated proteins or total proteins were then resolved on 10% SDS-PAGE. The gel was incubated with Amplify fluorogenic reagent (GE Biosciences) for 30 min before drying and exposure to film. Densitometric analysis was performed using Licor Odyssey software (LI-COR Biotechnology).

Quantitative RT-PCR. To measure relative mRNA expression, total RNA was isolated from U373MG cells 24 h after transient expression of GFP or NF45 (Absolutely RNA miniprep; Agilent Technologies, La Jolla, CA, USA) and cDNA generated (First-Strand cDNA synthesis kit; GE Biosciences). Quantitative PCR was performed on an ABI Prism 7000 real-time thermocycler using 1 μg total RNA together with SYBRGreen (Qiagen, Mississauga, ON, Canada) and gene-specific primers (cIAP1: TCTGGAGATGATCCATGGGTAGA, TGGCCTTTCATTCGTATCAAGA; β-actin: CTGGAACGGTGAAGGTGACA, AAGGGACTTCCTGTAACAATGCA; NF45: GACACAATGTGGCTGACCTG, GAAGATTGGGTGGCACTGTT). Relative expression levels were determined using the

standard curve method. Controls lacking RT showed no significant genomic DNA amplification (>10 cycle difference).

Polysome profiling. A total of 5×10^6 U373MG cells were nucleofected with 10 μg of GFP or NF45 plasmid DNA 72 h before polysome profiling. Cells were incubated with 0.1 mg/ml cycloheximide for 3 min, washed with cold PBS+cycloheximide and lysed in cold polysome lysis buffer (15 mM Tris-HCl (pH 7.4), 15 mM MgCl2, 300 mM NaCl, 1%(v/v) Triton X-100, 0.1 mg/ml cycloheximide, 100 U/ml RNasin). Equal OD254 units were loaded onto 10–50% linear sucrose gradients and centrifuged at 39 000 r.p.m. for 90 min at 4°C. Gradients were fractionated from the top (Densi-Flow; Labconco, Kansas City, MO, USA) and RNA/protein was monitored at 254 nm using a HPLC system (Akta Explorer; GE Biosciences). Fractions (1 ml) were collected and flash-frozen in liquid nitrogen. RNA was isolated from individual fractions by proteinase K digestion followed by phenol/chloroform extraction. Equal volumes of RNA from each fraction were used to generate cDNA using oligo-dT primers and a reverse transcription kit (First-Strand cDNA synthesis kit; GE Biosciences). PCR primers specific for cIAP1 or β-actin (c.f. last section for specific sequences) were used to amplify messages using a limited-cycle PCR. Amplified cDNA was resolved on agarose gel, and visualized with ethidium bromide. Genomic DNA contamination in controls lacking RT was undetectable.

IRES activity assay. A total of 1×10^6 U373MG cells were nucleofected with 6 μg βGAL/ cIAP1/CAT bicistronic vector containing the full-length cIAP1 5′ UTR (nucleotides −1222 to

−1) and 2 μg GFP or NF45 expression vector. For monocistronic experiments, CAT expression constructs with the 1.2 kb 5′ UTR or a mutant containing nucleotides −80 to −1 of the 5′ UTR were used together with a β-GAL expression construct. For *c* and *d5* HeLa cell experiments, we seeded 6 × 10^5 cells 24 h before Lipofectamine 2000 (Invitrogen) transfection with 2 μg bicistronic vectors harbouring cIAP1, APAF-1, BclxL, DAP5 and VCIP IRES. Protein lysates were harvested after 24 h using CAT lysis buffer (Roche Diagnostics, Laval, QC, Canada). β-GAL activity was assessed using an ONPG colorimetric assay. CAT expression was quantified by ELISA according to the manufacturer's protocol (Roche Diagnostics). Spurious splicing and potential cryptic promoter activity that could arise with the pBGAL/cIAP1/CAT bicistronic vector has been previously addressed.[27]

Recombinant NF45 expression and purification. The full-length ORF of human NF45 was amplified from pEF.NF45.HA by PCR and cloned into a bacterial GST expression plasmid (pGEX-KG). Expression of GST-NF45 (72 kDa) was induced with 100 nM IPTG for 4 h at 37°C. Cells were lysed on ice with lysozyme, 1.5% Sarkosyl, DNase I and protease inhibitors. Triton X-100 (4%) was added to solubilize proteins before clarification by centrifugation. Lysates were incubated with Glutathione Sepharose 4B beads (GE Biosciences) for 16 h and GST moieties were eluted with reduced glutathione (20 mM glutathione, 30 mM Na2HPO4, 0.1% (w/v) CHAPS, pH 9.5) for 2 h at 4°C. Purity was assessed by SDS-PAGE and Coomassie staining.

RNA UV cross-linking. [α-^{32}P]UTP-labeled, in vitro transcribed cIAP1 RNA (40 000 c.p.m.) was incubated with 300–500 ng of GST-NF45 for 25 min at room temperature in an RNA binding buffer (10 mM Tris-HCl (pH 7.4), 1.5 mM MgCl2, 150 mM KCl, 0.5 mM DTT, 0.1 mM PMSF, 10 mg/ml leupeptin). Samples were UV-irradiated (250 mJ/cm2) on ice using a Stratagene Stratalinker, followed by treatment with 2 U of RNase A/T1 and 100 μg of heparin. Complexes were resolved by SDS-PAGE and visualized by autoradiography.

Conflict of interest

The authors declare no conflict of interest.

Acknowledgements

We thank Dr. E Jan for the help with the ribosome electromobility shift assay. This work was supported by an operating grant from the Canadian Institutes for Health Research (FRN 74740) to MH and from the National Institutes of Health (NIH AI 034552) to MBM. TEG was supported by the Frederick Banting and Charles Best Canada Graduate Scholarships Doctoral Award. MH is the CHEO Volunteer Association Endowed Scholar.

References

1. Qin X, Sarnow P. Preferential translation of internal ribosome entry site-containing mRNAs during the mitotic cycle in mammalian cells. *J Biol Chem* 2004; **279**: 13721–13728.

2. Gerlitz G, Jagus R, Elroy-Stein O. Phosphorylation of initiation factor-2 alpha is required for activation of internal translation initiation during cell differentiation. *Eur J Biochem* 2002; **269**: 2810–2819.

3. Bushell M, Sarnow P. Hijacking the translation apparatus by RNA viruses. *J Cell Biol* 2002; **158**: 395–399.

4. Lewis SM, Cerquozzi S, Graber TE, Ungureanu NH, Andrews M, Holcik M. The eIF4G homolog DAP5/p97 supports the translation of select mRNAs during endoplasmic reticulum stress. *Nucleic Acids Res* 2008; **36**: 168–178.

5. Yoshimura FK, Luo X, Zhao X, Gerard HC, Hudson AP. Up-regulation of a cellular protein at the translational level by a retrovirus. *Proc Natl Acad Sci* USA 2008; **105**: 5543–5548.

6. Koritzinsky M, Magagnin M, Van Den Beucken T, Seigneuric R, Savelkouls K, Dostie J *et al.* Gene expression during acute and prolonged hypoxia is regulated by distinct mechanisms of translational control. *EMBO J* 2006; **25**: 1114–1125.

7. Yang DQ, Halaby MJ, Zhang Y. The identification of an internal ribosomal entry site in the 50-untranslated region of p53 mRNA provides a novel mechanism for the regulation of its translation following DNA damage. *Oncogene* 2006; **25**: 4613–4619.

8. Pestova TV, Lorsch JR, Hellen CUT. Translational control in biology and medicine. In: Mathews M, Sonenberg N, Hershey JWB (eds). Cold Spring Harbor Monograph Series. 3rd edn. Cold Spring Harbor Laboratory Press: Cold Spring Harbor, NY, 2007. pp 87–128.

9. Holcik M, Sonenberg N. Translational control in stress and apoptosis. *Nat Rev Mol Cell Biol* 2005; **6**: 318–327.

10. Bushell M, Stoneley M, Kong Y, Hamilton T, Spriggs K, Dobbyn H *et al.* Polypyrimidine tract binding protein regulates IRES-mediated gene expression during apoptosis. *Mol Cell* 2006; **23**: 401–412.

11. Lewis SM, Veyrier A, Hosszu Ungureanu N, Bonnal S, Vagner S, Holcik M. Subcellular relocalization of a trans-acting factor regulates XIAP IRES-dependent translation. *Mol Biol Cell* 2007; **18**: 1302–1311.

12. Holcik M, Korneluk RG. Functional characterization of the X-linked inhibitor of apoptosis (XIAP) internal ribosome entry site element: role of La autoantigen in XIAP translation. *Mol Cell Biol* 2000; **20**: 4648–4657.

13. Holcik M, Gordon BW, Korneluk RG. The internal ribosome entry site-mediated translation of antiapoptotic protein XIAP is modulated by the heterogeneous nuclear ribonucleoproteins C1 and C2. *Mol Cell Biol* 2003; **23**: 280–288.

14. Mitchell SA, Spriggs KA, Bushell M, Evans JR, Stoneley M, Le Quesne JP *et al.* Identification of a motif that mediates polypyrimidine tract-binding protein-dependent internal ribosome entry. *Genes Dev* 2005; **19**: 1556–1571.

15. Yaman I, Fernandez J, Liu H, Caprara M, Komar AA, Koromilas AE *et al.* The zipper model of translational control: a small upstream ORF is the switch that controls structural remodeling of an mRNA leader. *Cell* 2003; **113**: 519–531.

16. Vince JE, Wong WW, Khan N, Feltham R, Chau D, Ahmed AU *et al.* IAP antagonists target cIAP1 to induce TNF alpha-dependent apoptosis. *Cell* 2007; **131**: 682–693.

17. Varfolomeev E, Blankenship JW , Wayson SM, Fedorova AV, Kayagaki N, Garg P *et al.* IAP antagonists induce autoubiquitination of c-IAPs, NF-kappaB activation, and TNF alpha-dependent apoptosis. *Cell* 2007; **131**: 669–681.

18. Warnakulasuriyarachchi D. Translational induction of the inhibitor of apoptosis protein HIAP2 during endoplasmic reticulum stress attenuates cell death and is mediated via an inducible internal ribosome entry site element. *J Biol Chem* 2004; **279**: 17148–17157.

19. Van Eden ME, Byrd MP, Sherrill KW, Lloyd RE. Translation of cellular inhibitor of apoptosis protein 1 (c-IAP1) mRNA is IRES mediated and regulated during cell stress. *RNA* 2004; **10**: 469–481.

20. Kao PN, Chen L, Brock G, Ng J, Kenny J, Smith AJ *et al.* Cloning and expression of cyclosporin A- and FK506-sensitive nuclear factor of activated T-cells: NF45 and NF90. *J Biol Chem* 1994; **269**: 20691–20699.

21. Baird SD, Turcotte M, Korneluk RG, Holcik M. Searching for IRES. *RNA* 2006; **12**: 1755–1785.

22. Zuker M. Mfold web server for nucleic acid folding and hybridization prediction. *Nucleic Acids Res* 2003; **31**: 3406–3415.

23. Jan E, Sarnow P. Factorless ribosome assembly on the internal ribosome entry site of cricket paralysis virus. *J Mol Biol* 2002; **324**: 889–902.

24. Guan D, Altan-Bonnet N, Parrott AM, Arrigo CJ, Li Q, Khaleduzzaman M *et al.* Nuclear factor 45 (NF45) is a regulatory subunit of complexes with NF90/110 involved in mitotic control. *Mol Cell Biol* 2008; **28**: 4629–4641.

25. Merrill MK, Dobrikova EY, Gromeier M. Cell-type-specific repression of internal ribosome entry site activity by double-stranded RNA-binding protein 76. *J Virol* 2006;

80: 3147–3156.

26. Merrill M. The double-stranded RNA binding protein 76: NF45 heterodimer inhibits translation initiation at the rhinovirus type 2 internal ribosome entry site. *J Virol* 2006; **80**: 6936–6942.

27. Holcik M. Spurious splicing within the XIAP 50 UTR occurs in the Rluc/Fluc but not the gal/ CAT bicistronic reporter system. *RNA* 2005; **11**: 1605–1609.

28. Ungureanu NH, Cloutier M, Lewis SM, de Silva N, Blais JD, Bell JC *et al.* Internal ribosome entry site-mediated translation of Apaf-1, but not XIAP, is regulated during UV-induced cell death. *J Biol Chem* 2006; **281**: 15155–15163.

29. Yoon A. Impaired control of IRES-mediated translation in X-linked dyskeratosis congenita. *Science* 2006; **312**: 902–906.

30. Marash L, Liberman N, Henis-Korenblit S, Sivan G, Reem E, Elroy-Stein O *et al.* DAP5 promotes cap-independent translation of Bcl-2 and CDK1 to facilitate cell survival during mitosis. *Mol Cell* 2008; **30**: 447–459.

31. Blais JD, Addison CL, Edge R, Falls T, Zhao H, Wary K *et al.* Perk-dependent translational regulation promotes tumor cell adaptation and angiogenesis in response to hypoxic stress. *Mol Cell Biol* 2006; **26**: 9517–9532.

32. Ranpura SA, Deshmukh U, Reddi PP. NF45 and NF90 in murine seminiferous epithelium: potential role in SP-10 gene transcription. *J Androl* 2008; **29**: 186–197.

33. Shin HJ, Kim SS, Cho YH, Lee SG, Rho HM. Host cell proteins binding to the encapsidation signal epsilon in hepatitis B virus RNA. *Arch Virol* 2002; **147**: 471–491.

34. Baird SD, Lewis SM, Turcotte M, Holcik M. A search for structurally similar cellular internal ribosome entry sites. *Nucleic Acids Res* 2007; **35**: 4664–4677.

35. Xia X, Holcik M. Strong eukaryotic IRESs have weak secondary structure. *PLoS ONE* 2009; **4**: e4136.

36. Isken O, Baroth M, Grassmann CW, Weinlich S, Ostareck DH, Ostareck-Lederer A *et al.* Nuclear factors are involved in hepatitis C virus RNA replication. *RNA* 2007; **13**: 1675–1692.

37. Isken O, Grassmann CW, Sarisky RT, Kann M, Zhang S, Grosse F *et al.* Members of the NF90/NFAR protein group are involved in the life cycle of a positive-strand RNA

virus. *EMBO J* 2003; **22**: 5655–5665.

38. Ting NS, Kao PN, Chan DW, Lintott LG, Lees-Miller SP. DNA-dependent protein kinase interacts with antigen receptor response element binding proteins NF90 and NF45. *J Biol Chem* 1998; **273**: 2136–2145.

39. Kiledjian M, Dreyfuss G. Primary structure and binding activity of the hnRNP U protein: binding RNA through RGG box. *EMBO J* 1992; **11**: 2655–2664.

40. Ghisolfi L, Joseph G, Amalric F, Erard M. The glycine-rich domain of nucleolin has an unusual supersecondary structure responsible for its RNA-helix-destabilizing properties. *J Biol Chem* 1992; **267**: 2955–2959.

41. Darnell JC, Jensen KB, Jin P, Brown V, Warren ST, Darnell RB. Fragile X mental retardation protein targets G quartet mRNAs important for neuronal function. *Cell* 2001; **107**: 489–499.

42. Ramos A, Hollingworth D, Pastore A. G-quartet-dependent recognition between the FMRP RGG box and RNA. *RNA* 2003; **9**: 1198–1207.

43. Mathews DH, Disney MD, Childs JL, Schroeder SJ, Zuker M, Turner DH. Incorporating chemical modification constraints into a dynamic programming algorithm for prediction of RNA secondary structure. *Proc Natl Acad Sci* USA 2004; **101**: 7287–7292.

44. Parrott AM, Walsh MR, Reichman TW, Mathews MB. RNA binding and phosphorylation determine the intracellular distribution of nuclear factors 90 and 110. *J Mol Biol* 2005; **348**: 281–293.

45. Zhao TT, Graber TE, Jordan LE, Cloutier M, Lewis SM, Goulet I *et al.* hnRNP A1 regulates UV-induced NF-kappaB signalling through destabilization of cIAP1 mRNA. *Cell Death Differ* 2009; **16**: 244–252.

CHAPTER 4

Nucleotide composition of cellular IRES predicts a post-transcriptional operon

Preamble

"Nucleotide composition of cellular IRES predicts a post-transcriptional operon" is an unpublished manuscript. The article identifies XIAP as an additional target of NF45 ITAF activity. Further, the article provides evidence that other NF45-dependent IRES can be predicted based only on the nucleotide composition of their 5'UTRs. The identified NF45-dependent mRNAs are involved in common cellular pathways that serve to maintain genomic integrity and are hypothesized to represent an IRES-based RNA operon.

Author list: Tyson E. Graber and Martin Holcik

Author contributions: TEG wrote the article. TEG designed and performed experiments presented in Figures 4.1-5.

I would also like to thank Dr. Stephen Baird for spending a good chunk of his time helping me with the Perl script that allowed for the calculation of AU content within a sequence database (which completes the task in a few seconds rather than a few hours) and for allowing me to ~~play with~~ use the Cellomics HCS automated imaging system.

Introduction

The vast majority of cellular mRNAs initiate their translation through a well-defined mechanism of ribosome recruitment that occurs at the 5' terminal 7-methyl-GDP with the help of several canonical protein factors. A subset of cellular and viral mRNAs contain regulatory motifs in their 5' untranslated regions (UTR) termed Internal Ribosome Entry Sites (IRES) that usurp the canonical mode of initiation. In eukaryotes, this mechanism requires IRES trans-acting protein factors (ITAFs) that facilitate ribosome recruitment downstream of the 5' terminus. While several ITAFs and their target mRNAs have been empirically identified, in silico prediction of ITAF targets has proved difficult due to poor definition of consensus binding motifs within their target IRES. Here, we report that high AU content (>60%) of 5' untranslated regions harbouring IRES serves as an excellent predictor of dependence on the recently identified and evolutionarily conserved ITAF, NF45. Moreover, we provide evidence that cells deficient in NF45 ITAF activity exhibit dysregulated IRES-mediated translation of mRNAs that function in DNA damage repair, apoptosis and NF-κB signalling. This specific defect in IRES translation may explain the cytokinesis impairment observed in HeLa cells expressing NF45 RNAi that leads to aneuploidy and a senescent-like phenotype. Together, these data indicate that NF45 is required for appropriate cell growth and functions by controlling a post-transcriptional RNA operon that is necessary for the maintenance of genomic integrity, apoptotic threshold and appropriate NF-κB signalling within the cell.

Results and Discussion

NF45 regulates XIAP IRES and interacts outside of the polypyrimidine tract

We initially identified NF45 as an ITAF that regulates the cellular Inhibitor of Apoptosis Protein 1 (cIAP1) IRES during the unfolded protein response.[1] To address the question of whether NF45 ITAF activity was specific to the cIAP1 IRES or whether it could regulate other IRES, we screened several IRES-containing mRNAs for their dependence on NF45 expression. Our experimental system consists of HeLa cells that stably express shRNA targeting NF45 (*d5* cells) and cells expressing non-targeting shRNA (*c* cells). These cells have been previously characterized and exhibit significantly reduced expression of NF45, while the expression of its binding partner, NF90 remains largely unaffected.[2] We then transiently transfected these cell lines with bicistronic constructs harbouring various cellular or viral IRES to measure IRES activity in cells deficient in NF45 relative to cells expressing normal levels of NF45. Using this system we have previously shown in our initial screen of six cellular IRES that decreased expression of NF45 drastically affects the activity of cIAP1 (>2-fold decrease in activity) but spares the activity of other IRES such as APAF-1, BclxL, DAP5, and VCIP.[1] These results indicated that NF45 ITAF activity does not target all IRES.

Because cIAP1 is a member of the inhibitor of apoptosis family of proteins we extended our screen to determine whether another IRES-containing family member, the X-linked Inhibitor of Apoptosis Protein (XIAP) is regulated by NF45. We assessed XIAP IRES activity in *d5* versus *c* cells and found a significant (75%) decrease in activity (Figure 4.1B). To ensure that this assay accurately reflected NF45 ITAF function we also tested the activity of the encephalomyocarditis virus (EMCV) IRES in *d5* versus *c* cells. Unlike cellular IRES,

Figure 4.1

NF45 regulates IRES-mediated translation of XIAP and interacts outside of the polypyrimidine tract. (**A**) Schematic of bicistronic DNA constructs used to assess IRES activity. The XIAP IRES is inserted between the upstream (β-GAL ORF, reporting cap-dependent translation) and downstream (CAT ORF, reporting IRES-mediated translation). Cells were transiently transfected and the ratio of CAT/β-GAL was reported as relative IRES activity. (**B**) IRES activity of XIAP and EMCV IRES in *d5* versus *c* cells. Note that a ratio of 1.0 is indicative of no change in IRES activity between the two cell lines. (**C**) NF45 interacts specifically with the XIAP IRES. Western blot of an RNA affinity chromatography preparation with no RNA or XIAP IRES RNA used as bait. (**D**) Western blot showing that endogenous XIAP protein expression is impaired in *d5* cells relative to *c* cells. (**E**) Although the predicted secondary structures of the cIAP1 and XIAP IRES are dissimilar, a putative NF45 binding site defined by an AU-rich stem motif lies within the first stemloop (SLI) of the XIAP IRES. (**F**) NF45 interacts outside of the XIAP poypyrimidine tract (PPT). Western blot of an RNA affinity chromatography preparation with wildtype (wt) XIAP IRES RNA or SLII-deleted XIAP IRES (ΔSLII) used as bait. Blots were probed with antibodies detecting NF45 or polypyrimidine tract binding protein (PTB).

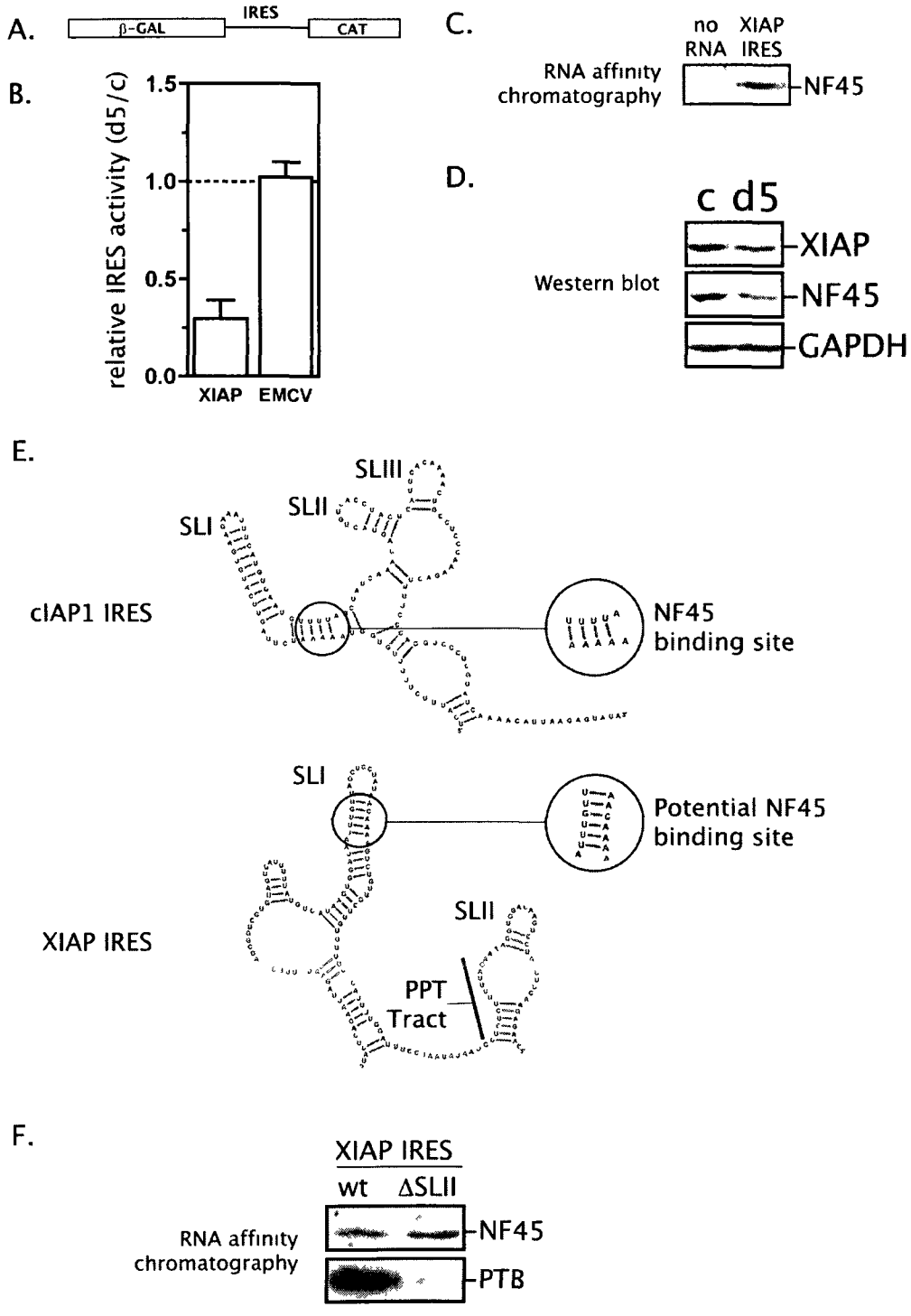
A.
IRES
β-GAL
CAT
B.
relative IRES activity (d5/c)
1.5
1.0
0.5
0.0
XIAP
EMCV
C.
no RNA
XIAP IRES
RNA affinity chromatography
NF45
D.
c d5
Western blot
XIAP
NF45
GAPDH
E.
SLIII
SLII
SLI
cIAP1 IRES
NF45 binding site
SLI
Potential NF45 binding site
SLII
XIAP IRES
PPT Tract
F.
XIAP IRES
wt
ΔSLII
RNA affinity chromatography
NF45
PTB

the EMCV IRES does not require ITAFs for its activity and should therefore be unaffected by the lack of NF45 in *d5* cells. Indeed, we found that EMCV IRES activity remained unchanged in cells expressing low amounts of NF45 (Figure 4.1B). To determine if NF45 is a bona fide XIAP ITAF we used an RNA affinity chromatography approach to pull down XIAP binding proteins from a HEK293T cytoplasmic lysate using in vitro transcribed XIAP IRES as bait. A western blot of this affinity preparation revealed that NF45 does specifically interact with the XIAP IRES but not with a matrix lacking RNA (Figure 4.1C). Importantly, we also found that decreased XIAP IRES activity in *d5* cells results in a concomitant decrease (~30%) in endogenous XIAP protein levels (Figure 4.1D).

Previously published data from our laboratory indicates that NF45 interacts with an AU-rich stem structure present within the cIAP1 IRES.[1] We therefore hypothesized that a NF45-dependent IRES sequence would contain an AU-rich stem. We compared the known RNA secondary structures of the cIAP1[1] and XIAP[3] IRES and noted an AU-rich stem motif present in the first stem-loop of the XIAP IRES that could conceivably participate in binding NF45 (Figure 4.1E). Supporting this assertion, we found that NF45 associated with either the wildtype (wt) XIAP IRES or a mutant IRES lacking stemloop II (ΔSLII) in our RNA affinity chromatography preparations, while polypyrimidine tract binding protein (PTB) failed to bind the stemloop II mutant (Figure 4.1F). Importantly, previous XIAP IRES mutants generated in our laboratory that lack this first stemloop were found to have significantly decreased IRES activity.[4] Together, these data indicate that NF45 interacts with the first stemloop of the XIAP IRES and positively affects its activity, leading to increased XIAP protein expression.

AU content of 5'UTRs correlates with NF45-dependent IRES activity

We next surveyed the nucleotide composition of the seven IRES tested in our NF45 ITAF activity assay along with the composition of their respective 5'UTRs to determine whether AU content correlates with NF45-dependent IRES activity. A diagonal plot of the %AU content of these 5'UTRs (APAF1, BclxL, cIAP1, DAP5, EMCV, VCIP, XIAP) against that of their IRES is shown in Figure 4.2. The nucleotide composition of known IRES does not significantly deviate from that of their 5'UTRs.[5] Therefore, this constraint alone cannot be used to predict novel IRES. However, the diagonal plot of our known NF45-dependent IRES (cIAP1 and XIAP) revealed a strong correlation between the AU content of these two IRES and their requirement for NF45. Specifically, cIAP1 and XIAP IRES are both AU-rich *and* NF45-dependent, while APAF1, BclxL, DAP5, VCIP and EMCV IRES are GC-rich *and* NF45-independent. These initial observations led us to the intriguing hypothesis that AU content of a 5'UTR could predict IRES that are dependent on NF45 for their activity.

To address this hypothesis, we surveyed the entire set of known IRES-containing RNAs[5] and calculated the AU content of their 5'UTR and minimal IRES (if known). We ranked a list of 90 known eukaryotic IRES based on AU content and further considered only human IRES in our experiments. This resulted in a list of 9 IRES with an AU content greater than 50% in their respective 5'UTRs to be carried forward for testing in the wet laboratory (Figure 4.2B).

Figure 4.2

AU content of 5'UTRs correlates with NF45-dependent IRES activity. **(A)** Diagonal plot showing relationship of NF45 ITAF activity and the AU content of 5'UTRs and IRES. We have previously shown that NF45 expression does not affect BclxL, DAP5, APAF-1, and VCIP IRES activities (closed-circle=NF45-independent IRES) but does impact cIAP1 and, as we have shown in Figure 4.1, XIAP IRES activities (open-circle=NF45-dependent).[1] **(B)** Table of IRES-containing human mRNAs that have >50% AU content within their 5'UTRs. The percent AU content of the minimal IRES (if unknown, content is equivalent to that of 5'UTR) is indicated in brackets.

A.

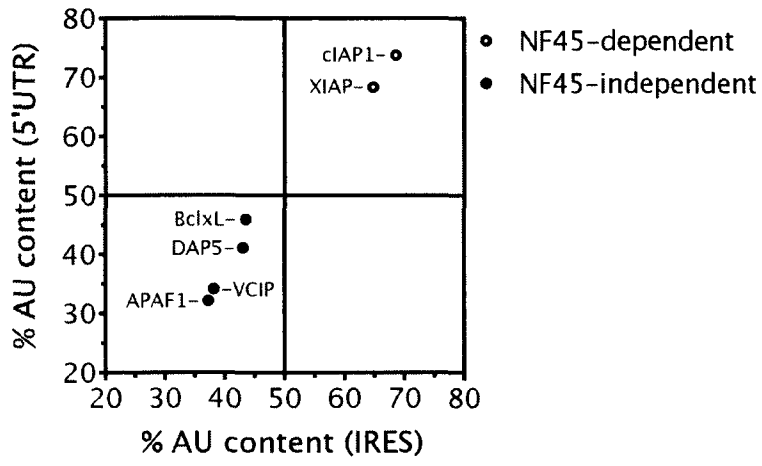

B.

% AU 5'UTR (IRES)	IRES name	IRESite ID[1]	Unigene symbol	Unigene ID
74 (68)	XIAP	109	XIAP	Hs.356076
68 (65)	cIAP1	259	BIRC2	Hs.696238
67 (68)	NRF	243	NKRF	Hs.437084
64 (69)	ELG1	492	C17ORF85	Hs.120963
60 (60)	SNM1	58	DCLRE1A	Hs.1560
58 (62)	MYT2	42	MYT2	Hs.123048
57 (58)	UNR	81	CSDE1	Hs.69855
56 (51)	AQP4	491	AQP4	Hs.315369
54 (54)	TEK	N/A	TEK	Hs.89640

[1] http://www.iresite.org

AU-rich 5'UTRs harbouring IRES are regulated by NF45

To determine whether NF45 acts as an ITAF for AU-rich IRES we measured IRES activity using a bicistronic β-GAL/CAT vector transfected into *d5* versus *c* cells. We have previously confirmed and validated IRES activity of cIAP1, XIAP, ELG1 and AQP4 IRES in the β-GAL/CAT vector expressed in HEK293 cells.[3] In addition to these IRES, we cloned the previously characterized NRF, SNM1, MYT2, UNR, and TEK IRES into the β-GAL/CAT bicistronic vector. Using these constructs, we observed that the ratio of IRES activity in *d5* versus *c* cells was significantly less (<50% of that in *d5* cells) for cIAP1, XIAP, NRF, and ELG1 IRES; strongly arguing that NF45 positively regulates these AU-rich IRES (Figure 4.3). Surprisingly, SNM1 IRES activity was significantly increased in NF45-deficient cells illustrating that NF45 ITAF activity can be pleiotropic, as has been previously demonstrated with other ITAF-IRES interactions.[5] Importantly, we found that IRES with an AU content of less than 60% (MYT2, UNR, AQP4, TEK, EMCV, BclxL, DAP5, VCIP, and APAF1) were largely unaffected by decreased expression of NF45 in *d5* cells.

Prediction of NF45-dependent IRES across Eukarya

We wished to use our results from the above IRES screen to establish specific constraints that could be used to confidently predict NF45-dependent IRES in silico. From a plot of $\log_2$-transformed mean IRES activity versus the AU content of the IRES-containing 5'UTRs, we can see that those IRES whose activity is affected by more than 2-fold up or down in NF45-deficient cells all lie within 5'UTRs with an AU content greater than or equal to 60% (Figure 4.4A). From this data, we propose that IRES-containing 5'UTRs with an AU

Figure 4.3

AU-rich 5'UTRs harbouring IRES are regulated by NF45. IRES activity was tested in *d5* (NF45 shRNA) cells relative to *c* (non-targeting shRNA) cells using a bicistronic assay for the IRES listed in Figure 4.2B in addition to GC-rich IRES (EMCV, BclxL, DAP5, VCIP, APAF1) as described in Materials and Methods (n=3, mean ±SD). IRES are ranked in order of decreasing 5'UTR AU content (from left to right, indicated at the bottom)

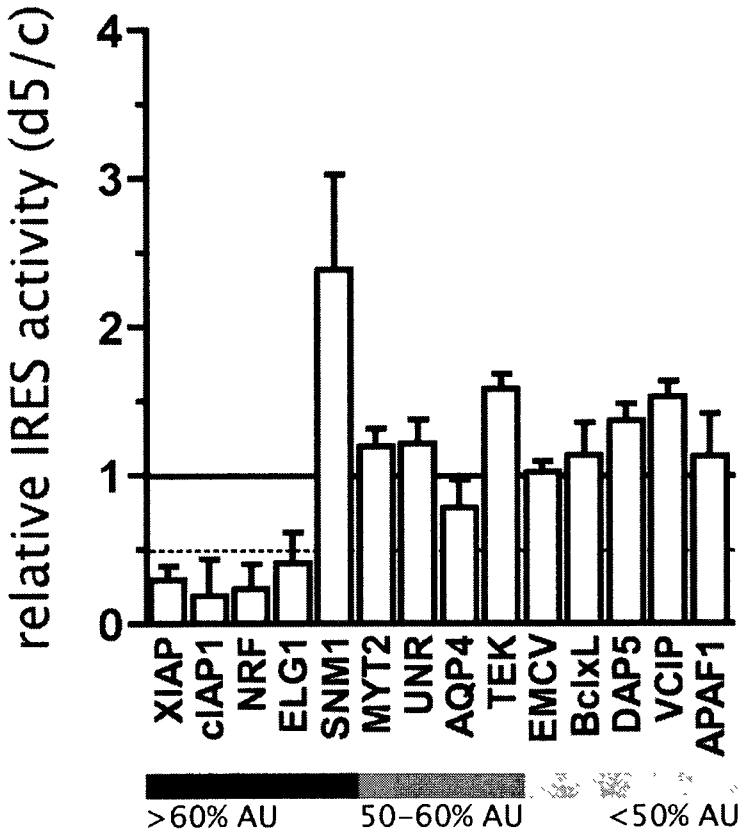
relative IRES activity (d5/c)
4
3
2
1
0
XIAP
cIAP1
NRF
ELG1
SNM1
MYT2
UNR
AQP4
TEK
EMCV
BclxL
DAP5
VCIP
APAF1
>60% AU
50-60% AU
<50% AU

Figure 4.4

A 5'UTR AU content of greater than 60% predicts cross-species dependence on NF45. **(A)** Determination of threshold AU content for NF45-dependent IRES. IRES activity data from Figure 4.3 was transformed into $\log_2$-space and plotted against the AU content of the 5'UTRs tested. A constraint of >60% AU content was chosen based on the clustered activities of IRES that changed by more than 2-fold up or down in *d5* versus *c* cells (shaded quadrants). **(B)** Conservation of NF45-IRES interactions allows prediction of an NF45-dependent IRES in *Canis familiaris*. The SCAMPER IRES (63% AU content) was cloned into a bicistronic vector as described in Materials and Methods and was tested for IRES activity as in Figure 4.3 (n=3, mean ±SD).

A.

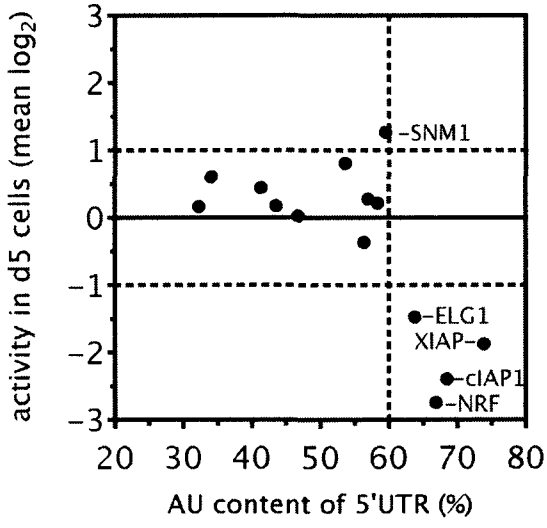
activity in d5 cells (mean log2)
3
2
1
0
−1
−2
−3
20
30
40
50
60
70
80
AU content of 5'UTR (%)
SNM1
ELG1
XIAP
cIAP1
NRF

B.

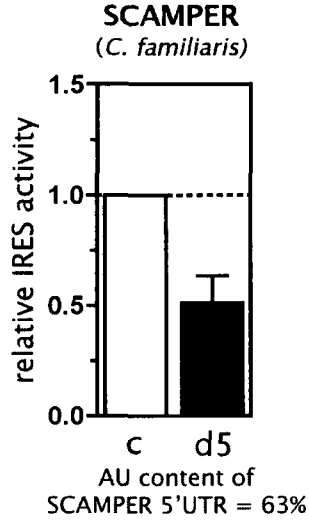
SCAMPER
(C. familiaris)
relative IRES activity
1.5
1.0
0.5
0.0
c
d5
AU content of
SCAMPER 5'UTR = 63%

content greater than 60% can be predicted to be affected by NF45. To confirm that this prediction holds across species, we screened for activity of the *Canis familiaris* IRES SCAMPER in *d5* cells. The AU content of the SCAMPER 5'UTR and its respective IRES is 63% and therefore fits our constraint. As predicted, we found that SCAMPER IRES activity was decreased by 50% in *d5* relative to *c* cells, confirming that SCAMPER expression is regulated by human NF45 and suggesting that AU-rich IRES from other species likely require NF45 for their activity (Figure 4.4A). It is important to note that *C. familiaris* NF45 is 99.7% identical to that of the *H. sapiens* orthologue, implying functional NF45-IRES interactions in *C. familiaris*. Further, the high degree of NF45 protein homology and target IRES sequence conservation between mammals suggest that NF45-IRES interactions are evolutionarily conserved and therefore functionally important. Outside of class Mammalia, the CG5641 protein in *D. melanogastor* is also homologous to mammalian NF45 and may regulate IRES in this species. Of the few *D. melanogastor* IRES insofar identified, antennapedia, hsp70, hsp90, reaper, and ultrabithorax possess more than 60% AU content in their respective 5'UTRs, and would therefore be predicted to be regulated at the level of translation by CG5641. Interestingly, no NF45 orthologue exists in *S. cerevisiae*, perhaps reflecting the apparent distinct mechanism of IRES regulation in this species that requires short stretches of adenosine nucleotides to recruit ribosomes through interaction with *D. melanogastor* poly-A binding protein (PAPB).[6]

NF45-dependent IRES define an RNA operon

We observed that the NF45-dependent mRNAs harbouring IRES identified herein appear to encode proteins involved in two intimately linked functional pathways; namely DNA damage repair (SNM1) and NF-κB signalling (NRF, cIAP1, XIAP). The ELG1 IRES regulates an uncharacterized protein (known as ELG and not to be confused with the DNA repair protein ELG1). NF-κB can be activated upon DNA damage induced by several chemotherapeutic drugs including camptothecin, etoposide and doxorubicin.[7] Does NF45 preserve genomic stability by maintaining IRES-mediated translation of critical DNA repair genes? Does NF45 keep the brake on NF-κB signalling through IRES-mediated translation of the NF-κB-repressing factor (NRF), cIAP1, and XIAP? Our laboratory is currently trying to answer these critical questions by continuing to look at the effect of RNAi-mediated NF45 knockdown in *d5* cells. This HeLa cell line exhibits a striking senescent-like morphology typified by an overall flat, non-elliptical shape, and increased F-actin expression (Figure 4.5). These cells also display multi-lobed nuclei, suggesting either a cell fusion event or a defect in cytokinesis. Recent time-lapse microscopy of nuclear division in NF45 siRNA-transfected HeLa cells that faithfully recapitulates the phenotype observed in *d5* cells clearly indicates a block in cytokinesis during mitosis.[8] Although *d5* cells exhibit a normal cell cycle profile (except for an increased polyploid population), there is a 50% decrease in ^{3}H-thymidine uptake that suggests severely impaired DNA synthesis and correlates with the slow growth kinetics of these cells.[2] Surprisingly, although aneuploidy is increased in *d5* cells, apoptotic threshold is unaffected.[2, 8] The absence of p53 protein in this HeLa cell line derivative may explain the lack of cell death in the face of dysregulated mitosis.

Figure 4.5

***d5* cells exhibit defects in cytokinesis and a senescent-like morphology.** Micrographs of fixed *c* (HeLa cells expressing non-specific shRNA) and *d5* (expressing NF45 shRNA) cells. Nuclei were stained with Hoechst dye and F-actin filament expression was assessed using the actin depolymerization inhibitor phalloidin conjugated to a fluorescent dye as described in Materials and Methods section. Arrow denotes a typical *d5* cell, exhibiting irregular shape, large cytoplasm, increased expression of F-actin filaments, and multi-lobed nuclei.

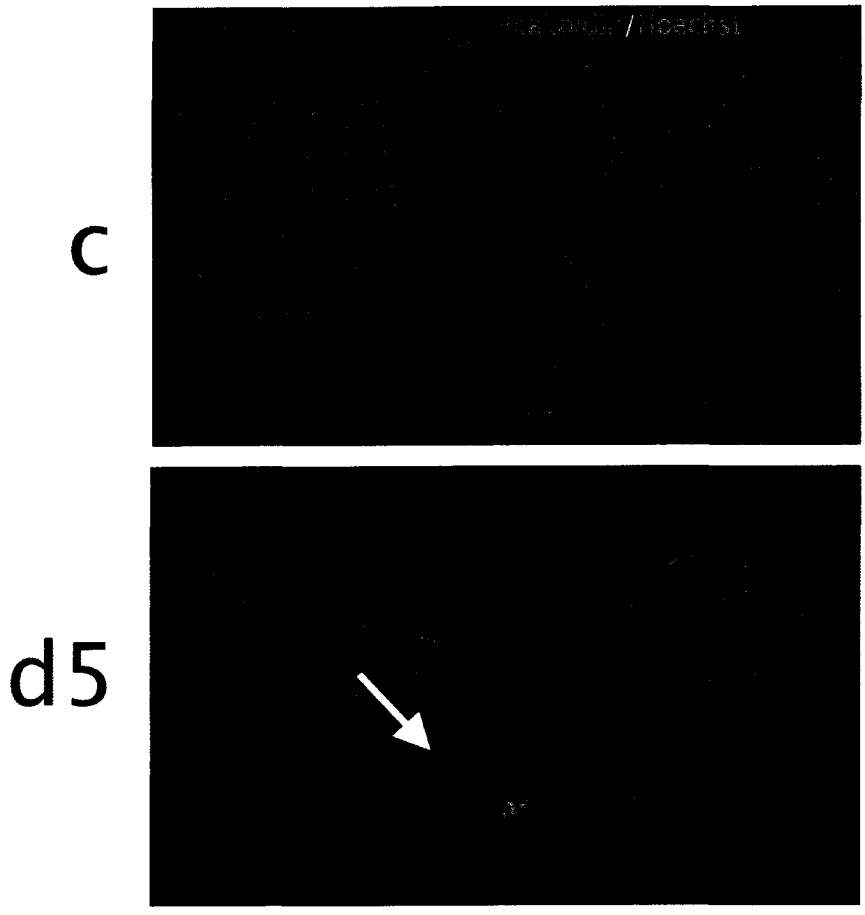
c
d5

A direct link between IRES-mediated translation and the *d5* phenotype has yet to be proven, but we have shown for the first time that NF45 expression affects translation of mRNAs encoding proteins involved in DNA repair, apoptosis, and NF-κB signalling, thus representing an IRES-based RNA operon. We were able to predict these NF45-dependent IRES based solely on the unusually high AU content (>60%) of their respective 5'UTRs, giving researchers a new in silico method to determine if newly discovered IRES are dependent on NF45 ITAF activity.

Materials and Methods

Cell culture, expression constructs and transfection. HeLa cells expressing shRNA (*c* and *d5*) were previously characterized[2] and were maintained under selective pressure with 400 μg/ml of G418 (Invitrogen, Burlington, ON, Canada) in serum- and antibiotic-supplemented Dulbecco's modified Eagle's medium (DMEM). Transient DNA transfections were performed using Lipofectamine 2000 (Invitrogen, Burlington, ON, Canada) as per the manufacturer's protocol. Unless otherwise stated, all assays were performed 24 hours following transfection.

RNA affinity chromatography. Affinity chromatography was performed with HEK293T cells and in vitro transcribed RNA corresponding to the full-length XIAP IRES or a mutant lacking stemloop II (containing the PPT) as previously described.[3] Briefly, RNA was end-labelled with biotin and conjugated to avidin-coated beads. A HEK293T cytoplasmic lysate

was incubated with the RNA beads or with beads alone, followed by extensive washing. Captured proteins were resolved by SDS-PAGE and transferred to a PVDF membrane. Membranes were probed with anti-NF45[1] or anti-PTB (Zymed Laboratories, San Francisco, CA, USA).

Western blot analysis. Cells were lysed in RIPA buffer for 30 minutes at 4°C, followed by centrifugation at 10,000xg to remove debris. Equal amounts of protein were resolved by 10% SDS-PAGE, transferred to PVDF membranes using a wet transfer protocol and probed with antibodies to Nuclear Factor 45[1], XIAP (anti-RIAP3[3]), or GAPDH (BD Biosciences, Mississauga, ON, Canada). Membranes were incubated with Alexa 680-conjugated (Invitrogen, Burlington, ON, Canada) or IR800-conjugated (LI-COR Biotechnology, Lincoln, NE, USA) secondary antibody followed by detection using the LICOR Odyssey infrared scanner.

Calculation of UTR nucleotide composition. A non-redundant human 5'UTR sequence database and a database containing known IRES sequences were used to calculate AU content.[5]

Cloning of IRES and bicistronic assays. The AQP4, cIAP1, ELG1, NRF, and XIAP IRES have been previously cloned into our β-GAL/CAT bicistronic vector and characterized as previously described.[1, 3] The SCAMPER[9] and MYT2[10] IRES were synthesized with flanking NheI/XhoI sites and cloned into a pUC57 vector (Bio Basic, Inc., Toronto, ON, Canada)

followed by sub-cloning into the β-GAL/CAT bicistronic vector. A portion of the SNM1 5'UTR containing IRES activity described in Zhang et al[11] (nucleotides -669 to -1, forward primer: CTC TTC CT GCT AGC GGG ATT GTT CAT TGC TGC, reverse primer: CTC TTC CT CTC GAG GGC AAA ATG ATT TTA TCA), the UNR 5'UTR containing IRES activity described in Cornelis et al[12] (nucleotides -462 to -1, forward primer: CTC TTC CT GCT AGC TGC TGC TTA TGG CGG CGC, reverse primer: CTC TTC CT CTC GAG CGC AGT GAT ACT CAA ATA), and the TEK 5'UTR containing IRES activity described in Park et al[13] (nucleotides -354 to -1, forward primer: CTC TTC CT GCT AGC GCA GCA GCA AAA GCA GCA, reverse primer: CTC TTC CT CTC GAG GCT TCC CCA AAT CTC TCC), were amplified by PCR from mammalian gene collection clones (SNM1, Genbank Accession:BI770136; UNR, GB:BI546285; TEK; GB:BI546285, all purchased from Thermo Fisher Scientific, Inc., Ottawa, ON, Canada) using primers with NheI/XhoI sites. The NRF 5'UTR (nucleotides -653 to -1, forward primer: CTC GAG CAG AGT AAT GAC ATG GTT CC, reverse primer: CTC TTC CAA GCG TGG GCT GTA CC) was PCR-amplified from a liver cDNA library using primers with NheI/XhoI sites. The amplified UTRs were then sub-cloned into the β-GAL/CAT bicistronic vector. All constructs were verified by sequencing and basal IRES activity in *c* cells (relative to cells transfected with empty bicistronic vector) was confirmed.

Fluorescence microscopy. $1.0x10^5$ *d5* and *c* cells were seeded in 12-well flat-bottom plates. 24 hours later, cells were fixed and simultaneously stained for nuclei and F-actin filaments by incubating them with 5μg/ml of Hoechst 3342 and 0.2U/ml Alexa 564-conjugated

Phalloidin (both from Invitrogen, Burlington, ON, Canada) in 3.7% formaldehyde in PBS for 30 minutes at room temperature. Nuclei and F-actin staining was captured with a Cellomics ArrayScan VTI automated fluorescence imaging system (Thermo Fisher Scientific, Inc., Ottawa, ON, Canada) using appropriate filters.

References

1. Graber TE, Baird SD, Kao PN, Mathews MB, Holcik M. NF45 functions as an IRES trans-acting factor that is required for translation of cIAP1 during the unfolded protein response. *Cell Death Differ* 2010; **17** (4): 719-729.

2. Guan D, Altan-Bonnet N, Parrott AM, Arrigo CJ, Li Q, Khaleduzzaman M, *et al.* Nuclear factor 45 (NF45) is a regulatory subunit of complexes with NF90/110 involved in mitotic control. *Molecular and Cellular Biology* 2008; **28** (14): 4629-4641.

3. Baird SD, Lewis SM, Turcotte M, Holcik M. A search for structurally similar cellular internal ribosome entry sites. *Nucleic Acids Res* 2007; **35** (14): 4664-4677.

4. Holcik M, Lefebvre C, Yeh C, Chow T, Korneluk RG. A new internal-ribosome-entry-site motif potentiates XIAP-mediated cytoprotection. *Nat Cell Biol* 1999 Jul; **1** (3): 190-192.

5. Baird SD, Turcotte M, Korneluk RG, Holcik M. Searching for IRES. *RNA* 2006 Oct; **12** (10): 1755-1785.

6. Gilbert WV, Zhou K, Butler TK, Doudna JA. Cap-independent translation is required for starvation-induced differentiation in yeast. *Science* 2007 Aug 31; **317** (5842): 1224-1227.

7. Jin HS, Lee DH, Kim DH, Chung JH, Lee SJ, Lee TH. cIAP1, cIAP2, and XIAP act cooperatively via nonredundant pathways to regulate genotoxic stress-induced nuclear factor-kappaB activation. *Cancer Res* 2009 Mar 1; **69** (5): 1782-1791.

8. Neumann B, Walter T, Heriche JK, Bulkescher J, Erfle H, Conrad C, *et al.* Phenotypic profiling of the human genome by time-lapse microscopy reveals cell division genes. *Nature* Apr 1; **464** (7289): 721-727.

9. De Pietri Tonelli D, Mihailovich M, Schnurbus R, Pesole G, Grohovaz F, Zacchetti D. Translational control of Scamper expression via a cell-specific internal ribosome entry site. *Nucleic Acids Res* 2003 May 15; **31** (10): 2508-2513.

10. Kim JG, Armstrong RC, Berndt JA, Kim NW, Hudson LD. A secreted DNA-binding protein that is translated through an internal ribosome entry site (IRES) and distributed in a discrete pattern in the central nervous system. *Mol Cell Neurosci* 1998 Oct; **12** (3): 119-140.

11. Zhang X, Richie C, Legerski RJ. Translation of hSNM1 is mediated by an internal ribosome entry site that upregulates expression during mitosis. *DNA Repair (Amst)* 2002 May 30; **1** (5): 379-390.

12. Cornelis S, Tinton SA, Schepens B, Bruynooghe Y, Beyaert R. UNR translation can be driven by an IRES element that is negatively regulated by polypyrimidine tract binding protein. *Nucleic Acids Res* 2005; **33** (10): 3095-3108.

13. Park EH, Lee JM, Blais JD, Bell JC, Pelletier J. Internal translation initiation mediated by the angiogenic factor Tie2. *J Biol Chem* 2005 Jun 3; **280** (22): 20945-20953.

CHAPTER 5

hnRNP A1 regulates UV-induced NF-κB signalling through destabilization of cIAP1 mRNA

Preamble

"hnRNP A1 regulates UV-induced NF-KB signalling through destabilization of cIAP1 mRNA" is a research article published in Cell Death and Differentiation (volume 16, February 2009). The article identifies classical AU-rich elements (ARE) within the cIAP1 3'UTR. These ARE were found to reduce cIAP1 mRNA stability following UV irradiation by interacting with the RNA binding protein hnRNP A1. hnRNP A1 translocation from the nucleus to the cytoplasm, rather than a change in its level of expression, following this stress was found to mediate cIAP1 mRNA instability. Together, these data ascribe an additional level of post-transcriptional control to cIAP1 mRNA.

Author list: Tong T. Zhao*, **Tyson E. Graber***, Lindsay E. Jordan, Mireille Cloutier, Stephen M. Lewis, Isabelle Goulet, Jocelyn Côté and Martin Holcik

*these authors contributed equally

Author contributions: TEG and MH wrote the article. TEG designed and performed experiments presented in Figures 5.1b, 5.4f (luciferase assay), 5.6. TEG designed and performed an additional experiment requested by a reviewer that was not included in the final published manuscript. TEG provided technical support and advice on experimental design for experiments presented in Figures 5.2, 5.3b. JC provided reagents.

Abstract

cIAP1 is an important member of the inhibitor of apoptosis family of proteins and is involved in the regulation of the NF-κB signalling pathway downstream of the TNF receptor. We report here that UV irradiation leads to downregulation of cIAP1 expression because of enhanced cIAP1 mRNA destabilization. An AU-rich element located within the 3' untranslated region of cIAP1 mRNA is sufficient to mediate cIAP1 mRNA instability. Furthermore, we have identified hnRNP A1 as a cIAP1 3'UTR-binding protein. hnRNP A1 is a primarily nuclear protein, but accumulates in the cytoplasm after exposure of cells to UV irradiation. Indeed, we find that hnRNP A1 enhances the destabilization of cIAP1 mRNA during UV irradiation. Moreover, siRNA-mediated knockdown of hnRNP A1 restores cIAP1 levels and prevents UV irradiation-induced activation of the NF-κB signal transduction pathway, suggesting that hnRNP A1 is an essential post-transcriptional modulator of cIAP1 expression, and thus cIAP1 activity.

Introduction

The inhibitor of apoptosis (IAP) family of proteins are key regulators of programmed cell death.[1] The IAP family comprises eight distinct members that participate in diverse cellular processes including cell cycle, signal transduction, ubiquitylation, and caspase inhibition.[2] Although it was initially believed that all IAPs are capable of inhibiting distinct caspases, the recent data suggest that only XIAP is a bona fide caspase inhibitor.[3] cIAP1 and cIAP2 were identified through an interaction with the TNF-receptor complex proteins TRAF1 and TRAF2, which regulate NF-κB signalling through the TNF receptor.[4] The C-terminal RING

finger domain of cIAP1 possesses an ubiquitin E3 ligase activity and may sensitize cells to apoptosis by direct ubiquitylation and removal of TRAF2 following activation of the TNF receptor, resulting in the inhibition of NF-κB pathways.[5] Indeed, cIAP1 degradation induced by Smac mimetics leads to activation of both the canonical and non-canonical NF-κB pathways, strengthening the importance of IAPs in the regulation of NF-κB signalling.[6–8]

Although cIAP1 and cIAP2 perform similar functions within the cell, their expression is regulated differently. The expression of cIAP2 is controlled primarily at the level of transcription in an NF-κB-dependent manner.[9] Also, the protein turnover of cIAP2 is regulated by the ubiquitin ligase activity of cIAP1.[10] In contrast, cIAP1 levels are controlled at the level of protein synthesis. The 5' untranslated region (UTR) of cIAP1 contains an upstream open reading frame that reduces the basal translation of cIAP1.[11] The 5'UTR of cIAP1 also harbours an internal ribosome entry site (IRES) element that mediates translational induction of cIAP1 in response to stress.[12,13] This complex regulatory network reflects the distinct spatial and temporal requirement for cIAP1 and cIAP2 proteins in response to various physiological conditions.

Here, we describe an additional regulatory mechanism that governs the expression of cIAP1. We find that following UV irradiation the levels of cIAP1 decrease dramatically. This reduction of cIAP1 protein is achieved by destabilization of cIAP1 mRNA. We have identified an AU-rich (ARE) sequence in the 3'UTR of cIAP1 that is sufficient and necessary to confer instability on a reporter mRNA. Furthermore, we find that the heterogeneous ribonucleoprotein A1 (hnRNP A1) interacts with the cIAP1 3'UTR and regulates cIAP1 mRNA stability. Importantly, UV irradiation mediates accumulation of hnRNP A1 in the

cytoplasm and subsequent destabilization of cIAP1 mRNA, which results in reduced cIAP1 protein levels and consequently increased NF-κB signalling.

Results

UV irradiation destabilizes cIAP1 mRNA and reduces cIAP1 protein levels

UV irradiation (UVR) causes cells to mount a response to deal with the potentially harmful effects of UV-induced damage. We have earlier reported that UVR results in an inhibition of global protein synthesis, whereas simultaneously enhancing translation of the proapoptotic protein Apaf-1 through an IRES-dependent mode of translation.[14] In the course of these experiments we observed that the levels of the anti-apoptotic gene cIAP1 were significantly reduced following UVR (Figure 5.1a). We wished to determine if this reduction in cIAP1 levels is because of changes in protein or mRNA stability. UV-irradiated cells were pulse-chased with ^{35}S-Met/Cys and cIAP1 was immunoprecipitated over the course of 24 h. We observed that UVR did not alter the stability of cIAP1 protein (Figure 5.1b). We next examined the steady-state levels of cIAP1 mRNA following UVR. When compared with the levels in non-irradiated HEK293 cells, the steady-state levels of endogenous cIAP1 mRNA decreased significantly in UV-irradiated cells (Figure 5.1c). This suggests that the decrease in cIAP1 protein levels following UVR could be because of changes in the stability of cIAP1 mRNA. We examined the stability of endogenous cIAP1 mRNA following UVR by quantitative RT-PCR (Figure 5.1d). Indeed, this experiment revealed that the half-life of cIAP1 mRNA ($t_{1/2}$=5.9 h) is significantly reduced by UVR ($t_{1/2}$=3.3 h). These results

demonstrate that UVR causes a significant decrease in cIAP1 protein levels by destabilizing cIAP1 mRNA.

Figure 5.1

UV irradiation destabilizes cIAP1 mRNA. (**a**) UV irradiation reduces cIAP1 protein levels. 293 cells were treated with UV radiation (UVR (150 mW/cm2)) or not (CTRL) and the expression of cIAP1 protein was determined 24 h later by western blot. (**b**) UV irradiation does not affect cIAP1 protein stability. Cells were pulsed with ^{35}S-Met/Cys for 25 min following UV irradiation and chased in the presence of cold Met/Cys for an additional 24 h. cIAP1 and β-actin were immunoprecipitated using specific antibodies at indicated time points and resolved on SDS-PAGE (left). The levels of remaining cIAP1 are shown relative to β-actin, and the cIAP1/β-actin ratio at the beginning of cold Met chase (0 h) was set as 1 for both control and UVR samples (right). (**c**) UV irradiation reduces steady-state levels of cIAP1 mRNA. 293 cells were treated with UV irradiation as in (**a**) and 5 h later the total RNA was extracted. The levels of cIAP1 and GAPDH mRNA were determined by quantitative RT-PCR analysis as described in the Material and Methods section; values are expressed as cIAP1 relative to GAPDH ($2^{-[Ct\ (cIAP1)-Ct(GAPDH)]}$), and the ratio for non-irradiated cells was set as 1. Mean ±SD of three experiments. (**d**) UV irradiation destabilizes cIAP1 mRNA. The cells were treated as in (**c**) and Actinomycin D (ActD, 10 μg/μl) was added immediately following UV exposure. Total RNA was extracted from parallel samples at 0, 4, 8, 12, and 16 h time points and the levels of cIAP1 and GAPDH mRNA were determined as in (**c**). Values are expressed as cIAP1 relative to GADPH ($^{2-[Ct(cIAP1)-Ct(GAPDH)]}$ normalized to the 0 h time point, which was set as 1. The mean ±SD of three independent experiments is shown.

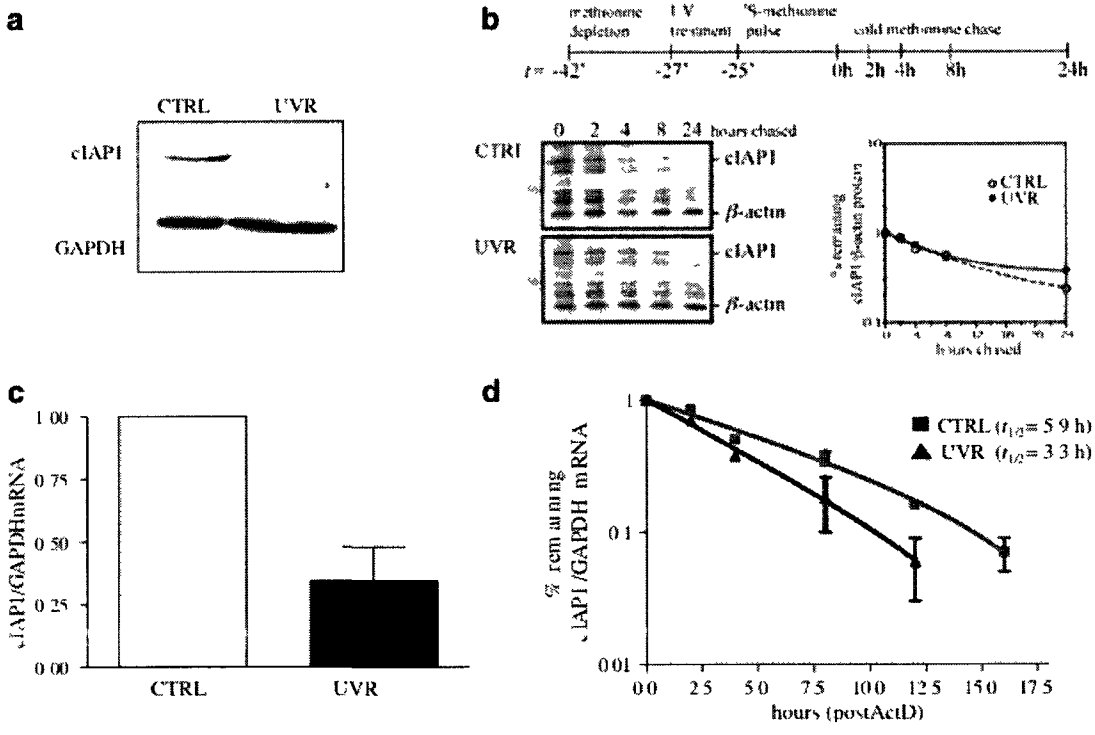
a
CTRL
UVR
cIAP1
GAPDH
b
methionine depletion
UV treatment
$S-methionine pulse
cold methionine chase
t = -42'
-27'
-25'
0h
2h
4h
8h
24h
0 2 4 8 24 hours chased
CTRL
cIAP1
β-actin
UVR
cIAP1
β-actin
CTRL
UVR
hours chased
c
cIAP1/GAPDH mRNA
1 00
0 75
0 50
0 25
0 00
CTRL
UVR
d
% remaining cIAP1 /GAPDH mRNA
CTRL ($t_{1/2}$= 5 9 h)
UVR ($t_{1/2}$= 3 3 h)
1
0 1
0 01
0 0
2 5
5 0
7 5
10 0
12 5
15 0
17 5
hours (postActD)

The 3'UTR of cIAP1 contains an AU-rich element that destabilizes cIAP1 mRNA following UVR

The stability of an mRNA is usually determined by sequence elements located within its 3'UTR. We therefore investigated whether the 3'UTR of cIAP1 can confer instability on a reporter mRNA. In the reporter vector pMC the expression of chloramphenicol acetyl transferase (CAT) reporter mRNA is driven by a CMV promoter and is post-transcriptionally regulated by the sequence elements inserted downstream of the CAT gene. This plasmid also expresses the neomycin phosphotransferase gene (NEO) from an independent promoter (SV40), which serves as an internal control. Insertion of the full-length 3'UTR of TNFα, known to confer mRNA instability, downstream of the CAT reporter gene resulted in an approximately 10-fold reduction in CAT mRNA levels (Figure 5.2a). Insertion of the full-length cIAP1 3'UTR resulted in an approximately 3-fold reduction in CAT mRNA levels. The levels of cIAP1 3'UTR-CAT mRNA decreased even further following UVR, confirming that the 3'UTR of cIAP1 harbours the necessary elements to destabilize reporter mRNA. To further delineate the sequences that are required for cIAP1 mRNA instability we constructed a series of deletion mutants of the cIAP1 3'UTR (Figure 5.2b). We observed that a 120 nucleotide fragment (120–240) is necessary and sufficient to confer instability on CAT mRNA (Figure 5.2c).

Inspection of the (120–240) fragment of the cIAP1 3'UTR revealed that it contains four ARE (Figure 5.2b). To determine if these sequences are involved in destabilization of cIAP1 mRNA, the individual ARE segments were mutated and tested for their ability to

Figure 5.2

A fragment of cIAP1 3'UTR that contains AREs is sufficient to destabilize a heterologous reporter mRNA. (**a**) 3'UTR of cIAP1 is sufficient to destabilize reporter mRNA. 293 cells were transiently transfected with the indicated plasmids and the total RNA was extracted 24 h later. The levels of CAT and NEO mRNA were determined by quantitative RT-PCR analysis. Values are expressed as CAT relative to NEO ($2^{-[Ct(CAT)-Ct(NEO)]}$) and the ratio in non-irradiated cells transfected with the control plasmid pMC was set as 100. The mean ±SD of three independent experiments is shown. (**b**) The complete sequence of the 3'UTR of cIAP1. The stop codon is shown in bold italics. The putative AU-rich elements (AREs) are made bold and underlined. The numbers in square brackets denote nucleotide position relative to the stop codon. A schematic diagram of reporter plasmids is shown below; AREs are indicated as black rectangles. (**c**) A 120 nt fragment harbouring the cIAP1 AREs is sufficient to destabilize the mRNA. 293 cells were transfected with the indicated plasmids and total RNA was extracted as in (**a**). The levels of CAT and NEO mRNA were determined 24 h later by quantitative RT-PCR analysis as in (**a**). The mean ±SD of three independent experiments is shown. (**d**) cIAP1 AREs no. 3 and no. 4 are necessary to confer mRNA instability. Mutations of individual ARE modules (shown above the graph) were introduced into the reporter plasmid pMC-cIAP1 (120–240) by site-directed mutagenesis. Indicated reporter plasmids were then transiently transfected into 293 cells and the levels of CAT and NEO mRNA were determined 24 h later by quantitative RT-PCR analysis as in (**a**). The mean ±SD of three independent experiments is shown.

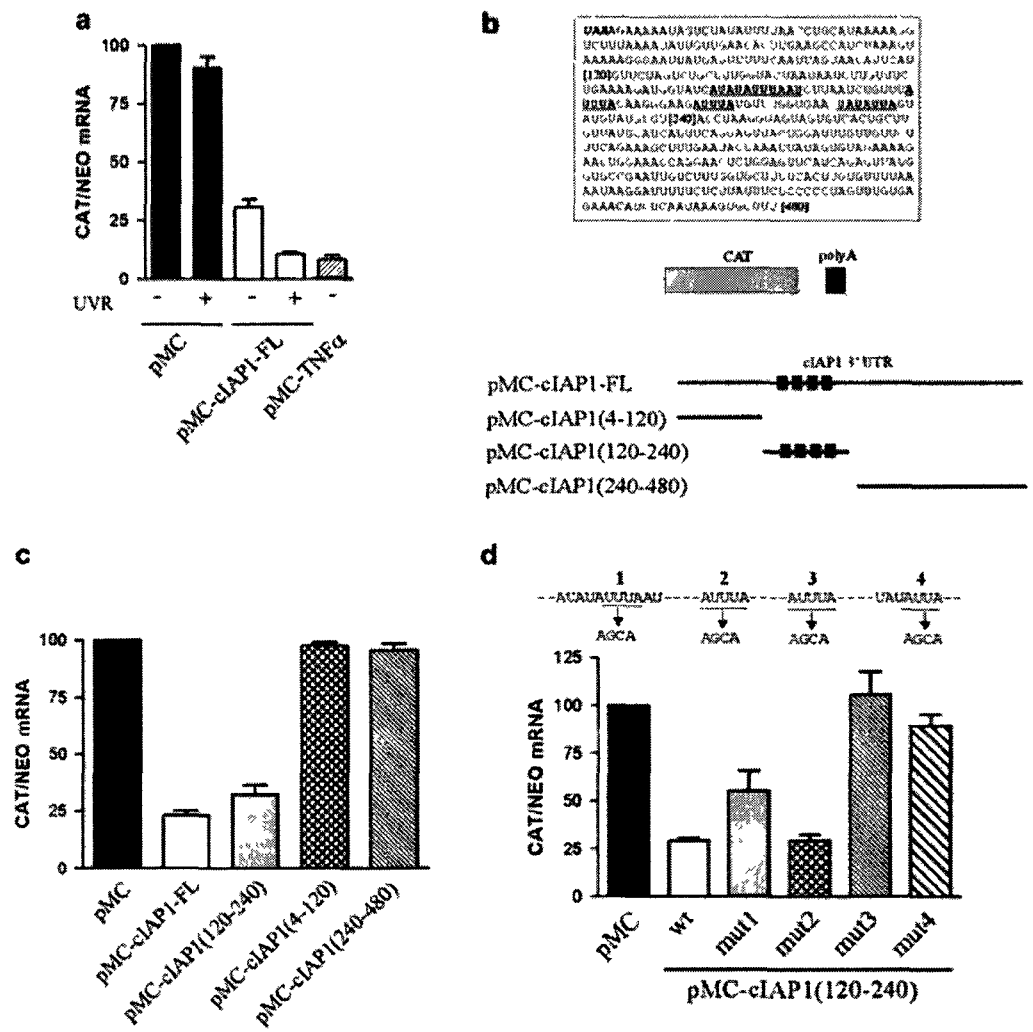
a
CAT/NEO mRNA
100
75
50
25
0
UVR
-
+
-
+
-
pMC
pMC-cIAP1-FL
pMC-TNFα
b
CAT
polyA
cIAP1 5'UTR
pMC-cIAP1-FL
pMC-cIAP1(4-120)
pMC-cIAP1(120-240)
pMC-cIAP1(240-480)
c
CAT/NEO mRNA
100
75
50
25
0
pMC
pMC-cIAP1-FL
pMC-cIAP1(120-240)
pMC-cIAP1(4-120)
pMC-cIAP1(240-480)
d
1
2
3
4
AGCA
AGCA
AGCA
AGCA
CAT/NEO mRNA
125
100
75
50
25
0
pMC
wt
mut1
mut2
mut3
mut4
pMC-cIAP1(120-240)

destabilize CAT mRNA (Figure 5.2d). We found that although mutation of the ARE no. 2 had no effect on the stability of the reporter mRNA (when compared with the wildtype sequence), mutations in either ARE no. 3 or ARE no. 4 completely abolished mRNA instability conferred by the cIAP1 3'UTR. In contrast, mutation of the ARE no. 1 produced an intermediate phenotype with partial restoration of CAT mRNA stability.

The results presented above confirm that the 3'UTR of cIAP1 contains an mRNA instability element, and that AU-rich elements no. 3 and no. 4 within the 3'UTR are the major elements contributing to destabilization of the mRNA.

hnRNP A1 binds the cIAP1 3'UTR ARE

To identify proteins that interact with the cIAP1 3'UTR we used an RNA affinity chromatography approach[15] followed by western blot with antibodies against candidate RNA binding proteins, which identified hnRNP A1 as a cIAP1 3'UTR-interacting protein (Figure 5.3a). In contrast, TIA-1, TIAR, and hnRNP C1/C2 (known RNA binding proteins) were not detected in the protein eluate from the cIAP1 3'UTR RNA affinity matrix, demonstrating the specificity of the hnRNP A1 interaction with the cIAP1 3'UTR in vitro.

We next investigated if hnRNP A1 binds directly to cIAP1 3'UTR RNA, and performed a UV-crosslinking experiment using a radiolabelled cIAP1 3'UTR RNA probe and purified recombinant GST-hnRNP A1 protein. In addition, we used the cIAP1 3'UTR ARE mutants, described in a previous experiment (Figure 5.2d). We find that cIAP1 3'UTR RNA is cross-linked to GST-hnRNP A1 (Figure 5.3b), indicating that hnRNP A1 does indeed bind directly to cIAP1 RNA. Importantly, GST-hnRNP A1 failed to bind to the ARE mutants

Figure 5.3

hnRNP A1 binds directly to the ARE-containing sequence of the cIAP1 3'UTR. (a) RNA affinity chromatography isolation of cIAP1 3'UTR binding proteins. Pre-cleared protein extracts from 293 cells were incubated with either agarose beads coated with cIAP1 3'UTR 120–240 RNA or agarose beads alone. After protein binding, beads were washed extensively, pelleted, and proteins were eluted by boiling. Following separation by SDS-PAGE the proteins were detected by western blot using the indicated antibodies. **(b)** Recombinant hnRNP A1 binds directly to the cIAP1 3'UTR. GST (lane 1) or GST-hnRNP A1 (lanes 2, 3) were incubated with [^{32}P]-labelled wildtype (wt) or mutated cIAP1 3'UTR RNA probes, UV-crosslinked, and then separated by SDS-PAGE and visualized by autoradiography. **(c)** hnRNP A1 binding curves for cIAP1 3'UTR wildtype and ARE mutant RNAs. Nitrocellulose filter-binding assays were performed and analyzed as described in Materials and Methods. Filter-bound RNA is plotted as a function of protein concentration. The data presented represent the mean ±SD of three independent experiments.

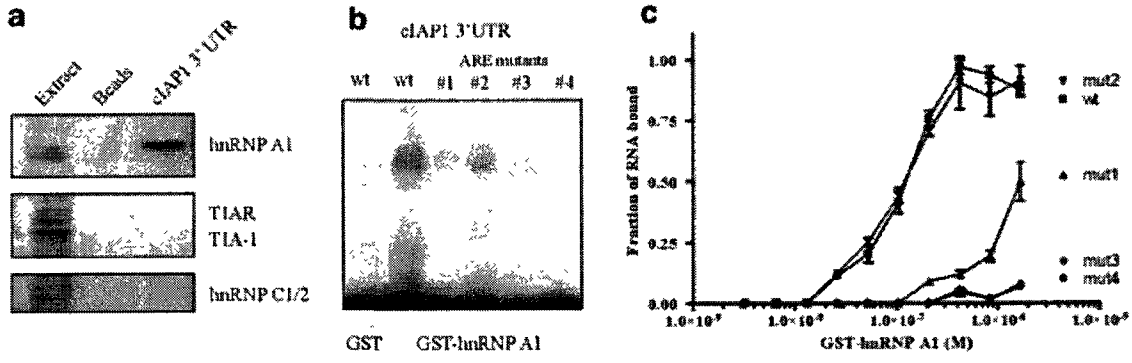
a
Extract
Beads
cIAP1 3'UTR
hnRNP A1
TIAR
TIA-1
hnRNP C1/2
b
cIAP1 3'UTR
ARE mutants
wt
wt
#1
#2
#3
#4
GST
GST-hnRNP A1
c
Fraction of RNA bound
1.00
0.75
0.50
0.25
0.00
mut2
wt
mut1
mut3
mut4
GST-hnRNP A1 (M)

no 1, no. 3 and no. 4, whereas it bound ARE mutant no. 2, implicating these ARE sites as hnRNP A1 binding sites within the cIAP1 3'UTR.

We further assessed the interaction between hnRNP A1 and the cIAP1 3'UTR by measuring the apparent equilibrium dissociation constant (*Kd*) of the recombinant GST-hnRNP A1 protein with both the wildtype cIAP1 3'UTR and ARE-mutant sequences by a nitrocellulose filter-binding assay. We find that the *Kd* for the interaction between GST-hnRNP A1 and cIAP1 3'UTR RNA is 122 nM (Figure 5.3c). Importantly, this *Kd* value is similar to the *Kd* values reported earlier for the interactions between hnRNP A1 and other target mRNAs,[16–18] suggesting a bona fide and specific interaction. An almost identical binding curve was observed for the ARE no. 2 mutant RNA (mut2), whereas the *Kd* for an interaction between GST-hnRNP A1 and ARE no. 1, no. 3, and no. 4 mutant RNAs (mut1, mut3, and mut4) is greater than 600 nM (we could not determine the actual value as we were unable to saturate binding). Interestingly, the binding affinity of GST-hnRNP A1 for the various cIAP1 3'UTR ARE mutants correlates with the ability of these mutants to destabilize CAT reporter mRNA (compare Figure 5.3c and Figure 5.2d), suggesting that hnRNP A1 is a major factor in the instability of cIAP1 mRNA.

hnRNP A1 regulates levels of cIAP1 in response to UVR

hnRNP A1 accumulates in the cytoplasm of cells exposed to UVR (Figure 5.4a and Van der Houven van Oordt et al[19]); therefore, UVR may cause a decrease in cIAP1 mRNA stability (and thus cIAP1 protein levels) because of this increase in cytoplasmic hnRNP A1. To test this hypothesis we used a mutant variant of hnRNP A1 that is defective in its interaction with

Figure 5.4

Cytoplasmic levels of hnRNP A1 regulate cIAP1 mRNA stability and NFκ-B signalling following UV irradiation. (**a**) hnRNP A1 accumulates in the cytoplasm of UV-irradiated cells. 293 cells were exposed to UVR as described in Materials and Methods and the nuclear (NE) and cytoplasmic (CE) protein fractions were harvested at 1 h intervals post-UVR, separated by SDS-PAGE, transferred to PVDF, and subjected to western blot analysis with antibodies against hnRNP A1 and actin. (**b**) Cytoplasmic hnRNP A1 reduces cIAP1 protein levels. 293 cells were transfected with a plasmid-expressing GFP, FLAG-hnRNP A1, or FLAG-hnRNP A1 F1 mutant. Expression levels of FLAG-hnRNP A1, FLAG-hnRNP A1 F1, cIAP1 and GAPDH were determined by western blot analysis using anti-hnRNP A1, anti-cIAP1, and anti-GAPDH antibodies. The asterisk (*) indicates the FLAG-tagged protein species. Relative cIAP1 levels are expressed as a ratio of cIAP1/GAPDH. The ratio in GFP-transfected cells was set as 1. (**c**) Reduced levels of hnRNP A1 stabilize cIAP1 3'UTR reporter mRNA following UVR. 293 cells were cotransfected with control non-silencing or hnRNP A1 siRNA and the indicated reporter plasmids. After 48 h the cells were UV-irradiated and the levels of CAT and NEO mRNA were determined by quantitative RT-PCR 5 h post-UVR. Values are expressed as CAT relative to NEO ($2^{-[Ct(CAT)-Ct(NEO)]}$) and the ratio in non-irradiated cells transfected with control siRNA and the plasmid pMC was set as 100. The mean ±SD of three independent experiments is shown. The levels of hnRNP A1 in cells transfected with control or hnRNP A1 siRNA were determined by western blot. (**d**) Reduced levels of hnRNP A1 increase endogenous cIAP1 protein levels following UVR. 293 cells were transfected with control or hnRNP A1 siRNA as in (**a**) and the cells were irradiated 48 h later. Cell lysates were prepared 24 h post-UVR and the levels of cIAP1 and GAPDH were determined by western blot. Relative cIAP1 levels are expressed as a ratio of cIAP1/ GAPDH. The ratio in mock-transfected non-irradiated cells was set as 1. Displayed data are representative of three independent experiments. (**e**) Reduced levels of hnRNP A1 stabilize cIAP1 mRNA following UVR. 293 cells were treated as in (**d**) and the total RNA was extracted 5 h post-UVR. The levels of cIAP1 and GAPDH mRNA were determined by quantitative RT-PCR analysis. Values are expressed as cIAP1 relative to GAPDH ($2^{-[Ct(cIAP1)-Ct(GAPDH)]}$) and the ratio in non-irradiated mock-transfected cells was set as 100. The mean ±SD of three independent experiments is shown. (**f**) hnRNP A1 levels affect NF-κB signalling following UVR. 293 cells were co-transfected with control, hnRNP A1, or cIAP1 siRNA and the NF-κB reporter plasmid pNF-κB-Luc as described in Materials and Methods. After 48 h the cells were UV-irradiated and luciferase levels were determined 18 h post-UVR. Values are presented as mean luminescence corrected to the number of live cells per plate. The relative luciferase activity in non-irradiated mock-transfected cells was set as 100. The mean ±SD of three independent experiments is shown. The levels of hnRNP A1, cIAP1 and GAPDH were determined by western blot analysis in parallel untreated samples.

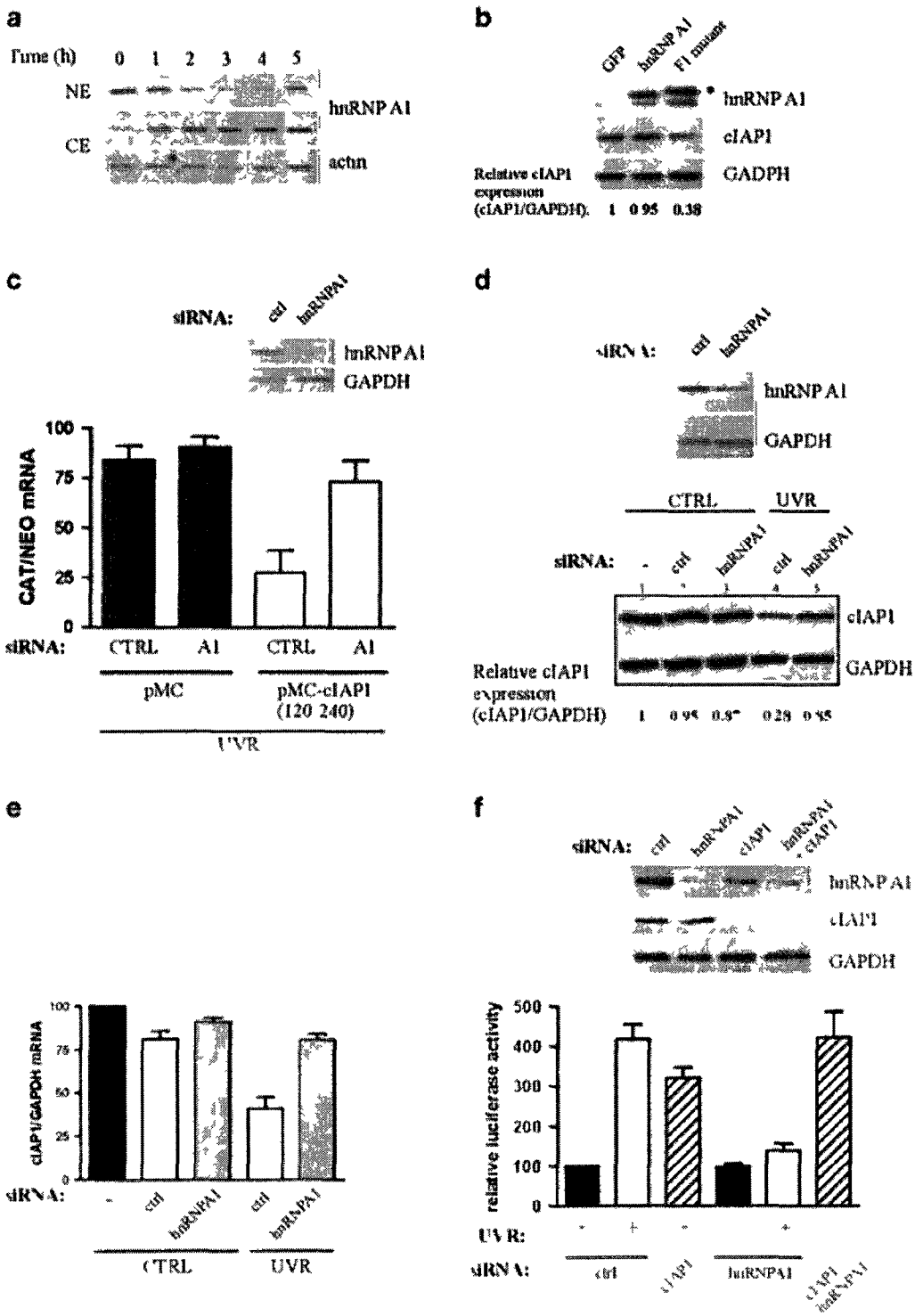
a
Time (h) 0 1 2 3 4 5
NE
CE
hnRNP A1
actin
b
GFP
hnRNP A1
F1 mutant
hnRNP A1
cIAP1
GAPDH
Relative cIAP1 expression (cIAP1/GAPDH). 1 0.95 0.38
c
siRNA: ctrl hnRNPA1
hnRNP A1
GAPDH
CAT/NEO mRNA
100
75
50
25
0
siRNA: CTRL A1 CTRL A1
pMC
pMC-cIAP1 (120 240)
UVR
d
siRNA: ctrl hnRNPA1
hnRNP A1
GAPDH
CTRL UVR
siRNA: - ctrl hnRNPA1 ctrl hnRNPA1
cIAP1
GAPDH
Relative cIAP1 expression (cIAP1/GAPDH) 1 0.95 0.87 0.28 0.35
e
cIAP1/GAPDH mRNA
100
75
50
25
0
siRNA: - ctrl hnRNPA1 ctrl hnRNPA1
CTRL UVR
f
siRNA: ctrl hnRNPA1 cIAP1 hnRNPA1 + cIAP1
hnRNP A1
cIAP1
GAPDH
relative luciferase activity
500
400
300
200
100
0
UV R: - + - +
siRNA: ctrl cIAP1 hnRNPA1 cIAP1 hnRNPA1

the Trn1 transporter protein and thus fails to enter the nucleus and accumulates in the cytoplasm (the F1 mutant[20]). Indeed, we found that the transient transfection of HEK293 cells with FLAG-tagged hnRNP A1 F1-expressing plasmid resulted in a significant reduction of cIAP1 protein (Figure 5.4b). This was in contrast to cells transfected with FLAG-tagged wildtype hnRNP A1, which had a negligible effect on the levels of cIAP1 (Figure 5.4b). Thus, accumulation of hnRNP A1 in the cytoplasm, even in the absence of UVR, is sufficient to decrease the levels of cIAP1 protein.

We further hypothesized that any decrease in cIAP1 levels because of UVR should be dependent on hnRNP A1. Cells were co-transfected with a cIAP1 3'UTR reporter plasmid and either a non-silencing control siRNA or hnRNP A1-targeting siRNA, exposed to UVR 48h later, and the levels of CAT reporter mRNA were determined by qRT-PCR 5 h post-irradiation. As observed earlier, exposure of cells to UVR significantly reduced the levels of CAT mRNA. Importantly, reduction of hnRNP A1 levels by siRNA restored CAT mRNA levels almost to the levels of a control mRNA that does not harbour the cIAP1 3'UTR (Figure 5.4c). Similarly, the decrease in endogenous cIAP1 levels following UVR was also dependent on hnRNP A1, as transient reduction of hnRNP A1 allowed cIAP1 levels to be maintained in response to UVR (Figure 5.4d; compare lanes 4 and 5). In contrast, transient reduction of TIAR, an RNA-binding protein that does not bind the cIAP1 3'UTR (Figure 5.3a) had no effect on cIAP1 protein levels following UVR (Figure 5.5). To confirm that the stabilization of cIAP1 protein levels in UV-irradiated cells is because of the stabilization of cIAP1 mRNA we examined the steady-state levels of cIAP1 mRNA. We observed that although UVR reduced cIAP1 mRNA levels in control siRNA-transfected

Figure 5.5

Transient decrease in TIAR levels does not affect levels of cIAP1 in UV-treated cells. 293 cells were transfected with control or TIAR siRNA as in Figure 5.4c and the cells were irradiated 48 h later. Cell lysates were prepared 24 h post-UVR and the levels of cIAP1, TIAR, and GAPDH were determined by western blot.

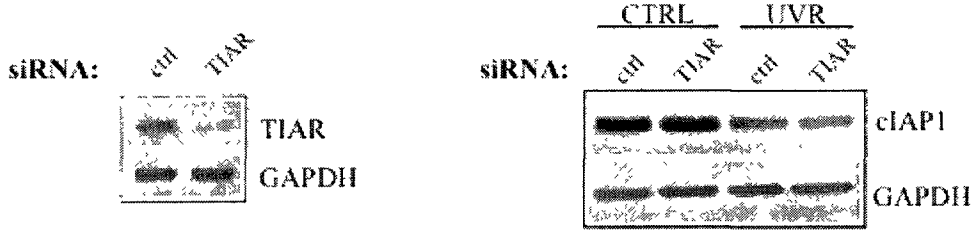
siRNA:
ctrl
TIAR
TIAR
GAPDH
CTRL
UVR
siRNA:
ctrl
TIAR
ctrl
TIAR
cIAP1
GAPDH

cells, transient knockdown of hnRNP A1 in UVR-treated cells allowed cIAP1 mRNA to be maintained at levels seen in non-irradiated cells (Figure 5.4e). Together these results indicate that accumulation of hnRNP A1 in the cytoplasm following exposure of cells to UV radiation causes a decrease in cIAP1 protein levels through the ability of the cytoplasmic hnRNP A1 to interact with the cIAP1 3'UTR, resulting in destabilization of cIAP1 mRNA.

hnRNP A1 modulates NF-κB signalling through destabilization of cIAP1 mRNA

It emerged recently that the primary role of cIAP1 is to modulate NF-kB signalling.[6–8] We therefore wished to examine whether the destabilization of cIAP1 mRNA that is brought about by cytoplasmic accumulation of hnRNP A1 following exposure of cells to UVR affects NF-κB signalling. To quantitate changes in total NF-κB activity we co-transfected cells with a commercially available NF-κB-luciferase reporter plasmid and siRNA-targeting cIAP1, hnRNP A1 or non-targeting siRNA as a control. Following transfection cells were allowed to recover for 48 h and then exposed to UVR. Relative luciferase activity was determined 18 h post-UV irradiation, and the levels of cIAP1 and hnRNP A1 were assessed by western blot analysis. We observed that UVR enhanced the basal NF-κB reporter activity (Figure 5.4f) as shown earlier.[21] Also as expected, transient knockdown of cIAP1 had a similar effect and enhanced the basal NF-κB reporter activity in the absence of UV irradiation (Figure 5.4f). In contrast, transient reduction of hnRNP A1 levels prevented the UVR-mediated induction of NF-κB reporter activity. Importantly, the attenuation of NF-κB activity seen in UVR-treated and hnRNP A1 siRNA-transfected cells is dependent on cIAP1 levels, as concomitant reduction of hnRNP A1 and cIAP1 levels by siRNA resulted in enhanced NF-κB reporter

expression. Taken together these results confirm that cIAP1 levels are required for proper NF-κB signalling activity[6–8] and uncover a role for the cytoplasmic accumulation of hnRNP A1 in this pathway following exposure of cells to UV radiation.

Discussion

An important finding of this study is that UV irradiation reduces the expression of cIAP1, a member of the inhibitor of apoptosis family of proteins and a critical regulator of NF-κB signalling. We demonstrated that UVR results in a 40% decrease in the half-life of cIAP1 mRNA. Examination of the 3'UTR of cIAP1 revealed the presence of four AU-rich elements, two of which are sufficient and necessary to confer instability on a reporter mRNA. Furthermore, we have identified hnRNP A1 as a stress-regulated cIAP1 ARE-binding protein. Importantly, cytoplasmic relocalization of hnRNP A1 triggered by UV irradiation causes a significant reduction in cIAP1 mRNA levels and a concomitant decrease in the level of endogenous cIAP1 protein. On the basis of these findings we conclude that hnRNP A1 is a negative regulator of cIAP1 expression and thus contributes to the regulation of NF-κB signalling following UV stress. In addition, our findings strengthen the hypothesis that post-transcriptional control of gene expression can be exercised through subcellular relocalization of mRNA binding proteins.

The regulation of mRNA decay is a central mechanism for the control of gene expression and is mediated by distinct RNA regulatory elements. AREs are one such class of elements and are found in the 3'UTRs of specific mRNAs. Although initially believed to be restricted to mRNAs of genes encoding cytokines, growth factors and oncogenes, recent data

suggest that ARE occurrence is much more prevalent, possibly in as much as 8% of the human transcriptome.[22] AREs typically function as RNA destabilizing elements that target mRNA for rapid degradation in the cytoplasm.[23] We have identified four AU-rich sequences within the 3'UTR of cIAP1. Mutational analysis revealed that only the last two segments, ARE no. 3 and ARE no. 4, are required for the instability conferred by cIAP1 3'UTR (Figure 5.3). AREs in general contain multiple copies of A/U nucleotides,[23] and the cIAP1 3'UTR thus appears to be a typical example of this class of regulatory sequences.

AREs exert their effect on target mRNAs through interaction with specific mRNA binding proteins. We identified hnRNP A1 as a cIAP1 3'UTR-binding protein (Figure 5.3). This is in contrast to TIAR, TIA-1, or hnRNP C1/C2 (known ARE binding proteins), which were not found to interact with cIAP1 3'UTR. Furthermore, the direct interaction of hnRNP A1 with cIAP1 3'UTR was demonstrated by in vitro crosslinking and filter-binding assays. Importantly, binding of hnRNP A1 correlates with the instability of cIAP1 3'UTR-containing mRNA, providing strong evidence that hnRNP A1 functions as a major destabilizing factor for cIAP1 mRNA. hnRNP A1 is a multifunctional protein that is implicated in diverse steps of RNA metabolism including splicing,[24] mRNA stability[25] and translation.[17] hnRNP A1 has been previously shown to bind several labile mRNAs that contain the AUUUA sequence, including the granulocyte–macrophage colony-stimulating factor (GM-CSF),[25] human angiotensin receptor AT_1,[26] and cytochromes P450, 2A6 and 2A5.[27,28] A similar AUUUA sequence is found in ARE no. 1, ARE no. 2, and ARE no. 3 of the cIAP1 3'UTR. Surprisingly, using mutational analysis we find that only ARE no. 3 and ARE no. 4 are bound by hnRNP A1, and that the presence of both intact sequences is required for binding (Figure

5.3). Mutations that abolished binding of hnRNP A1 resulted in stabilization of reporter mRNA. ARE no. 1, in which the AUUUA pentanucleotide is embedded within a larger stretch of A/U nucleotides exhibited only partial binding to hnRNP A1, and the reporter mRNA carrying this mutation was partially stabilized. It has been recognized that the binding of proteins to AREs is dependent on both the primary sequence and sequence context, and that the presence of AUUUA in itself does not guarantee a functional ARE.[23] This applies to the nature of the cIAP1 AREs within the 3'UTR and their surrounding sequence. In addition, a permissive secondary structure of the 3'UTR and proper presentation of the ARE for the ARE-binding protein are thought to contribute to the function of AREs. For example, the RNA-binding protein HuR requires both the presence of the HuR-binding site within the ARE as well as the presentation of this site in a single-stranded conformation within the 3'UTR structure for proper binding.[29] Although hnRNP A1 is usually considered an RNA and single-stranded DNA-binding protein,[30] accumulated evidence indicates that hnRNP A1 is capable of binding double-stranded DNA and RNA regions as well. In fact it was shown that hnRNP A1 could bind simultaneously to bipartite sequence elements with its two RRM domains, or as a dimer.[31–33] Our data fits well with this model suggesting that simultaneous contact of hnRNP A1 with ARE no. 3 and ARE no. 4 is required for proper binding of hnRNP A1 to cIAP1 3'UTR. Thus, mutations in either one of these sites would result in the attenuation of binding and consequent stabilization of the mRNA, as we have observed.

hnRNP A1 is predominantly a nuclear protein involved in the regulation of splicing.[34] However, hnRNP A1 has been shown to shuttle from the nucleus to the cytoplasm, where it exhibits a different ligand specificity, thus leading to the postulation that cytoplasmic hnRNP

A1 performs roles distinct from splicing.[34] Indeed, recent experimental data implicate hnRNP A1 in the regulation of mRNA translation, turnover, and viral replication. The subcellular localization of hnRNP A1 is dictated by the phosphorylation status of its C terminus, which affects the Trn1-dependent nuclear import of hnRNP A1.[20] The phosphorylation of hnRNP A1 occurs under conditions of diverse stresses such as osmotic shock,[19] UV irradiation,[19] heat shock,[35] or treatment of cells with sodium butyrate [36] and arsenite.[35] Cytoplasmic hnRNP A1 accumulates in stress granules, the sites of mRNA triage from which target mRNAs are exported to processing bodies for degradation.[35] Congruent with this model we find that cIAP1 mRNA and reporter mRNA harbouring the 3'UTR of cIAP1 is rapidly degraded upon irradiation of cells with UV (Figures 5.1 and 5.2), conditions that result in an accumulation of hnRNP A1 in the cytoplasm. This reduction in cIAP1 levels can be reversed by transient knockdown of hnRNP A1 (Figure 5.4d) confirming that the repression of cIAP1 expression following UVR is dependent on hnRNP A1. It is important to note that under normal conditions hnRNP A1 is predominantly present in the nucleus, and thus depletion of hnRNP A1 in untreated cells would be predicted to have only a minimal effect on cIAP1 levels, as we have indeed observed (Figure 5.4d).

Ultraviolet radiation is a common environmental stress that causes DNA damage and induces cell death in mammalian cells.[37] Previous work showed that exposure of cells to UVR results in an inhibition of global protein synthesis.[14,38,39] This observation leads to the question of why an additional regulatory mechanism, such as degradation of cIAP1 mRNA, would be employed by cells to silence the expression of target genes following UVR. It is interesting to note that several genes involved in the regulation of cell proliferation and

survival are translated by an IRES-dependent mode of translation that escapes some of the control steps that govern global, cap-dependent translation. For example, translation of the apoptosis protease-activating factor Apaf-1 is driven by an IRES element activity that is enhanced following UVR.[14] We and others have shown previously that translation of cIAP1 is also driven by an IRES.[12,40] Importantly, cIAP1 IRES activity is induced by cellular stresses such as endoplasmic reticulum stress,[12] etoposide,[40] and sodium arsenite.[40] As cIAP1 IRES would allow bypass of the global inhibition of protein synthesis induced by UVR and thus continued expression of cIAP1 protein, the degradation of cIAP1 mRNA by an hnRNP A1-dependent mechanism following UVR can be viewed as an additional control step aimed at the reduction of cIAP1 levels and a return to homeostasis.

Recent evidence suggests that the primary cellular role of cIAP1 is to regulate NF-κB signalling, as specific degradation of cIAP1 results in activation of both the canonical and non-canonical NF-κB signalling pathways.[6–8] NF-κB plays a critical role in cell proliferation and apoptosis, and activation of NF-κB by UV irradiation is an important protective mechanism for mammalian cells.[21] However, the molecular mechanisms involved in the activation of NF-κB following UV irradiation are poorly understood. Our data provide new insight into the regulation of NF-κB-signalling pathways and suggest a mechanism in which targeted degradation of cIAP1 mRNA, and thus a reduction in cIAP1 protein, is mediated by cytoplasmic accumulation of hnRNP A1 in response to UV irradiation.

Materials and Methods

Cell culture and reagents. Human embryonic kidney (HEK293), or human cervical carcinoma (HeLa) cells were maintained in standard conditions in Dulbecco's modified Eagle's medium (DMEM; Wisent Inc.) supplemented with heat inactivated 10% fetal calf serum (FCS), 2mM L-glutamine and 1% antibiotics (100U/ml penicillin–streptomycin). Transient transfections were performed using LipofectAMINE PLUS reagent (Invitrogen; Carlsbad, CA, USA) according to the manufacturer's protocol. Briefly, cells were seeded at a density of $6x10^5$ cells per well in 6-well plates and were transfected 24 h later in serum-free OPTI-MEM medium (Invitrogen) with 0.5μg of DNA per well. The transfection mixture was supplemented 3 h later with 1 ml DMEM containing 10% fetal calf serum, glutamate, and antibiotics. Cells were collected for analysis 24 h after transfection. siRNA transfections were performed using Lipofectamine 2000 reagent (Invitrogen) according to the protocol provided by the manufacturer. Briefly, cells were seeded at a density of $3x10^5$ cells per well in 6-well plates and were transfected 24 h later in serum-free DMEM with either a 10nM final concentration of hnRNP A1 or TIAR siRNA (Santa Cruz Biotechnology, Santa Cruz, CA, USA), a 5nM final concentration of HIAP2 siRNA (Dharmacon) or a nonsilencing scrambled control siRNA (Qiagen). Cells were collected for analysis 48 h after transfection. In the case of co-transfections, 0.5 μg per well of reporter plasmid DNA was co-transfected at the same time as siRNA.

For UV irradiation (UVR) experiments, cells were seeded at a density of $6x10^5$ cells per well in 6-well plates. After 24 h, cells were washed with phosphate-buffered saline (PBS) and irradiated at room temperature in 2 ml fresh medium with a 30-watt UVC light source

(254 nm) with the cover removed. After irradiation, cells were further incubated in culture medium for the indicated times and harvested. PBS washed cells not exposed to UVR served as controls. The intensity of UVR was measured prior to each experiment with a UVX radiometer (UVP Inc., Upland, CA, USA). For the Actinomycin D (ActD) experiments, cells were treated with 10 μg/ml of ActD immediately following UVR (150 mW/cm2) and harvested 0, 1, 2, 4, 8 h later. Cells not treated with UVR served as a control. Cells transfected with a siRNA were treated with UVR (150 mW/cm2) 48 h post-siRNA transfection and harvested 5 h later, as described above.

The expression plasmid pMC was constructed by inserting a synthetic polylinker (5'-AGC TTG CGG CCG CTA GCC TCG AGG GAT CCT CTA GAA TGC A-3') into a pcDNA3 vector (Invitrogen) followed by insertion of the chloramphenicol acetyl transferase (CAT) coding sequence. The CAT insert was generated by PCR amplification using pCAT as a template. The 3'UTRs were generated by PCR amplification from a liver cDNA library (Invitrogen). Expression plasmids pMC-cIAP1-FL and pMC-TNFα were thus constructed by inserting the 3'UTR of cIAP1, and TNFα, respectively downstream of CAT in the pMC construct. Deletion derivatives of pMC-cIAP1-FL were generated using a similar method; cIAP1 3'UTR segments were PCR amplified and cloned into pMC. The primers for amplification of respective 3'UTR fragments are listed in Table 5.1. The site-directed mutagenesis of cIAP1 3'UTR was carried out using the Quickchange II site-directed mutagenesis kit (Stratagene) following the manufacturer's instructions. All plasmid constructs were confirmed by nucleotide sequencing. FLAG-hnRNP A1 and FLAG-hnRNP A1 F1 expression plasmids were described earlier.[17]

Table 5.1
The sequences of primers used in this study to amplify 3'UTRs.

TNFα:
Forward primer: 5′-GGA TCC GGA GGA CGA ACA TCC AAC CTT-3′
Reverse primer: 5′-TCT AGA CTA AGC AAA CTT TAT TTC TCG-3′

cIAP1 (4-120):
Forward primer: 5′-GGA TCC AGA AAA ATA GTC TAT ATT TTA AC-3′
Reverse primer: 5′-TCT AGA GTA CCA AAG CAG ACT AGA AC-3′

cIAP1 (120-240):
Forward primer: 5′-GGA TCC GTT CTA GTC TGC TTT GGT AC-3′
Reverse primer: 5′-TCT AGA CAG TGA CAC TAC TCC CTT AGG-3′

cIAP1 (240-480):
Forward primer: 5′-GGA TCC CCT AAG GGA GTA GTG TCA CTG-3′
Reverse primer: 5′-TCT AGA CAC TTT ATT GAG ATG TTT CTC AC-3′

Western blot analysis. Cells were washed in 1 ml of ice-cold PBS and lysed in 150 µl RIPA buffer (1% Nonidet P-40, 1% sodium deoxycholate, 0.1%. SDS, 150 mM NaCl, 10 mM sodium phosphate (pH 7.2), 2 mM EDTA, 0.1 mM phenylmethylsulphonyl fluoride) containing 10 µg/ml each of aprotinin, pepstatin A and leupeptin (all from Sigma) for 30 min at 4°C, followed by centrifugation at 14 000xg for 10 min and supernatants were collected. Protein concentration in the supernatants was determined by a protein assay kit (Bradford; Bio-Rad, Richmond, CA, USA), and equal amounts of protein extract were separated by 10% SDS-PAGE. Proteins were subsequently transferred onto PVDF membrane and analyzed by western blotting with the following antibodies: rabbit polyclonal anti-cIAP1 (abCAM), mouse-monoclonal anti-GAPDH (Advanced ImmunoChemical), mouse-monoclonal anti TIA-1/TIAR (clone 3E6; generous gift from P. Anderson), mouse monoclonal anti-hnRNP C (clone 4F4, generous gift from G. Dreyfuss), and goat polyclonal anti-hnRNP A1 (Santa Cruz Biotechnology). All antibodies were used at the manufacturer's suggested dilutions and conditions followed by secondary antibody (horseradish peroxidase-conjugated sheep anti-mouse, anti- goat or anti-rabbit IgG; GE Healthcare, Piscataway, NJ, USA). Antibody complexes were detected using the ECL Plus and ECL western blotting detection systems (GE Healthcare). For the purposes of quantification of protein expression, parallel western blots were performed as described above but the secondary antibody used was Alexa Fluor 680-coupled goat anti-mouse, or anti-rabbit IgG (LI-Cor Inc.). Antibody complexes were then detected and quantified using the Odyssey Infrared Imaging system (LI-Cor Inc.). All quantification data are shown as an average ±SD from at least three independent experiments. As some confusion exists in the literature as to the specificity of

the cIAP1 Abcam antibody, we have verified that the antibody used in this study specifically detects cIAP1 but not cIAP2 (Figure 5.6).

Subcellular fractionation. Cells were washed in 1ml of ice-cold PBS, resuspended in 400 µl of Buffer A (10 mM HEPES-KOH (pH 7.5), 10 mM KCl, 1 mM DTT, 1 mM PMSF) containing protease inhibitors, and incubated on ice for 15 min. Nonidet P-40 was added to a final concentration of 0.3% and cells were incubated for an additional 10 min on ice. Nuclei were pelleted by centrifugation at 1500xg for 5 min, the cytoplasmic fraction was collected to a new tube and clarified by centrifugation at 13000xg for 15 min. The nuclei pellet was washed 2 times with 1 ml of Buffer A, and then resuspended in 50 µl of Buffer B (20mM HEPES-KOH (pH 7.5), 400 mM NaCl, 1 mM DTT, 1 mM PMSF) containing protease inhibitors and incubated on ice for 30 min, with mixing every 5 min. Nuclear debris was pelleted at 13000xg for 5 min and the nuclear fraction was collected to a new tube.

Pulse–chase immunoprecipitation. HEK293 ($6x10^5$) cells were seeded in 6-well plates 24 h prior to UV irradiation. Cells were incubated with DMEM lacking methionine and cysteine and supplemented with 10% FCS for 15 min at 37°C. Cells were then irradiated with UVC as described above and pulse-labelled with 0.1 mCi/ml ^{35}S-methionine and cysteine mix (EasyTagt EXPRESS Protein Labelling Mix, PerkinElmer) for 25 min at 37°C. Labelled cells were washed once in PBS and chased with cold methionine/cysteine-containing DMEM. At indicated time points cells were harvested in cold PBS and boiled in 50µl of denaturing lysis buffer (50 mM Tris, pH 7.4, 5 mM EDTA, 1% SDS, 10 mM DTT, 1 mM

Figure 5.6

Abcam 25939 antibody recognizes human cIAP1 but not cIAP2. (**A**) The protein band detected by Abcam 25939 antibody is ablated in antisense cIAP1-transduced cells. 293T cells were transduced with either GFP-expressing adenovirus (Ad.GFP; MOI=5) or cIAP1 antisense-expressing adenovirus (Ad.cIAP1as; MOI=50) for 24 hours and the levels of cIAP1 and Hsp70 were determined by western blot in cell lysates using Abcam cIAP1 rabbit pAb #25939 and Santa Cruz Hsp70 sc-24 mouse mAb. Relative cIAP1 levels are expressed as a ratio of cIAP1/Hsp70, and are shown below the blot. The ratio in Ad.GFP-transduced cells was set as 1. The lower panel shows PCR amplification of the adenovirus genome with primers specific for cIAP1 to verify the transduction. (**B**) Abcam 25939 antibody does not cross-react with cIAP2 protein. 293T cells were treated with recombinant mouse TNFα (R&D systems) at indicated doses for 20 hours and cell lysates were probed with Abcam cIAP1 rabbit pAb #25939, Santa Cruz Hsp70 sc-24 mouse mAb, and rabbit polyclonal RIAP1 antibody that recognizes both cIAP1 and cIAP2 .[41] Treatment of cells with TNFα results in an induction of cIAP2 protein level that is readily detected by RIAP1 antibody but not detected by Abcam 25939.

Abcam antibody recognizes human cIAP1 but not cIAP2

A.

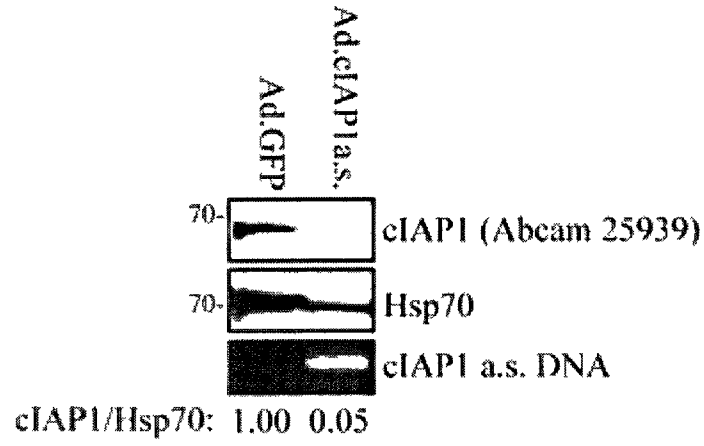

B.

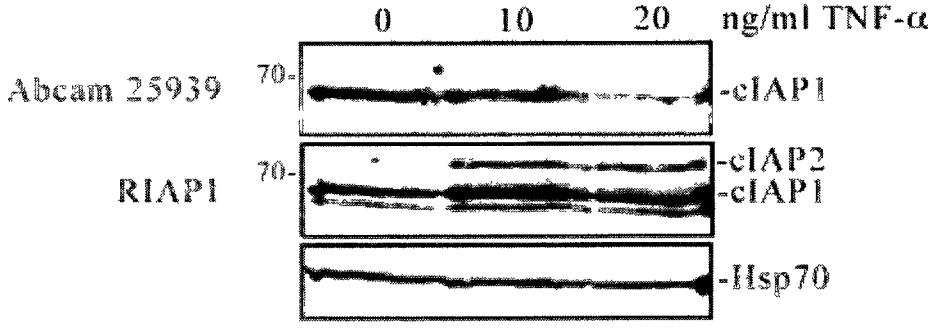

PMSF, 2 μg/ml leupeptin, 15 U/ml DNaseI) for 5 min. A cold non-denaturing buffer of 450 μl (50 mM Tris, pH 7.4, 5 mM EDTA, 300 mM NaCl, 1% Triton X-100, 10 mM iodoacetamide, 1 mM PMSF, 2 μg/ml leupeptin) was then added and the lysate was passed through a 25-G syringe needle 10 times. Following centrifugation to remove debris, the lysate was pre-cleared prior to immunoprecipitation with Pansorbin® cells (Calbiochem) for 2 h at 4°C. Co-immunoprecipitation of cIAP1 and b-actin from the pre-cleared lysates was performed at 4°C for 16 h using Protein G/Protein A-Agarose beads (Calbiochem) coated with antibodies specific for β-actin and cIAP1 at a dilution of 1:500 and 1:150, respectively. The beads were then washed extensively with cold wash buffer (50 mM Tris, pH 7.4, 300 mM NaCl, 0.1% Triton X-100), resuspended in Laemmli buffer and boiled to elute bound proteins. Immunoprecipiated proteins or total proteins were then resolved on 10% SDS-PAGE and stained with PageBlue (Fermentas) Coomassie stain. The gel was incubated with Amplify fluorogenic reagent (GE Biosciences) for 30 min prior to drying and exposure to film.

mRNA stability analysis. Cells were treated or not with UVR (150mW/cm2) as described above and Actinomycin D (10 μg/ml) was then added immediately to each well. Total RNA was isolated using the Absolutely RNA miniprep kit (Stratagene) at 0 (immediately after adding the Actinomycin D), 2, 4, 8, 12 and 16 h time points and the levels of cIAP1 and GAPDH mRNA was determined by quantitative RT-PCR as described below.

Quantitative RT-PCR. Total RNA was isolated using the Absolutely RNA miniprep kit (Stratagene) following manufacturer's instructions. For quantitative RT-PCR, reverse transcription was carried out using the First-Strand cDNA Synthesiskit (GE Healthcare) with oligo d(T)18 primers. The quantitative PCR was performed using the QuantiTect SYBR green PCR kit (Qiagen) and analysed on an ABI Prism 7000 sequence detection system using the ABI Prism 7000 SDS Software. Quantitative PCRs were carried out to detect cIAP1, GAPDH, CAT and NEO genes using primers listed in Table 5.2. Average data from at least three experiments ±SD is presented as ($2^{-[Ct(cIAP1)-Ct(GAPDH)]}$) and ($2^{-[Ct(CAT)-Ct(NEO)]}$). For the Actinomycin D experiment, ($2^{-[Ct(cIAP1)-Ct(GAPDH)]}$) normalized to 0 h Ct values ($2^{-\Delta\Delta Ct}$)is shown.

RNA affinity chromatography. Identification of cIAP1 3'UTR RNA-binding proteins was performed as described earlier.[17] Briefly, in vitro transcribed cIAP1 3'UTR RNA was biotinylated at the 5' end with the 5' EndTag Nucleic Acid Labelling System according to the manufacturer's instructions (Vector Laboratories). The biotinylated RNA (10 μg) was conjugated to Avidin-agarose beads (Sigma) in the presence of incubation buffer (10 mM Tris-Cl (pH 7.4), 150 mM KCl, 1.5 mM MgCl2, 0.5 mM DTT, 0.5 mM phenylmethylsulphonyl fluoride, 0.05% (v/v) Nonidet P-40) at 4°C for 2 h with continuous rotation. Unbound RNA was removed by washing the beads two times with incubation buffer. A 293T (500 μg) protein extract (in incubation buffer) was added to the coated beads, along with 30 μg yeast tRNA (Sigma) and 200 units of Prime RNase inhibitor (Eppendorf). Reactions were incubated at room temperature with continuous rotation for 30 min, followed

Table 5.2
The sequences of quantitative RT-PCR primers used in the study.

cIAP1:
Forward primer: 5′-TCT GGA GAT GAT CCA TGG GTA GA-3′
Reverse primer: 5′-TGG CCT TTC ATT CGT ATC AAG A-3′

GAPDH:
Forward primer: 5′-ACA GTC AGC CGC ATC TTC TT-3′
Reverse primer: 5′-ACG ACC AAA TCC GTT GAC TC-3′

NEO:
Forward primer: 5′-TGA ATG AAC TGC AGG ACG AG-3′
Reverse primer: 5′-CAA TAG CAG CCA GTC CCT TC-3′

CAT:
Forward primer: 5′-GCG TGT TAC GGT GAA AAC CT-3′
Reverse primer: 5′-GGG CGA AGA ACT TGT CCA TA-3′

by incubation at 4°C with continuous rotation for 2.5 h. Beads were washed five times with 500 µl incubation buffer, resuspended in 20 µl of 1X SDS-PAGE loading dye, and boiled for 5 min to elute bound proteins. Proteins were separated by 10% SDS- PAGE and detected by western blot analysis.

UV crosslinking of RNA-protein complexes and nitrocellulose filter-binding assay. RNA-protein UV-crosslinking experiments were performed using purified GST-hnRNP A1 and [^{32}P]-labelled cIAP1 3'UTR RNA as described earlier.[17] Similarly, the filter-binding assays were performed using the purified GST-hnRNP A1 as described.[17]

NF-κB reporter assay. A reporter plasmid containing NF-κB enhancer elements upstream of a luciferase reporter gene (pNF-κB-Luc, Stratagene) was used to assess NF-κB activity in HEK293T following exposure to UVR. Cells seeded in 6-well plates were transfected with DNA and/or siRNA as described above. After 24 h the cells were exposed to UVR (150 mW/ cm2) followed by incubation at 37°C for 18 h. To measure luciferase activity, 200 ng/ml of D-luciferin (BD Biosciences) was added to the cell media and incubated for 5 min at room temperature. Luminescence was recorded using the IVIS Imaging system (Xenogen) and quantified with IVIS Liveimage 2.5 software. Values are presented as mean luminescence corrected to the number of cells per plate.

Acknowledgements

This work was supported by a discovery grant from the National Sciences and Engineering Research Council of Canada (NSERC). J.C. is the recipient of Canada Research Chair (Tier 2) in RNA Metabolism. I.G. is supported by a scholarship from Fonds pour la Recherche en Santé du Québec (FRSQ). T.E.G. is supported by the Frederick Banting and Charles Best Canada Graduate Scholarships Doctoral Award. M.H. is the CHEO Volunteer Association Endowed Scholar.

References

1. Salvesen GS, Duckett CS. Apoptosis: IAP proteins: blocking the road to death's door. *Nat Rev Mol Cell Biol* 2002; **3**: 401–410.

2. Vaux DL, Silke J. IAPs, RINGs and ubiquitylation. *Nat Rev Mol Cell Biol* 2005; **6**: 287–297.

3. Eckelman BP, Salvesen GS, Scott FL. Human inhibitor of apoptosis proteins: why XIAP is the black sheep of the family. *EMBO Rep* 2006; **7**: 988–994.

4. Rothe M, Pan MG, Henzel WJ, Ayres TM, Goeddel DV. The TNFR2-TRAF signaling complex contains two novel proteins related to baculoviral inhibitor of apoptosis proteins. *Cell* 1995; **83**: 1243–1252.

5. Li X, Yang Y, Ashwell JD. TNF-RII and c-IAP1 mediate ubiquitination and degradation of TRAF2. *Nature* 2002; **416**: 345–347.

6. Vince JE, Wong WW, Khan N, Feltham R, Chau D, Ahmed AU *et al.* IAP antagonists target cIAP1 to induce TNF alpha-dependent apoptosis. *Cell* 2007; **131**: 682–693.

7. Petersen SL, Wang L, Yalcin-Chin A, Li L, Peyton M, Minna J *et al.* Autocrine TNF alpha signaling renders human cancer cells susceptible to Smac-mimetic-induced apoptosis. *Cancer Cell* 2007; **12**: 445–456.

8. Varfolomeev E, Blankenship JW, Wayson SM, Fedorova AV, Kayagaki N, Garg P *et al.* IAP Antagonists Induce autoubiquitination of c-IAPs, NF-kappaB Activation, and

TNFalpha-Dependent Apoptosis. *Cell* 2007; **131**: 669–681.

9. Wang CY, Mayo MW, Korneluk RG, Goeddel DV, Baldwin Jr AS. NF-kappaB antiapoptosis: induction of TRAF1 and TRAF2 and c-IAP1 and c-IAP2 to suppress caspase-8 activation. *Science* 1998; **281**: 1680–1683.

10. Conze DB, Albert L, Ferrick DA, Goeddel DV, Yeh WC, Mak T *et al.* Posttranscriptional downregulation of c-IAP2 by the ubiquitin protein ligase c-IAP1 in vivo. *Mol Cell Biol* 2005; **25**: 3348–3356.

11. Warnakulasuriyarachchi D, Ungureanu NH, Holcik M. The translation of an antiapoptotic protein HIAP2 is regulated by an upstream open reading frame. *Cell Death Differ* 2003; **10**: 899–904.

12. Warnakulasuriyarachchi D, Cerquozzi S, Cheung HH, Holcik M. Translational induction of the inhibitor of apoptosis protein HIAP2 during endoplasmic reticulum stress attenuates cell death and is mediated via an inducible internal ribosome entry site element. *J Biol Chem* 2004; **279**: 17148–17157.

13. Yoshimura FK, Luo X, Zhao X, Gerard HC, Hudson AP. Up-regulation of a cellular protein at the translational level by a retrovirus. *Proc Natl Acad Sci* USA 2008; **105**: 5543–5548.

14. Ungureanu NH, Cloutier M, Lewis SM, de Silva N, Blais JD, Bell JC *et al.* Internal ribosome entry site-mediated translation of Apaf-1, but not XIAP, is regulated during UV-induced cell death. *J Biol Chem* 2006; **281**: 15155–15163.

15. Kim JH, Paek KY, Ha SH, Cho S, Choi K, Kim CS *et al.* A cellular RNA-binding protein enhances internal ribosomal entry site-dependent translation through an interaction Downstream of the hepatitis C virus polyprotein initiation codon. *Mol Cell Biol* 2004; **24**: 7878–7890.

16. Bonnal S, Pileur F, Orsini C, Parker F, Pujol F, Prats AC *et al.* Heterogeneous nuclear ribonucleoprotein A1 is a novel internal ribosome entry site trans-acting factor that modulates alternative initiation of translation of the fibroblast growth factor 2 mRNA. *J Biol Chem* 2005; **280**: 4144–4153.

17. Lewis SM, Veyrier A, Hosszu Ungureanu N, Bonnal S, Vagner S, Holcik M. Subcellular relocalization of a trans-acting factor regulates XIAP IRES-dependent translation. *Mol Biol Cell* 2007; **18**: 1302–1311.

18. Cammas A, Pileur F, Bonnal S, Lewis SM, Leveque N, Holcik M *et al.* Cytoplasmic relocalization of heterogeneous nuclear ribonucleoprotein A1 controls translation

initiation of specific mRNAs. *Mol Biol Cell* 2007; **18**: 5048–5059.

19. van der Houven van Oordt W, Diaz-Meco MT, Lozano J, Krainer AR, Moscat J, Caceres JF. The MKK(3/6)-p38-signaling cascade alters the subcellular distribution of hnRNP A1 and modulates alternative splicing regulation. *J Cell Biol* 2000; **149**: 307–316.

20. Allemand E, Guil S, Myers M, Moscat J, Caceres JF, Krainer AR. Regulation of heterogenous nuclear ribonucleoprotein A1 transport by phosphorylation in cells stressed by osmotic shock. *Proc Natl Acad Sci* USA 2005; **28**: 28.

21. Bender K, Gottlicher M, Whiteside S, Rahmsdorf HJ, Herrlich P. Sequential DNA damage-independent and -dependent activation of NF-kappaB by UV. *EMBO J* 1998; **17**: 5170–5181.

22. Khabar KS, Bakheet T, Williams BR. AU-rich transient response transcripts in the human genome: expressed sequence tag clustering and gene discovery approach. *Genomics* 2005; **85**: 165–175.

23. Chen CY, Shyu AB. AU-rich elements: characterization and importance in mRNA degradation. *Trends Biochem Sci* 1995; **20**: 465–470.

24. Mayeda A, Krainer AR. Regulation of alternative pre-mRNA splicing by hnRNP A1 and splicing factor SF2. *Cell* 1992; **68**: 365–375.

25. Hamilton BJ, Nagy E, Malter JS, Arrick BA, Rigby WF. Association of heterogeneous nuclear ribonucleoprotein A1 and C proteins with reiterated AUUUA sequences. *J Biol Chem* 1993; **268**: 8881–8887.

26. Pende A, Contini L, Sallo R, Passalacqua M, Tanveer R, Port JD *et al.* Characterization of RNA-binding proteins possibly involved in modulating human AT(1) receptor mRNA stability. *Cell Biochem Funct* 2008; **26**: 493–501.

27. Christian K, Lang M, Maurel P, Raffalli-Mathieu F. Interaction of heterogeneous nuclear ribonucleoprotein A1 with cytochrome P450 2A6 mRNA: implications for post-transcriptional regulation of the CYP2A6 gene. *Mol Pharmacol* 2004; **65**: 1405–1414.

28. Glisovic T, Ben-David Y, Lang MA, Raffalli-Mathieu F. Interplay between hnRNP A1 and a cis-acting element in the 30 UTR of CYP2A5 mRNA is central for high expression of the gene. *FEBS Lett* 2003; **535**: 147–152.

29. Meisner NC, Hackermuller J, Uhl V, Aszodi A, Jaritz M, Auer M. mRNA openers and closers: modulating AU-rich element-controlled mRNA stability by a molecular switch in mRNA secondary structure. *Chembiochem* 2004; **5**: 1432–1447.

30. Schenkel J, Sekeris CE, Alonso A, Bautz EK. RNA-binding properties of hnRNP proteins. *Eur J Biochem* 1988; **171**: 565–569.

31. Ding J, Hayahsi MK, Zhang Y, Manche L, Krainer AR, Xu RM. Crystal structure of the two RRM domain of hnRNP A1 (UP1) complexed with single-stranded telomeric DNA. Genes Dev 1999; **13**: 1102-1115.

32. Burd CG, Dreyfuss G. RNA binding specificity of hnRNP A1: significance of hnRNP A1 high-affinity binding sites in pre-mRNA splicing. *EMBO J* 1994; **13**: 1197–1204.

33. Xu RM, Jokhan L, Cheng X, Mayeda A, Krainer AR. Crystal structure of human UP1, the domain of hnRNP A1 that contains two RNA-recognition motifs. *Structure* 1997; **5**: 559–570.

34. Pinol-Roma S, Dreyfuss G. Shuttling of pre-mRNA binding proteins between nucleus and cytoplasm. *Nature* 1992; **355**: 730–732.

35. Guil S, Long JC, Caceres JF. hnRNP A1 relocalization to the stress granules reflects a role in the stress response. *Mol Cell Biol* 2006; **26**: 5744–5758.

36. Tan HT, Zubaidah RM, Tan S, Hooi SC, Chung MC. 2-D DIGE analysis of butyrate-treated HCT-116 cells after Enrichment with heparin affinity chromatography. *J Proteome Res* 2006; **5**: 1098–1106.

37. Rehemtulla A, Hamilton CA, Chinnaiyan AM, Dixit VM. Ultraviolet radiation-induced apoptosis is mediated by activation of CD-95 (Fas/APO-1). *J Biol Chem* 1997; **272**: 25783–25786.

38. Deng J, Harding HP, Raught B, Gingras AC, Berlanga JJ, Scheuner D *et al.* Activation of GCN2 in UV-irradiated cells inhibits translation. *Curr Biol* 2002; **12**: 1279–1286.

39. Wu S, Hu Y, Wang J-L, Chatterjee M, Shi Y, Kaufman RJ. Ultraviolet light inhibits translation through activation of the unfolded protein response kinase PERK in the lumen of the endoplasmic reticulum. *J Biol Chem* 2002; **277**: 18077–18083.

40. Van Eden ME, Byrd MP, Sherrill KW, Lloyd RE. Translation of cellular inhibitor of apoptosis protein 1 (c-IAP1) mRNA is IRES mediated and regulated during cell stress. *RNA* 2004; **10**: 469–481.

41. Holcik M, Lefebvre CA, Hicks K, Korneluk RG. Cloning and characterization of the rat homologues of the inhibitor of apoptosis protein 1, 2, and 3 genes. *BMC Genomics* 2002; **3**: 5–10.

CHAPTER 6

General discussion

The cIAP1 IRES pre-initiation complex.

Prior to the work outlined in this thesis, our laboratory identified a unique stress-inducible IRES within the 5'UTR of cIAP1 mRNA. Following an effort to identify specific protein(s) that modulate activity of this inducible IRES, it was found that p86, the caspase-cleavage product of the DAP5/p97 protein, was responsible for mediating caspase-dependent cIAP1 IRES activity during the ER stress response. Surprisingly, I could not produce evidence for direct interaction of either p86 or p97 with the cIAP1 IRES in vitro. Thus was borne my central hypothesis that additional, non-canonical protein factors are required to modulate cIAP1 expression. I successfully identified a cohort of proteins that interact with the cIAP1 IRES, namely NF45, NF90, IGF2BP1, and RHA. Given that this protein-IRES complex was isolated using an in vitro affinity chromatography approach, one cannot rule out that some of these interactions may be RNA independent. I therefore further characterized the interaction between NF45 and the IRES and observed direct binding of the recombinant protein to in vitro transcribed IRES RNA. This observation was unexpected given the lack of a canonical RNA binding motif within the NF45 protein, however it is possible that the N-terminal RGG motif or the DNA zinc finger motif may play roles in RNA binding. Canonical RNA binding motifs are present in all three of the other putative cIAP1 ITAFs (NF90, IGF2BP1, RHA). Therefore, it is likely that one or more of these proteins interact directly with the cIAP1 IRES. UV-crosslinking of cell lysate components to labelled cIAP1 IRES followed by SDS-PAGE did reveal a prominent band migrating at approximately 90-100 kilodaltons (along with a band assumed to be NF45) that one could surmise to be NF90 (Figure 3.1). Future

experiments with recombinant proteins to recapitulate the cIAP1 ITAF complex in vitro will have to be performed to delineate the exact nature of the participation of these proteins.

What we have learned from this work is that both p86 and NF45 are required for an appropriate induction of IRES-mediated cIAP1 mRNA translation during the unfolded protein response. The lack of p86 (either through RNAi-mediated reduction in p97 expression, or inhibition of caspase-mediated cleavage of p97) prevents induction of cIAP1 IRES activity and concomitant protein expression. Conversely, overexpression of p86 significantly enhances cIAP1 protein expression through its IRES. Importantly, preliminary data not included for publication in the original manuscript indicates that induction of cIAP1 protein following overexpression of p86 is dependent on NF45 expression (refer to western blot in appendix B). Further, this western blot indicates that p86 enhances steady-state expression of both NF90 and NF45. How this occurs is not known although it is an intriguing possibility to consider that the p86/NF45/NF90 heterotrimer is shielded from proteasome degradation, that has been demonstrated for the NF90/NF45 heterodimer.[11] Alternatively, p86 may enhance translation of NF90 mRNA through a yet unidentified IRES, subsequently enhancing NF45 protein stability.

Together, these data provide significant evidence that points to NF45 directly interacting with the cIAP1 IRES and playing a critical role in initiation during the cellular response to ER stress. Further, we can conclude that NF45 acts downstream of p86 although we do not yet know whether this involves direct p86-NF45 interactions. Clearly, further in vitro work needs to be done to clarify whether p97/86 interacts directly with NF45 or through other cIAP1 ITAFs. Given the high homology of p97/86 with the eIF4GI and II

family members, it does not seem unreasonable to think that p97/86 acts as a general scaffold protein for the other ITAFs present on the cIAP1 IRES. This idea has been proposed by several laboratories, although it has not been formally shown.[12-14]

The closed loop model of cIAP1 IRES-mediated initiation.

The discovery of classical AU-rich elements (AREs) in the cIAP1 3'UTR by our laboratory led to the work outlined in chapter 5. Therein, we demonstrated that cIAP1 expression is also regulated at the level of RNA stability. We found that cIAP1 mRNA instability is mediated by the RNA binding protein hnRNP A1 interacting with the cIAP1 ARE. This instability is more pronounced following UVR stress that causes a quantitative relocalization of hnRNP A1 from the nucleus to the cytoplasm and a concomitant increase in the number and/or activity of cIAP1 decay mRNPs.

hnRNP A1 acts as a destabilizing ARE-binding protein in the context of the cIAP1 mRNP. This raises the question whether other ARE-binding proteins could act in an opposite manner and stabilize the cIAP1 mRNP. I noted that NF90, one of the cIAP1 IRES binding proteins, is a known ARE-binding protein that stabilizes the IL-2, p21 and MyoD mRNPs.[15] Using our RNA affinity chromatography system, I was able to find that NF90 interacts with the cIAP1 ARE. This unpublished and preliminary data is included in appendix C for the purposes of discussion. Importantly, this data indicates that NF90 does not interact with a mutant ARE, showing that NF90 interacts specifically with the ARE sequence. Owing to the propensity for NF45 and NF90 to heterodimerize in vivo, it is conceivable that these two proteins bridge the cIAP1 UTRs via specific interactions with the IRES and ARE (Figure

6.1). Supporting this model, I have observed that both steady-state levels of cIAP1 mRNA and cIAP1 IRES activity are significantly reduced in HEK293T cells transiently transfected with NF90 siRNA (refer to appendix D). These data indicate that NF45/NF90 might coordinately regulate the stability and IRES-dependent translation of cIAP1 mRNA through bridging of its UTRs. Similar bridging of UTRs mediated by the canonical cap-binding complex eIF4F (interacting with the m7G cap structure) and the polyA-binding protein, PABP (interacting with the polyA tail) synergistically enhance translational efficiency.[3] This eIF4F/PABP-dependent closed loop species of mRNA has been directly visualized using atomic force microscopy.[16] Evidence for NF45/NF90-dependent closed loop RNA species exists in the context of HCV and BVDV viral RNAs, where NF45/NF90 interactions with their IRES (in the 5'NTR) and AU-rich sequences in the 3'NTR are hypothesized to coordinate viral replication and translation.[17]

In the context of the cIAP1 mRNP, we do not yet know if NF45/90 interactions lead to looping of the RNA or if this event could mediate coordinated regulation of its stability and translational efficiency. Perhaps NF45/90 interactions with the UTRs constitute an auxilliary pre-initiation complex that catalyzes the rate-limiting step of translation when the eIF4F/PABP-dependent initiation complex is rendered non-functional (e.g. during stress such as hypoxia, ER stress or viral infection). In eukaryotes, a redundantly looped mRNA species consisting of both eIF4F/PABP-dependent and NF45/90-dependent complexes would provide an efficient switch to IRES-mediated translation initiation during the cellular stress response (refer to Figure 6.1). An extension of this hypothesis would be the prediction that mRNA sub-populations associating with identical ITAF complexes would be regulated

Figure 6.1

Proposed models of the cIAP1 translation and stability mRNPs and their modification following cellular stress. (**A**) The closed loop model of cIAP1 mRNA. Under basal conditions, formation of the cap-dependent pre-initiation complex is favoured, but inefficient scanning (due to a long 5'UTR) and non-productive translation of the upstream ORF leads to low levels of cIAP1 protein. Preliminary data indicate that NF90 interactions with the ARE in the 3'UTR may stabilize cIAP1 mRNA. It is likely that the cIAP1 ITAF complex identified in this thesis (comprising p97, NF45, NF90 IGF2BP1, and RHA) is already in place at the IRES (with 5'-3'UTR interactions mediated by NF45/NF90 binding) following export of the mRNP from the nucleus. This complex constitutes an auxilliary but inactive pre-initiation complex (**B**) IRES-dependent translation of cIAP1 mRNA. Following ER stress and initiation of the unfolded protein response, the cap-dependent pre-initiation complex is rendered non-functional, and caspase-mediated cleavage of p97 allows NF45-dependent recruitment of the ribosome at the IRES. Although the exact mechanism remains unknown it is likely that ribosome binding is mediated by eIF3. The end result is an increase in cIAP1 expression and an increase in apoptotic threshold (**C**) Should the stress be too great for the cell to cope with (e.g. ultraviolet radiation), hnRNP A1 relocalizes to the cytoplasm and associates with the ARE present in the cIAP1 3'UTR, targeting the message for degradation and resulting in decreased cIAP1 protein and apoptotic threshold. It is possible that hnRNP A1 displaces NF90 in this process owing to the former's high binding affinity for the cIAP1 ARE.

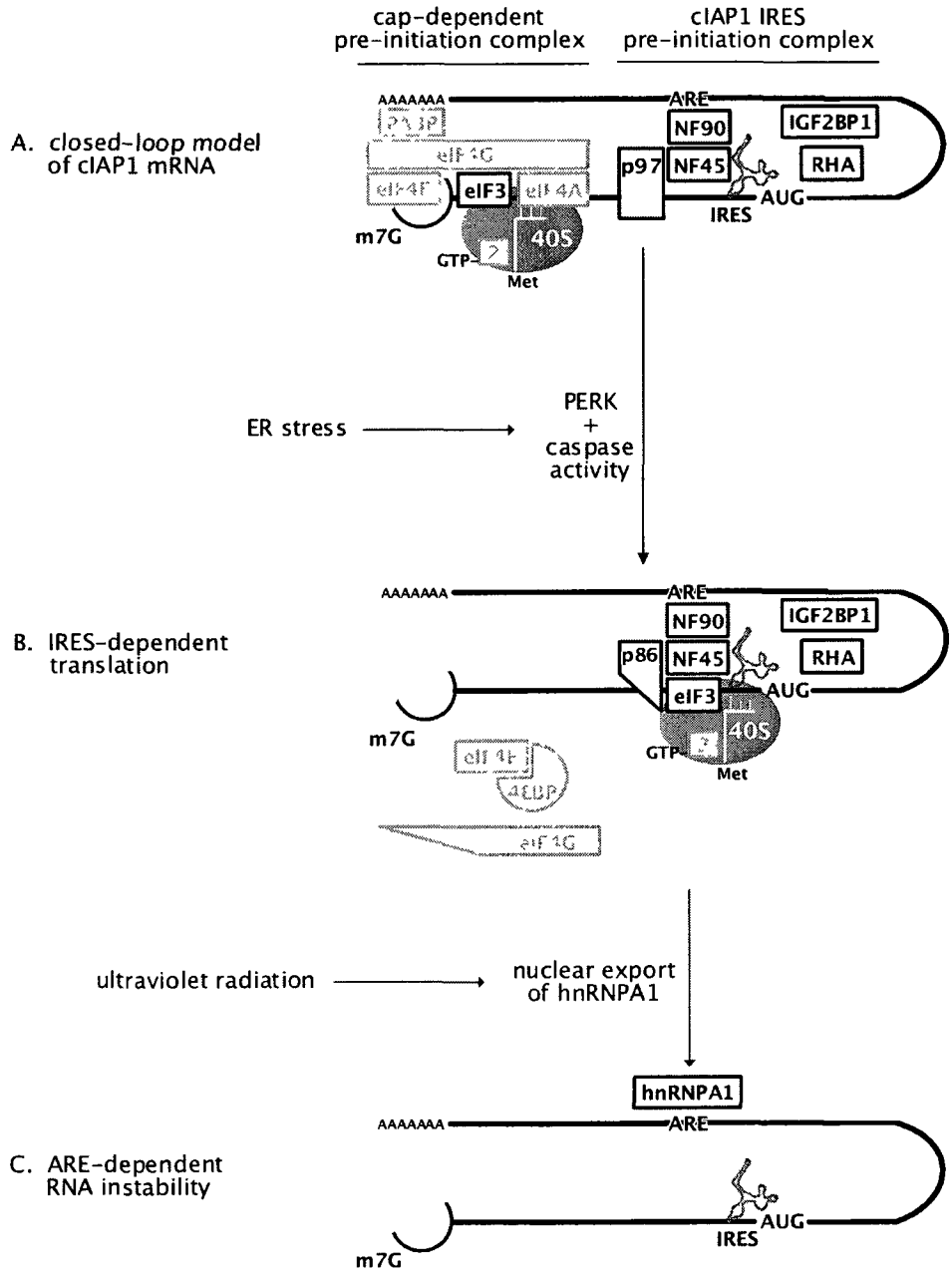
cap-dependent
pre-initiation complex
cIAP1 IRES
pre-initiation complex
A. closed-loop model
of cIAP1 mRNA
AAAAAAA
ARE
NF90
IGF2BP1
p97
NF45
RHA
eIF3
AUG
IRES
m7G
40S
GTP
Met
ER stress
PERK
+
caspase
activity
B. IRES-dependent
translation
p86
ultraviolet radiation
nuclear export
of hnRNPA1
hnRNPA1
C. ARE-dependent
RNA instability

together at the level of stability and translation. These RNA translation operons would function by allowing coordinated expression of proteins involved in maintaining critical biosynthetic pathways.

Does NF45 control an RNA operon?

Chapter 4 of this thesis presents data clearly demonstrating that NF45 ITAF activity is not specific to the cIAP1 IRES. Unexpectedly, I was able to confidently predict other NF45-dependent IRES based solely on the nucleotide composition of their 5'UTRs. Specifically, I found that decreased NF45 expression impairs translational efficiency of those mRNAs harbouring an IRES *and* an AU-rich (>60%) 5'UTR. An astute observer might ask whether *all* 5'UTRs with an AU content >60% possess IRES activity. This question has not been formally answered. Given that 9% (3051/33673) of human non-redundant 5'UTRs have an AU content >60%, testing this hypothesis using the classical bicistronic assay would be cumbersome. The implicit statement within this hypothesis is that AU-rich IRES are NF45-dependent. Therefore, it would be desirable to perform a Translation State Array Analysis (DNA microarray analysis of polyribosomal RNA) to determine the translational efficiency of transcripts containing AU-rich 5'UTRs in *d5* versus *c* cells. Transcripts whose translational efficiency is reduced (or enhanced) in cells lacking NF45 would thus be excellent candidates for novel IRES-containing mRNAs.

Importantly, the NF45-dependent and IRES-containing mRNAs identified herein encode proteins involved in three intimately linked functional pathways, namely DNA damage repair (SNM1), apoptosis, and NF-κB signalling (NRF, cIAP1, XIAP), while the

ELG1 IRES regulates an uncharacterized protein (known as ELG). NF-κB can be activated upon DNA damage induced by several chemotherapeutic drugs including camptothecin, etoposide and doxorubicin.[18] Does NF45 preserve genomic stability by maintaining IRES-mediated translation of critical DNA repair genes? Does NF45 keep the brake on NF-κB signalling through IRES-mediated translation of the NF-κB-repressing factor, cIAP1, and XIAP? Our laboratory is currently trying to answer these critical questions by continuing to look at the effect of RNAi-mediated NF45 knockdown in *d5* cells.

The *d5* cells exhibit a striking senescent-like morphology typified by an overall flat, non-elliptical shape. This is accompanied by multi-lobed nuclei indicative of aborted cytokinesis (Figure 4.5). This phenotype has recently been confirmed with time-lapse microscopy of HeLa cells transiently transfected with siRNA targeting NF45, where although cells undergo seemingly normal nuclear division, there is a clear block in cytokinesis leading to the identical phenotype (multi-lobed nuclei and slow growth) observed in *d5* cells.[19] Although there is no cell cycle arrest in *d5* cells, there is a 50% decrease in ^{3}H-thymidine uptake that suggests severely impaired DNA synthesis and correlates with the slow growth kinetics of these cells.[11] Interestingly, while polyploidy is increased in *d5* cells, and IRES-mediated translation of cIAP1 and XIAP is impaired, cells are not undergoing apoptosis.[11] I hypothesize that the lack of apoptosis is due to severe attenuation of the intrinsic mitochondrial apoptotic pathway, as a result of continuous p53 degradation by the resident E6 protein of the human papilloma virus that is resident in HeLa cells.[20] Work is ongoing to determine whether the striking senescent-like phenotype observed in cells expressing RNAi targeting NF45 is a result of impaired IRES-mediated translation of these specific transcripts.

The most important experiment yet to be performed is to rescue impaired IRES-mediated translation in *d5* cells by overexpression (or knockdown in the case of SNM1) of one or more of the targeted proteins in an attempt to revert the defect in cytokinesis.

The interconnected and fundamental biological pathways that are perturbed by the lack of NF45 ITAF activity would suggest that the NF45-IRES RNP constitutes an RNA operon. Analogous to a DNA operon, the post-transcriptional RNA operon theory postulates that specific populations of eukaryotic mRNAs are coregulated at the level of RNA export, stability, and/or translation by virtue of their cis-acting UTR elements and interactions with trans-acting factors (proteins and/or small RNAs).[4] The power of an RNA operon lies in its ability to coordinately regulate multiple mRNAs through distinct mRNPs in response to discreet cell signals. These mRNPs can be organized into functional operons that ensure an efficient, spatio-temporal response to cellular perturbations. No study to-date has looked directly at how NF45 expression and/or localization would be affected by changes in cellular homeostasis that could lead to co-regulation of NF45-dependent IRES. Indirect evidence from the NF45 binding partner, NF90 (which stabilizes NF45 levels) indicates that its Akt-dependent phosphorylation mediated by CD28 stimulation causes it to shuttle from the nucleus to the cytoplasm.[21] Other studies found that phosphorylation of NF90 during mitosis causes a similar redistribution to the cytoplasm.[22, 23] NF45 may come along for the ride in these situations, perhaps affecting IRES-mediated translation along the way (although this might be a naive assumption, as post-translational modification of NF90 could very well affect its interaction with NF45).

Singular changes in NF45 expression and/or localization cannot however explain the differing activities of the XIAP and cIAP1 IRES in response to the same cellular stresses. For example, XIAP but not cIAP1 IRES activity is induced by gamma irradiation, anoxia and serum starvation. Conversely, cIAP1 but not XIAP IRES is induced upon ER stress, etoposide-induced DNA damage, and sodium arsenite treatment. In the case of XIAP, a number of ITAFs have already been identified that have opposing effects on IRES activity. For example, hnRNP A1 represses XIAP IRES activity[24], while hnRNP C1/C2 enhances activity.[25] A scenario that reconciles these observations requires IRES activity to be viewed as an integrated signal arising from the combinatorial activities of pleiotropic ITAFs assembled in a macromolecular complex at the IRES. Thus, in a cell responding to ER stress, NF45 maintains both XIAP and cIAP1 IRES activities, but additive p86 ITAF activity only targets the cIAP1 IRES causing its induction compared to the unstressed cell.

Future directions

The evolutionarily conserved NF45-IRES interaction has been uncovered by studying post-transcriptional control of cIAP1. NF45-dependent IRES appear to be defined by unusually high AU content and this constraint was sufficient to accurately predict those existing cellular IRES whose activity can be modified by NF45. This constraint may also be useful in predicting novel cellular IRES. To this end, a useful experiment might be to test for IRES activity in a manageable number of AU-rich (>60%) 5'UTRs to determine if IRES activity occurs more frequently in this subset than by chance.

Understanding the mechanism through which NF45 enhances IRES-mediated translation of its target mRNAs is of critical importance, as it may shed light on how cellular IRES function, that to-date is poorly understood. To begin to address questions on mechanism of action (i.e. how NF45 mediates ribosomal recruitment), our laboratory is attempting to recapitulate the cIAP1 IRES pre-initiation complex in vitro to determine: 1) if any canonical initiation factors are required for NF45-dependent IRES activity, 2) how NF45 may affect IRES structure, and 3) whether NF45 can directly interact with the ribosome. Additionally, the possibility of coordinated regulation of RNA stability and translation through NF45/NF90-mediated looping of cIAP1 mRNA (and by implication other NF45-dependent mRNAs) needs to be explored further.

Together, the work detailed in this dissertation has added significantly to our understanding of how RNA binding proteins affect the stability and translation of mRNA and builds a strong argument for the role that post-transcriptional operons might play in organizing functional units of gene expression in higher eukaryotes.

Appendix A:
References for chapter 1 (sections 2-3) and chapter 6

1. Jacob F, Perrin D, Sanchez C, Monod J. [Operon: a group of genes with the expression coordinated by an operator.]. *C R Hebd Seances Acad Sci* 1960 Feb 29; **250:** 1727-1729.

2. Gros F, Gilbert W, Hiatt HH, Attardi G, Spahr PF, Watson JD. Molecular and biological characterization of messenger RNA. *Cold Spring Harb Symp Quant Biol* 1961; **26:** 111-132.

3. Mathews M, Sonenberg N, Hershey JWB. *Translational control in biology and medicine*, [3rd edn. Cold Spring Harbor Laboratory Press: Cold Spring Harbor, N.Y., 2007, x, 934 p.pp.

4. Keene J. RNA regulons: coordination of post-transcriptional events. *Nat Rev Genet* 2007 Jul 1; **8** (7): 533-543.

5. Eckelman BP, Salvesen GS. The human anti-apoptotic proteins cIAP1 and cIAP2 bind but do not inhibit caspases. *J Biol Chem* 2006 Feb 10; **281** (6): 3254-3260.

6. LaCasse EC, Mahoney DJ, Cheung HH, Plenchette S, Baird S, Korneluk RG. IAP-targeted therapies for cancer. *Oncogene* 2008 Oct 20; **27** (48): 6252-6275.

7. Baud V, Karin M. Is NF-kappaB a good target for cancer therapy? Hopes and pitfalls. *Nat Rev Drug Discov* 2009 Jan; **8** (1): 33-40.

8. Warnakulasuriyarachchi D, Ungureanu NH, Holcik M. The translation of an antiapoptotic protein HIAP2 is regulated by an upstream open reading frame. *Cell Death Differ* 2003 Aug; **10** (8): 899-904.

9. Warnakulasuriyarachchi D. Translational Induction of the Inhibitor of Apoptosis Protein HIAP2 during Endoplasmic Reticulum Stress Attenuates Cell Death and Is Mediated via an Inducible Internal Ribosome Entry Site Element. *Journal of Biological Chemistry* 2004 Feb 3; **279** (17): 17148-17157.

10. Barreau C, Paillard L, Osborne HB. AU-rich elements and associated factors: are there unifying principles? *Nucleic Acids Res* 2005; **33** (22): 7138-7150.

11. Guan D, Altan-Bonnet N, Parrott AM, Arrigo CJ, Li Q, Khaleduzzaman M, *et al.* Nuclear factor 45 (NF45) is a regulatory subunit of complexes with NF90/110 involved in mitotic control. *Mol Cell Biol* 2008 Jul; **28** (14): 4629-4641.

12. Hundsdoerfer P, Thoma C, Hentze MW. Eukaryotic translation initiation factor 4GI and p97 promote cellular internal ribosome entry sequence-driven translation. *Proc Natl Acad Sci U S A* 2005 Sep 20; **102** (38): 13421-13426.

13. Lee SH, McCormick F. p97/DAP5 is a ribosome-associated factor that facilitates protein synthesis and cell proliferation by modulating the synthesis of cell cycle proteins. *EMBO J* 2006 Sep 6; **25** (17): 4008-4019.

14. Frank F, Virgili G, Sonenberg N, Nagar B. Crystallization and preliminary X-ray diffraction analysis of the MIF4G domain of DAP5. *Acta Crystallogr Sect F Struct Biol Cryst Commun* Jan 1; **66** (Pt 1): 15-19.

15. Shi L, Zhao G, Qiu D, Godfrey WR, Vogel H, Rando TA, *et al.* NF90 regulates cell cycle exit and terminal myogenic differentiation by direct binding to the 3'-untranslated region of MyoD and p21WAF1/CIP1 mRNAs. *J Biol Chem* 2005 May 13; **280** (19): 18981-18989.

16. Wells SE, Hillner PE, Vale RD, Sachs AB. Circularization of mRNA by eukaryotic translation initiation factors. *Mol Cell* 1998 Jul; **2** (1): 135-140.

17. Isken O, Grassmann CW, Sarisky RT, Kann M, Zhang S, Grosse F, *et al.* Members of the NF90/NFAR protein group are involved in the life cycle of a positive-strand RNA virus. *EMBO J* 2003 Nov 3; **22** (21): 5655-5665.

18. Jin HS, Lee DH, Kim DH, Chung JH, Lee SJ, Lee TH. cIAP1, cIAP2, and XIAP act cooperatively via nonredundant pathways to regulate genotoxic stress-induced nuclear factor-kappaB activation. *Cancer Res* 2009 Mar 1; **69** (5): 1782-1791.

19. Neumann B, Walter T, Heriche JK, Bulkescher J, Erfle H, Conrad C, *et al.* Phenotypic profiling of the human genome by time-lapse microscopy reveals cell division genes. *Nature* Apr 1; **464** (7289): 721-727.

20. Wesierska-Gadek J, Schloffer D, Kotala V, Horky M. Escape of p53 protein from E6-mediated degradation in HeLa cells after cisplatin therapy. *Int J Cancer* 2002 Sep 10; **101** (2): 128-136.

21. Pei Y, Zhu P, Dang Y, Wu J, Yang X, Wan B, *et al.* Nuclear export of NF90 to stabilize IL-2 mRNA is mediated by AKT-dependent phosphorylation at Ser647 in response to CD28 costimulation. *J Immunol* 2008 Jan 1; **180** (1): 222-229.

22. Parrott AM, Walsh MR, Reichman TW, Mathews MB. RNA binding and phosphorylation determine the intracellular distribution of nuclear factors 90 and 110. *J Mol Biol* 2005 Apr 29; **348** (2): 281-293.

23. Aoki Y, Zhao G, Qiu D, Shi L, Kao PN. CsA-sensitive purine-box transcriptional regulator in bronchial epithelial cells contains NF45, NF90, and Ku. *Am J Physiol* 1998 Dec 1; **275** (6 Pt 1): L1164-1172.

24. Lewis SM, Veyrier A, Hosszu Ungureanu N, Bonnal S, Vagner S, Holcik M. Subcellular relocalization of a trans-acting factor regulates XIAP IRES-dependent translation. *Mol Biol Cell* 2007 Apr; **18** (4): 1302-1311.

25. Holcik M, Gordon BW, Korneluk RG. The internal ribosome entry site-mediated translation of antiapoptotic protein XIAP is modulated by the heterogeneous nuclear ribonucleoproteins C1 and C2. *Mol Cell Biol* 2003 Jan; **23** (1): 280-288.

Appendix B:
p86-dependent translation of cIAP1 requires NF45 expression.

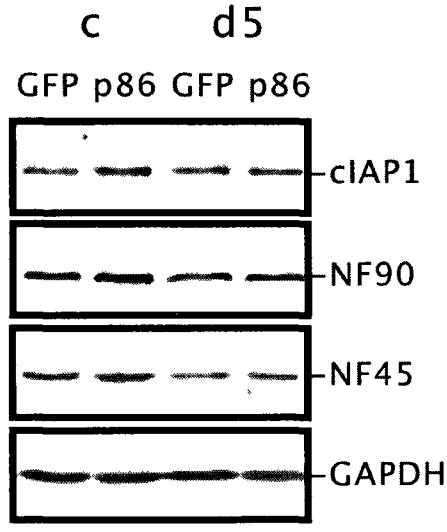

Western blot showing that p86-mediated induction of cIAP1 protein expression is impaired in cells expressing NF45 shRNA (*d5*) relative to cells expressing non-targeting shRNA (*c*). Cells were transiently transfected with 1μg of GFP or p86 overexpression plasmid and harvested 24 hours later (as described in Materials and Methods section in chapter 2). Western blots were performed with antibodies against the indicated proteins (sources described in Materials and Methods section in chapter 3). Blot represents a single experiment.

Appendix C:
NF90 interacts with cIAP1 ARE present in the cIAP1 3'UTR.

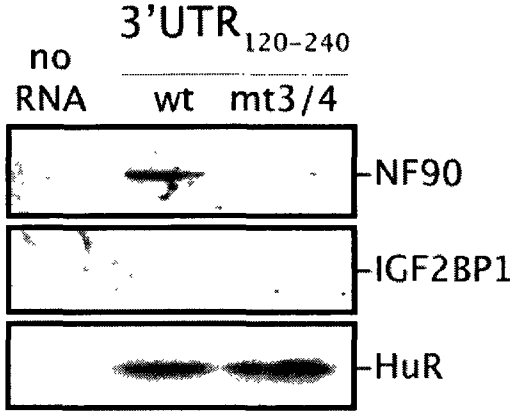

Western blot of an RNA affinity chromatography preparation. A HEK293T cytoplasmic lysate was incubated with biotin-end-labelled in vitro transcribed RNA corresponding to the wildtype (wt) ARE-containing portion of the cIAP1 3'UTR ($3'UTR_{120-240}$) or RNA with point mutations in ARE no. 3 and no. 4 (mt3/4) or no RNA (see chapter 5 for specific protocol and details about mutations). Captured proteins were pulled down on streptavidin beads and resolved by SDS-PAGE. Western blots were performed with antibodies against the indicated proteins (sources described in Materials and Methods section in chapter 3).

Appendix D:
cIAP1 IRES activity and mRNA levels are reduced in cells with targeted knockdown of NF90 expression.

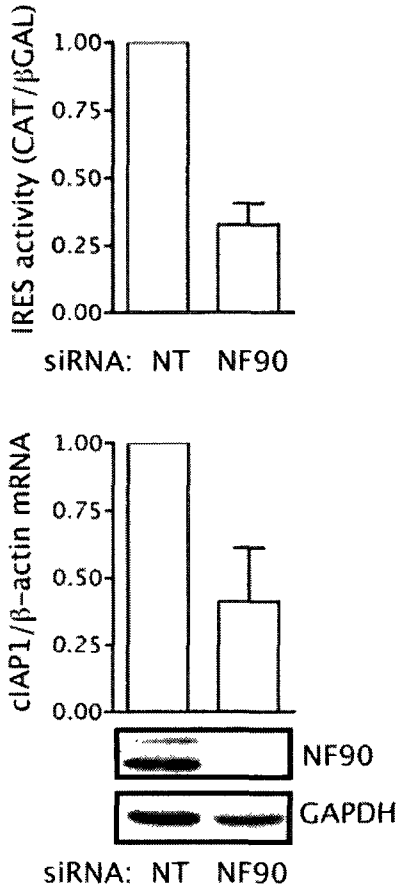

HEK293T cells were incubated with two rounds of 50 nM siRNA targeting NF90 and NF110 (NF90: 5'-GCU UGC UGC UGU AAC AGA AGA CAA G-3') or non-targeting (NT) siRNA for 48+48 hours using Lipofectamine 2000. (**Top panel**) IRES activity of cells transfected with NF90 or NT siRNA (n=3, mean ±SD). (**Middle panel**) Steady-state expression of cIAP1 mRNA relative to β-actin mRNA in cells transfected with NF90 or NT siRNA and assessed by quantitative RT-PCR (n=3, mean ±SD). (**Bottom panel**) Western blot probed with antibodies specific for NF90/NF110 or GAPDH showing efficiency of NF90/110 knockdown. Detailed protocols, primers and sources of antibodies for all assays are found in Materials and Methods section in chapter 2.

Appendix E:
Curriculum vitae

Contact Information

Tyson GRABER
Apoptosis Research Centre
Children's Hospital of Eastern Ontario Research Institute
401 Smyth Road, Ottawa, Ontario, Canada, K1H 8L1
e: tyson@arc.cheo.ca
p: 613.738.4176

Languages

English; French; German (working knowledge)

Relevant Work Experience

Position	Organization	Department	Supervisor	Start-End Date
Graduate student	Children's Hospital of Eastern Ontario	Apoptosis Research Centre	Dr. Martin Holcik	09/2004 - present
Teaching Assistant (various courses)	University of Ottawa	Faculty of Science	various	01/2005-05/2007
Research Technician	Children's Hospital of Eastern Ontario	Apoptosis Research Centre	Dr. Martin Holcik	05/2003 - 08/2004
Application Scientist, part-time consultant	United Bioinformatica, Inc.	Microarray analysis software	Independent consultant	04/2004 -12/2006
Technical Officer	National Research Council Canada	Biological Sciences Division	Dr. John P. MacManus	01/2001 - 04/2003
Infantryman	Canadian Forces Primary Reserve	Governor General's Footguards and 28th Medical	N/A	05/1997 - 02/2002
Research Technician	University of Ottawa	Cellular and Molecular Medicine	Dr. Henry Fliss	07/2000 - 12/2000
Fourth year Honour's student	Ottawa Hospital Research Institute	Molecular Medicine	Dr. Sharon Cassol	09/1999 - 05/2000
Summer student	Ottawa Hospital Research Institute	Cancer Therapeutics	Dr. Chaim Birnboim	05/1999 - 08/1999

Academic Background and Training

Degree	Specialty	Organization	Country	Date received
Doctorate (Ph.D.)	Biochemistry	University of Ottawa	Canada	2010 (in progress)
Bachelor's, Honours (B.Sc.)	Biochemistry	University of Ottawa	Canada	06/2000

Awards and Distinctions

Award	Agency	Amount	Start-End Date
AACR Scholar-in-Training Travel Award	American Association of Cancer Researchers	$1 000	02/2010
Biochemistry programme Travel Award	University of Ottawa, Dept. of Biochemistry, Microbiology and Immunology	$1 000	02/2010
FGPS Travel Award	University of Ottawa, Faculty of Graduate and Postdoctoral Studies	$550	02/2010
Keystone Symposia Travel Scholarship	Keystone Symposia	$1 000	01/2008
Frederick Banting and Charles Best Canada Graduate Scholarship – Doctoral Award	Canadian Institutes of Health Research	$105 000	05/2007-05/2010
University of Ottawa Excellence Scholarship	University of Ottawa	$20 000 (equivalent to tuition fees)	05/2007-05/2010
1st place, departmental research seminar award	University of Ottawa, Dept. of BMI	nil	02/2006
FGPS Travel Award	University of Ottawa, Faculty of Graduate and Postdoctoral Studies	$400	05/2005
3rd place, departmental poster presentation	University of Ottawa, Dept. of BMI	nil	03/2005

Award	Agency	Amount	Start-End Date
John C. Wiley research award	Children's Hospital of Eastern Ontario	$1 500	09/2004

Expertise

I have technical expertise in the following specialized areas: DNA microarray analysis, Quantitative PCR, RNA affinity chromatography, polyribosome profiling.

Consulting activities

I worked as a part-time consultant with United Bioinformatica Inc., a small company that sold and distributed software for life scientists. I was tasked with presenting and demonstrating several DNA microarray analysis software packages to a number of academic and commercial entities. I was also responsible for providing clients on-line technical support across Canada. My consulting activity ended following acquisition of small microarray analysis software producers by larger companies that provide in-house sales, distribution and technical support. My experiences with United Bioinformatica Inc. lead me to better appreciate and understand the dynamics of working with a commercial enterprise.

Mentoring activities

I have volunteered as a judge for the Ottawa Regional (2008 and 2010) and Canada-Wide science fairs (2009). I also volunteered to participate as a mentor in the 2009 Sanofi-Aventis BioTalent Challenge where I provided a Grade 9 student with 3 months of hands-on training and experience in a medical research laboratory. The student was allowed to design and conduct her own research project under my direct supervision. This was followed by presentation of the results to her peers and judging by members of the scientific community.

Teaching/Supervisory experience

I worked as a teaching assistant for a number of undergraduate laboratory courses. I have also helped to train and supervise both undergraduate and fellow graduate students. Therefore, teaching figures prominently in my career aspirations.

Other relevant activities

• *City-wide research seminar calendar*

I have created a centralized on-line calendar that brings together listings of medical research seminars that take place at the University of Ottawa, Ottawa Health Research Institute, University of Ottawa Heart Institute, and the Children's Hospital of Eastern Ontario. Before this calendar, each seminar series could only be accessed from separate websites. The calendar provides students and faculty with centralized and mobile listings that make it easy to see when and where a seminar of interest is scheduled to take place.

• *Wiki-LIMS*

I am a co-creator of a wiki-based Laboratory Information Management Service (LIMS) for the institute where I currently work/study. The wiki-LIMS provides a user-friendly electronic notebook option to the end user.

Published refereed papers

1. **Graber TE**, Baird SD, Kao PN, Mathews MB, Holcik M. (2010) *NF45 functions as an IRES trans-acting factor that is required for translation of cIAP1 during the unfolded protein response.* Cell Death and Differentiation. 17, 719-729.

2. Zhao TT*, **Graber TE***, Jordan LE, Cloutier M, Lewis SM, Goulet I, Cote J, Holcik M. (2008) *hnRNP A1 regulates UV-induced NFKB signaling* via *destabilization of cIAP1 mRNA.* Cell Death and Differentiation. 16, 244-252. *Equal contributors

3. LewisSM, Cerquozzi S, **Graber TE**, Ungureanu NH, Andrews M, Holcik M.(2008). *The eIF4G homologue p97 supports the translation of select mRNAs during endoplasmic reticulum stress.* Nucleic Acids Research. 36, 168-178.

4. **Graber TE** and Holcik M. (2007). *Cap-independent regulation of gene expression in apoptosis.* Molecular Biosystems. 3, 825-834.

5. **Graber TE**, Lewis SM, Holick M. (2006). *An approach to whole-genome identification of IRES elements.* Current Genomics. 7, 205-215.

6. Costain WJ, Rasquinha I, **Graber T**, Luebbert C, Preston E, Slinn J, Xie X, Macmanus JP. (2006). *Cerebral ischemia induces neuronal expression of novel VL30 mouse retrotransposons bound to polyribosomes.* Brain Res. 1094, 24-37.

7. Holcik M, **Graber T**, Lewis SM, Lefebvre CA, Lacasse E, Baird S. (2005). *Spurious splicing within the XIAP 5'UTR occurs in the Rluc/Fluc but not the β-gal/CAT bicistronic reporter system.* RNA. 11, 1605-9.

8. MacManus JP, **Graber T**, Luebbert C, Preston E, Rasquinha I, Smith B, Webster J. (2004). *Translation-state analysis of gene expression in mouse brain after focal ischemia.* J. Cereb. Blood Flow Metab. 24, 657-67.

Contributions to a collective work (Non-reviewed article)

- I contributed a review article of Microarray Gene Expression Analysis Software (in my capacity as a consultant for UBI Bioinfomatica, Inc.) to the Canadian Bioinformatics Help Desk newsletter (a service of Genome Canada).

Presentations as guest speaker

1. **Graber TE**, Baird SD, Kao PN, Mathews MB, Holcik M. *NF45 functions as an IRES trans-acting factor that is required for translation of cIAP1 during the unfolded protein response.* Presented at RiboWest 2009 meeting, Prince George, B.C., Canada, 2009

2. **Graber TE**, Holcik M. *Identification of repressor proteins regulating IRES-mediated translation of HIAP2.* Presented at Cold Spring Harbor Laboratory Translational Control meeting, Cold Spring Harbor, NY, USA, 2006

Published abstracts (conference posters)

1. **Graber TE**, and Holcik M. *Nucleotide Composition Defines a Class of Cellular IRES.* Presented at the American Association for Cancer Research, San Diego, CA, USA, *2010*

2. **Graber TE**, Baird SD, Zhao TT, Holcik M. *Identification of common protein factors regulating translation and RNA stability of the inhibitor of apoptosis protein cIAP1 in response to cell stress.* Presented at RNA-Protein Interactions in Development and Cancer Workshop, Baeza, Spain, 2009

3. **Graber TE**, Holcik M. *NF45 is a novel translation regulator of the inhibitor of apoptosis protein cIAP1.* Presented at Cold Spring Harbor Laboratory Translational Control meeting, Cold Spring Harbor, NY, USA, 2008

4. **Graber TE**, Holcik M. *Repression of HIAP2 translation is mediated by a novel cellular IRES trans-acting factor.* Presented at Keystone Symposium - Translational Regulatory Mechanisms, Coeur d'Alene, Idaho, USA, 2008

5. **Graber TE**, Lewis S, Holcik M. *Identification of proteins enhancing cap-independent translation of the inhibitor of apoptosis protein HIAP2 and their role in ER stress-induced apoptosis.* Presented at the annual meeting of the RNA Society, Banff, Alberta, Canada, 2005

6. **Graber TE**, Luebbert C, Preston E, Rasquinha I, Smith B, Webster J, and MacManus JP. *Translation-state analysis of gene expression in mouse brain after focal ischemia.* Presented at Genomics Health Initiative conference, Ottawa, Ontario, Canada, 2002

Artistic works

- I have published full-page photographs (Mountain Equipment Co-Op 2006 summer catalogue, p.46 English and French editions) as well as a photograph-mural (Mountain Equipment Co-Op, Toronto store)

***